THE UNIVERSITY of ADELAIDE

Three-Dimensional Measurement of Spinal Kinematics and Whole-Body Activity Recognition

Sammuel Aleck Sobey

A thesis submitted for the degree of

Doctor of Philosophy

at The University of Adelaide

July 2019

I certify that this work contains no material which has been accepted for the award of any other degree or diploma in my name in any university or other tertiary institution and, to the best of my knowledge and belief, contains no material previously published or written by another person, except where due reference has been made in the text. In addition, I certify that no part of this work will, in the future, be used in a submission in my name for any other degree or diploma in any university or other tertiary institution without the prior approval of the University of Adelaide and where applicable, any partner institution responsible for the joint award of this degree.

The author acknowledges that copyright of published works contained within this thesis resides with the copyright holder(s) of those works.

I give permission for the digital version of my thesis to be made available on the web, via the University's digital research repository, the Library Search and also through web search engines, unless permission has been granted by the University to restrict access for a period of time.

I acknowledge the support I have received for my research through the provision of an Australian Government Research Training Program Scholarship.

A list of published works includes:

- Sobey S.A., Grimshaw P.N., Grainger S, Robertson W.S.P, Taylor I., Weston M., *A Low Cost, Wireless Spinal Motion Measurement Device*, Intelligent Environments, London, 2016.

International conference presentations:

- Sobey S.A., Grimshaw P.N., Grainger S, Robertson W.S.P, *Comparison of Different Sensors When Measuring Dynamic Range of Motion*, European Society of Biomechanics, Lyon, 2016.
- Sobey S.A., Grimshaw P.N., Grainger S, Robertson W.S.P, Taylor I., Weston M., *A Low Cost, Wireless Spinal Motion Measurement Device*, Intelligent Environments, London, 2016.
- Sobey S.A., Grimshaw P.N., Grainger S, Robertson W.S.P, *Design of a New Inertial Based Spinal Motion Measurement Device*, International Society of Biomechanics, Brisbane, 2017.

Sammuel Sobey

2nd of July 2019

I dedicate this work to my parents Angela and Phillip, without whose support none of this work would be possible. To my brothers and sister, Matthew, Thomason, Gregory, and Brieanna, for all the incredible times we have shared. To my Grandma Yvonne and my late Grandparents Hugh and Dawn, some of the greatest and most loving people in my world, thank you for all you have done for me.

To my supervisors Paul, Will, and Steven for their guidance and support throughout my candidature, for without it, this thesis would not have been completed.

To all my friends in the School of Mechanical Engineering, but mostly David, Erica, Ryan, and Amy for all the great times we have had, especially Friday weekly lunches and the ISB conference in Brisbane 2017.

To my numerous housemates throughout my candidature; Tom, Joel, James, David, Mitchell, and Nic, thank you for helping me by picking up the slack at home when I was too busy to do so myself. And to all my other friends for everything along the way.

And lastly, but certainly not least, to Lucy. I cannot thank you enough for all you have done for me in our lives together so far and during the writing of my thesis.

"No matter how you get there or where you end up, human beings have this miraculous gift to make that place home"

Creed Bratton, 2013

Acknowledgements

There are many people I would like to acknowledge for their continuous support over the duration of my thesis. Firstly, to my primary supervisor Paul and my co-supervisors Will and Steven; without your extensive and continued guidance and support, this thesis would not be possible. Thank you for the many hours of work you have all put in over the last few years to get me in a position to submit this thesis, it is greatly appreciated.

Thank you to one of my fellow PhD students Ryan Quarrington, who took some time from his very busy schedule to give consultation to me in regard to some of the data analysis performed in Chapter 6.

I would also like to acknowledge the contributions made by students Isaac Taylor and Melissa Weston who, over the course of six weeks, assisted with my thesis, particularly in Chapter 5.

Abstract

Back pain is one of the leading causes of disability, being the second largest contributor to work days missed, and sixth largest disability when expressed in terms of an overall burden measured in disability-adjusted life years. Back pain is a large economic burden, where indirect costs from work days missed far outweigh the direct costs due to treatment. As such, it is economically better to prevent back pain from occurring, rather than treating it after the onset of pain. Some risk factors of back pain which can be monitored to help in the prevention of pain include poor posture and prolonged sedentary behaviour. Inactivity, being similar to prolonged sedentary behaviour, is also a risk factor for some of the major non-communicable diseases responsible for death including heart diseases, stroke, breast and colon cancer, and diabetes.

The aims of the thesis were to: 1) compare a number of commonly used measurement systems, including a low-cost wearable sensor, in their ability to measure motion typically seen in the human spine; 2) develop an activity classification model capable of predicting everyday activities including standing, sitting, lying, and walking; 3) create a new, inexpensive device that can simultaneously track user spine posture/kinematics and activity; and 4) validate the device to have accuracy within ±5° for spine posture, and an average positive activity classification rate of 90% or above.

This research demonstrates the accuracy of a low-cost wearable sensor in its ability to track motion similar to that of the human spine under typical conditions and compare this to more expensive systems. Using two accelerometers and machine learning, a new activity recognition model was created with the ability to track 13 distinct activities commonly used in daily living, being: standing, sitting, prone, supine, right-side, and left-side lying, walking, jogging, jumping, stair ascending, stair descending, walking on an incline, and transitions. From this new knowledge, a new concept inertial-sensor-based device was created with the capabilities of measuring spinal kinematics and whole-body activity tracking. The device has been developed

to measure spinal motions with mean errors of ±2.5°, and therefore meeting the aim to have an accuracy within ±5°, while also showing that the more superior the position on the spine an inertial sensor is placed, the higher the errors in measurement. The device can also predict standing, sitting, lying, and walking with an average accuracy of 95.6%, and therefore above the desired accuracy of 90%. When including all activities, the classifier has an average accuracy of 90.3%.

To reduce the global effect of back pain, the developed device has the capabilities to aid in the prevention, management, and rehabilitation of back pain by focussing on two risk factors: poor posture and inactivity. For use in this research, the definition of a good posture is one that compromises between minimising spinal load and minimise muscle activity, therefore a poor posture is one that doesn't adhere to this requirement which could significantly increase the risk of the onset of back pain. For widespread use, the device created in this research has been developed to be as inexpensive as possible. To meet these goals, the future work of the device has been outlined, including size and cost reduction, as well as increasing the aesthetic appeal, thus making it a more appealing product to the general population.

Contents

List of Figures

List of Tables

Glossary of Abbreviations

Abbreviation	Full Term
3D	Three-dimensional
3DSSPP	3D Static Strength Prediction Program
AR	Axial rotation
AU	Australian
Avg	Average
BA	Bland-Altmann
C	Cervical
C7	Seventh cervical vertebra
CI	Confidence interval
CM	Coupled motion
CRF	Cardiorespiratory fitness
CT	Computed tomography
DALY	Disability-adjusted life years
DOF	Degrees of freedom
DW	Disability weight
$ET_{10\%ROM}$	Percentage of time the IMU errors were within ±10% of the range of motion of the VICON measurements
f	Fast
FE	Flexion-extension
FOI	Frame of interest
FTDI	Future Technology Devices International
GBD 2010	Global Burden of Disease study 2010
GCS	Global coordinate system
GUI	Graphical user interface
ICC	Intraclass correlation coefficients
IMU	Inertial measurement unit
KNN	K-nearest neighbour
L	Lumbar
LB	Lateral bending
LBP	Low back pain
LCS	Local coordinate system
LMM	Lumbar Motion Monitor
m	Medium
Max	Maximum
MET	Metabolic equivalent of task

MRI	Magnetic resonance imaging
PSIS	Posterior superior iliac spine
RMSE	Root-mean-square error
ROM	Range of motion
S	Sacrum
s	Slow
SD	Standard deviation
SMA	Signal magnitude area
SMM	Spinal Motion Measurement device
STA	Soft tissue artefact
SVM	Support vector machine
T	Thoracic
T12	Twelfth thoracic vertebra
US	United States
YLD	Years lived with disability
YLL	Years of life lost

Chapter 1

Introduction

1.1 Motivation

1.1.1 Back Pain

Back pain is one of the most significant ailments in modern society as it is the highest contributor to disability when ranked in terms of years lived with disability (YLD) and sixth highest in terms of disability-adjusted life years (DALYs) [9]. This is evident in the prevalence rates of the disease, with point, year, and lifetime rates of 9.4%, 25-50%, and 60-80% respectively [9-11]. As it is a common disability, back pain equates to the second most leading reason for sick leave from work [12].

The high occurrence of back pain leads it to be a very costly disability to both the suffering individual and the economy. Although it is difficult to obtain an exact figure on how much back pain costs, there have been several studies that have offered an estimate. Walker et al. [13] estimated that in total, low back pain (LBP) cost AU$9.17 billion in Australia in 2003, in which AU$8.15 billion (89% of total costs) were due to indirect costs from productivity loss. In the United States, low back pain is estimated to cost US$100-200 billion annually, where two-thirds of these costs are due to indirect reasons [14].

The detrimental impact that low back pain has gives reason for the prevention of the disability. Although the aetiology of back pain is often multifaceted, with there being numerous risk factors [10, 11, 14-19], when taking preventative measures task related risk factors (e.g., poor posture, prolonged static behaviour, high spinal loads, etc.) have been considered more important [15, 20].

To help with prevention, it is important to measure these task-related risks. Intra-discal pressure measurement offers direct in vivo measurement of spine loads through the use of pressure sensors inserted into the intervertebral discs of the spine and is thus considered to give the most accurate measurement method for these loads [21, 22]. This is required to be performed by a surgeon, can be costly, and leave the patient vulnerable to disc herniation in the future [23, 24]. Therefore, spine load

models are generally used to estimate the loads acting on the spine [25] based on inputs such as kinematics, muscle activation, and anthropometrics. It has also been shown that posture and activity can significantly affect the loads on the spine [10, 26-28]. Therefore, due to the difficulty of measuring spinal loads, as well as loads being affected by spinal posture, spinal kinematics, and activity, this research will not investigate spinal loads directly. Rather, this research will primarily focus on spinal posture and kinematics, and prolonged sedentary behaviour as the risk factors of interest for back pain.

1.1.2 Inactivity and Prolonged Sedentary Behaviour

Inactivity has a significant effect on the number of premature deaths and was responsible for 5.3 million, or approximately 9%, of all premature deaths worldwide in 2008 [29], being the fourth leading contributor to death [30]. This is due to inactivity being a risk factor for, and causing 6-10% of cases of, numerous non-communicable diseases, including: coronary heart disease, stroke, type II diabetes, and breast and colon cancer [29].

The classifications of prolonged sedentary behaviour and inactivity are related but slightly different. Prolonged sedentary behaviour is the event in which an individual remains performing sedentary activity (lying, sitting, etc.), or activities that do not increase energy expenditure substantially above resting level, for an extended period of time whereas inactivity is when an individual performs an inadequate level of activity, and therefore has a low energy expenditure [31, 32]. An example of the difference between these two is when an individual performs frequent bouts of activity but for a small amount of time. The individual will, therefore, have low energy expenditure and thus exhibit inactivity, but not prolonged sedentary behaviour due to the frequency of activity.

Although prolonged sedentary behaviour has been identified as a risk factor for back pain, inactivity can also have a great impact on an individual's health as it is

a risk factor for numerous non-communicable diseases. Inactivity, like prolonged sedentary behaviour, requires some form of activity monitoring for it to be quantified. Therefore, this research focussed on both inactivity and prolonged sedentary behaviour as important metrics for assessing back pain risk.

1.2 Background

Towards the measurement of poor posture, prolonged sedentary behaviour, and inactivity, there are numerous options available for measuring spinal posture and kinematics in a laboratory or clinical setting. These options include radiography, optical motion capture, inertial sensors, electro-goniometers, electromagnetic tracking systems, and others. More clinically accurate methods, such as radiography and optical motion capture have a restricted capture volume and are therefore not capable of tracking posture throughout daily living. Commercially available posture trackers therefore generally make use of wearable inertial sensors. Such devices include the ViMove (DorsaVi, Melbourne, Australia), Lumo Lift (Lumo Bodytech Inc., Palo Alto, United States), Upright Pro and Upright Go (UpRightTechnologies Ltd., Tel Aviv, Israel), and Alex (NAMU Inc., Seoul, Korea). These types of devices provide long-term, real-time measures of spinal posture and bio-feedback to the user when poor posture is maintained, in which bio-feedback has been shown to have positive effects in the past [33]. The issue with the majority of these devices is no spinal kinematic output (orientation, angular velocity, etc.) can be received, with exception to the ViMove device. The ViMove, however, is very expensive compared to the other devices, with an upfront cost of AU$2000 and a monthly subscription of AU$149.

For tracking of prolonged sedentary behaviour and inactivity, long-term activity classification can be used. This allows for comparisons between the activity levels of the individual and healthy activity levels. For the classification of activity, video capture is the gold standard as this method offers the highest accuracy and has been used in previous studies [34-36]. The process of using video capture for manual activity classification, however, is very time consuming and has a limited capture volume in which activities must be performed. Therefore, other methods are commonly used for the classification of activity, one being the use of accelerometry [36-44]. Although this method can have lower accuracy than video analysis, it does allow for the activities of interest to be performed in an unlimited volume and has faster processing times.

In previous research, activity classifiers of daily living have used accelerometers and other sensors to predict user activity using predefined thresholds or machine learning [36-42, 44, 45]. These activity classifiers can use raw acceleration data, as well as the gravitational (low-pass filtered raw data) and bodily motion components (high-pass filtered raw data) to calculate various parameters on acceleration used to predict activity [36, 37, 39, 44]. Such parameters can include mean acceleration, the standard deviation of acceleration, maximum amplitude, minimum-to-maximum range, tilt angle, and energy expenditure.

Of interest for this research, are basic static and dynamic activities which can be used to define sedentary and active times. These activities include standing, sitting, lying, walking, jogging, jumping, stair ascending, stair descending, incline walking, and transitions. The accuracy of previously reported classifiers in static activities is generally high, with ranges of 81.3% to 91.9% for standing, 84.1% to 95.0% for sitting, 94.0% to 99.4% for lying. The accuracy for dynamic activities, however, is normally lower, with ranges of 70.3% to 95.9% for walking, 76.8% to 98.3% for jogging/running, 61.5% to 71.0% for stair ascending, and 44.3% to 69.6% for stair descending [36, 37, 40, 41]. Jumping and walking on an incline have high respective energy expenditure [46-48], however, to the best of the authors knowledge, these activities have not been included in an activity classifier using accelerometer data previously.

1.3 Aims

Back pain is very common, and it is expensive to treat, and therefore research should be performed to aid in the prevention of back pain. Two major risk factors for back pain, which can also be monitored on a day-to-day basis to help in prevention, are poor posture and prolonged sedentary behaviour. Therefore, the goal of this research is to develop a device which can monitor user spinal kinematics and classify activity such that poor posture, prolonged sedentary behaviour, and inactivity can all be monitored. The aims of the thesis are to:

1. Compare a number of commonly used spinal kinematic measurement systems, including a low-cost (<AU$1000) wearable sensor, in their ability to measure motion typically seen in the human spine.

2. Develop an activity classification model capable of predicting everyday activities including standing, sitting, lying, and walking. Extending from this set of activities, it is beneficial to include other commonly used activities of daily living, including jogging, stair ascending and descending, jumping, walking on an incline, and transitions.

3. Create a new, inexpensive (<AU$1000) device with the ability to simultaneously track user spine posture/kinematics and activity. This device should be highly portable, and therefore consist of wearable sensors such that it can be worn during activities of daily living.

4. Validate the device to have accuracy within ±5° for spine kinematics. This accuracy range (±5°) was selected such that it had similar accuracies to previous posture trackers [49] and was within the 10% range of motion threshold used to test clinical significance [50].

5. Validate the device to have an average positive activity classification rate of 90% or above for standing, sitting, lying, and walking. Extending this aim is to achieve an average classification rate of at least 90% for all activities the created classifier can predict.

1.4 Significance and Contribution

Continued research into the measurement of various risk factors for back pain, including poor posture and prolonged sedentary behaviour, will aid in the reduction of the number of occurrences of the disorder. This research has contributed in a number of ways.

Firstly, this research has also contributed by comparing the accuracy of low-cost wearable inertial sensors, to more expensive wearable sensors and optical motion capture, a commonly used measurement system in human kinematics.

This research has also contributed by creating a new activity classifier which can classify 13 distinct activities, including standing; sitting; prone, supine, right-side, and left-side lying; walking; jogging; stair ascending and descending; jumping; walking on an incline; and transitions between activities. This activity classifier is the first model with the capabilities to predict jumping and incline walking, and to include all other activities within the same model with accuracies that match or exceed previous activity classifiers. This has significance as it gives researchers a tool to track activity to a higher resolution using accelerometry and therefore broadening the motions that can be used during experimentation. The activity classifier also demonstrates the use of machine learning in the classification of activity and biomechanics, as was the method used to create the classifier.

Finally, a new inexpensive device, called the Spinal Motion Measurement device (SMM), has been developed to be a measurement tool to track both spinal kinematics and activity of the user for long-term use. The development of this tool has a contribution to both researchers and the general population. For researchers, it is a device that can be used for long-term tracking of spinal kinematics and whole-body activity for patients with and without back pain and other conditions of interest. Due to the device being inexpensive it allows for many devices to be built and used simultaneously, thus permitting the time spent on data collection in studies to be kept to a minimum. This is particularly useful in long-term studies where patients may have their spinal kinematics and activity tracked for weeks. Thus, by monitoring a

greater number of participants simultaneously due to the inexpensive nature of the device, the researchers can save a lot of time and effort during data collection. For Ph.D. researchers and masters students, who often have little funding, it gives them the opportunity to minimise costs for equipment that they may require.

For the general population, this research develops a new concept device that a user can wear to track numerous risk factors for back pain and other non-communicable diseases. Although not finalised for commercial use, this research has provided the fundamental foundations for the device to be usable for the general population. With the recommended future work undertaken, including further reduction of price, removal of cables, and software development, the device will be more suited to the general population.

1.5 Thesis Outline

The focus of the thesis is primarily based on the conceptual design and implementation of a novel device for measuring user spinal kinematics and whole-body activity. This includes research concerned with sensor and component selection for the device, the creation of an activity classifier, the assembly of the components, developing software for this application, and the validation of the device in the measurement of spinal kinematics and activity classification. What is not included within the scope of this project is a large-scale validation of the device to reduce the incidence of back pain and other non-communicable diseases or developing the device to be a commercial product beyond keeping the off-the-shelf parts inexpensive. For example, no significant work has been put into making the device aesthetically appealing or in developing easy to use software specific to the device. The definition of a good posture in this thesis is one that compromises between minimising spinal load and minimise muscle activity, therefore a poor posture is one that doesn't adhere to this requirement which could significantly increase the risk of the onset of back pain. Numerous commercial devices define a poor posture when a certain pre-define threshold on spine angle is reached [51-54]. It should be noted that the development of a pre-defined threshold for poor posture is outside the scope of this research. These thresholds, however, could be adopted from previous studies such as that performed by Marras, et al (2010) [55] which describes the thresholds for numerous continuous variables, including trunk angle and the risk associated with them.

This thesis outlines the design and validation of a novel tool to assess physical risk factors associated with back pain. Therefore, a significant literature review into back pain has been completed and is detailed in Chapter 2. In this chapter, information is outlined on the human back; including regions of the spine, bones, muscles, and movement, as well as the prevalence of back pain, the effects it has on the suffering individual and society, and the risk factors for back pain. A review is then given on two of the major risk factors, which are also able to be measured to aid in the prevention of back pain, include poor posture and prolonged sedentary behaviour.

Inactivity, being similar to prolonged sedentary behaviour, is also a risk factor for numerous other health issues. Therefore, a background is given on some of the major diseases that inactivity can affect. Finally, in Chapter 2, the gaps in the literature are given which were used to help form the area of investigation in this research.

Chapter 3 relates to the first aim of this research and is the preliminary investigation into measuring spinal kinematics. This chapter involves comparing numerous measurement systems in their ability to measure the range of motion (ROM) and absolute orientation during random motion of a highly repeatable Katana robot arm. From this analysis, it was found that the SparkFun Razor inertial measurement unit (IMU) was a suitable, inexpensive device to measure motions that simulate normal spinal kinematics.

Chapter 4 relates to the second and fifth aim of this research by detailing the method used to create a new activity classification model, as well as the methods used, and results obtained in the validation of the classifier. In this chapter, a comparison of various machine learning algorithms and filter designs is performed. From these comparisons, the best performing activity classification model, based on accuracy and prediction speed, was chosen for further analysis.

Based on the information and new knowledge obtained in Chapters 2, 3, and 4, it was possible to design and build a new concept device, the Spinal Motion Measurement device (SMM). This device was designed with the capabilities to measure spinal posture and kinematics, as well as classify the activity of the user and thus answering aim three of this research. Chapter 5, therefore, details the hardware design of this device and the software required to obtain raw data, including: three-dimensional orientation and angular velocities of the IMUs, and three-dimensional accelerations of the accelerometers, where the IMUs and accelerometers are the sensors included within the SMM.

Chapter 6 refers to the fourth aim of this research and thus discusses the experiment used in the validation of the spinal kinematics measurement aspect of the SMM on human participants. This SMM is validated in its ability to measure spinal kinematics using a VICON MX Vantage V8 (Vicon Motion Systems Ltd., Oxford,

United Kingdom) motion capture system as the reference system. This chapter provides a comparison of the accuracy of the SMM at various levels of the spine, during different speeds of motion, and different motion planes.

Finally, Chapter 7 concludes the research by giving an overall summary of the work performed and how it pertained to the aims of the research conducted. Included in Chapter 7 are limitations of this current research and some suggested future work to overcome these.

Chapter 2

Literature Review

The narrative literature review presented in this chapter gives a discussion on various aspects of back pain. A brief introduction is given on the anatomy of the human back, including the various spinal regions and their respective degree of motion. Then, a discussion on back pain, including its prevalence rates, the effects it has on suffering individuals and society, and the risk factors that increase the likelihood of back pain occurring. Of the identified risk factors, task-related risk factors, including poor posture and prolonged sedentary behaviour, are considered more important in designing for preventative measures. Therefore, an in-depth discussion is given on the measurement of spinal kinematics, and the classification of human activity. Inactivity, which is similar to prolonged sedentary behaviour, is also discussed in the literature review. The discussion of inactivity includes its impact globally on mortality rates and on various non-communicable diseases, as well as previous research performed into the classification of human activity. This chapter is concluded by a summary and a list of gaps in previous research.

2.1 The Human Back

The human back consists of: the bones that form the spine, muscles, nerves, ligaments, tendons, and intervertebral discs. The spine is a curved linkage of 33 individual vertebrae bones that form the vertebral column, which has the function to allow support, protect the spinal cord, and provide muscle attachment to allow movement. The vertebral column is split up into five distinct sections; the cervical (neck), thoracic (upper back), lumbar (lower back), sacrum, and coccyx (Figure 2.1 (a)). Only the cervical, thoracic and lumbar regions allow movement [5] and consist of seven, twelve, and five vertebrae respectively.

The spinal muscles are used to provide movement, stability, and to maintain good posture, where a good posture is one that compromises between minimising spinal load and minimise muscle activity. The major muscles associated with movement and stabilisation of the neck are the upper trapezius and sternocleidomastoid muscles. The muscles that are predominately responsible for maintaining posture in the lumbosacral area include the erector spinae, rectus

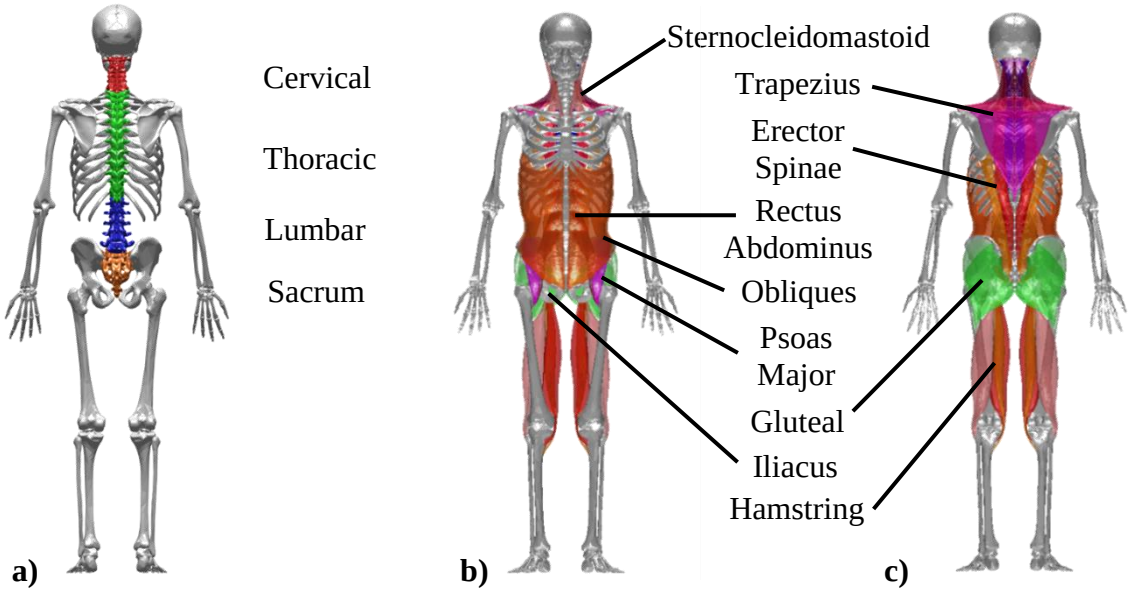

Figure 2.1 a) shows the cervical (red), thoracic (green), lumbar (blue), and sacrum (orange) regions of the spine, and b) Anterior view & c) posterior view of the major muscles responsible for stabilisation and movement of the spine where the psoas major is in front of the iliacus. (Source: [7, 8])

abdominus, internal and external obliques, psoas major, iliacus, gluteal, and hamstring muscles [5] (Figure 2.1).

Global ranges of motion for the cervical, thoracic and lumbar regions have been studied previously [1-6], with normal values shown in Table 2.1. Translation between adjacent vertebrae is relatively small, with the typical translation in the lumbar region being approximately 1-3 mm depending on the vertebral level [3, 4].

Due to the limited movement of the thoracic region, it is uncommon to experience pain in this area [56]. Pain in the cervical and lumbar regions are, however, a very common condition, and can be due to numerous causes which include: disc degeneration and herniation, nerve impingement, muscle strain and spasms, osteoarthritis and many others. However, many suffering individuals back pain is idiopathic. Back problems may also cause pain to radiate through the limbs, known as radiculopathy, which is due to the compression of nerves [57, 58]. Within the lumbar region, the two lowest vertebral joints labelled L4-L5 and L5-S1 carry the most load and are therefore the most prone to injury [57].

Table 2.1 Typical number of vertebrae, the total range of motion, and mean range of motion between adjacent vertebrae for the cervical, thoracic and lumbar regions of the spine. (Source: [1-6])

Region	Number of Vertebrae	Flexion-Extension (°)		Lateral Bending (°)		Axial Rotation (°)	
		Total	Mean	Total	Mean	Total	Mean
Cervical	7	45 - 58	6.4 - 8.3	32 - 47	4.6 - 6.7	63 - 78	9 - 11.1
Thoracic	12	37 - 44	3.1 - 3.7	25 - 27.5	2.1 - 2.3	41 - 53	3.4 - 4.4
Lumbar	5	83 - 102	16.6 - 20.4	20 - 35	4.0 - 7.0	25 - 40	5.0 - 8.0
Total	24	165 - 204	6.9 – 8.5	77 – 109.5	3.2 – 4.6	129 - 171	5.4 – 7.1

2.2 Back Pain

2.2.1 Prevalence of Back pain

When discussing the prevalence of disease, terminology including point, one-year, and lifetime prevalence rates, as well as years lived with disability (YLDs), are commonly used. Point, one-year, and lifetime prevalence rates for a disease are the percentage of the population that suffer from that disease at any given point in time, at least once during a given year, or at least once in their lifetime respectively. YLDs are calculated as the total cumulative time in which the population suffers from a disease. Disability-adjusted life years (DALYs) is also frequently used and is the sum of YLDs and years of life lost (YLL), or mortality before life-expectancy, due to the disease [59].

Low back pain has point, one-year, and lifetime prevalence rates of 9.4% [9], 25-50% and 60-80% respectively [10, 11]. Low back pain is also the second most reported reason for sick leave, and a leading cause for activity limitation [12]. Low back pain has been ranked as the largest contributor to global disability when expressed in YLDs, and sixth highest in terms of an overall burden when measured in DALYs [9]. In Australasia and Western Europe, it was the highest contributor to the overall burden. In the years between 1990 and 2010, DALYs due to LBP increased from 58.2 million to 83 million years, a 24.8 million rise. The majority of this increase was due to the increase in world population, however, 7.5 million years of the increase in DALYs was due to the ageing population [9]. This shows that as the world population and life expectancy increases, so will the issue of back pain in society.

2.2.2 The Effects of Back Pain on the Individual

Disability weights (DWs) reflect the severity of a disease and is given as a score between 0 (equal to full health) to 1 (equal to death). Five major musculoskeletal conditions were highlighted as being most likely to contribute the largest proportion of musculoskeletal burden in *The Global Burden of Disease Study 2010* (GBD 2010)[1]. These conditions were low back pain, neck pain, osteoarthritis (hip and knee), rheumatoid arthritis, and gout. Of these five conditions, only severe rheumatoid arthritis (DW = 0.606) had a higher disability weight than LBP (DW = 0.269 to 0.374) depending on the type of LBP (acute with/without leg pain, chronic with/without leg pain) [61]. People with severe rheumatoid arthritis and severe polyarticular gout are described to have severe and constant pain, and deformity in most joints, all of which can cause difficulty moving around, using the hands, and performing normal tasks of daily living. Suffering individuals can also often feel sadness, anxiety, and extreme fatigue [61].

Although not as serious as severe rheumatoid arthritis, LBP is a disability that can affect people of all ages. The effects of LBP on the individual are varied depending on the type of pain. LBP is commonly divided into acute or chronic, and specific or non-specific pain. Acute LBP occurs suddenly and lasts no more than four to twelve weeks, whereas chronic LBP lasts longer than 12 weeks [62]. Non-specific LBP is defined as LBP not attributable to a known specific pathology, whereas specific back pain is [63]. Nonetheless, common effects of LBP include severe pain, activity limitation, work days missed, poor sleep, and sufferers can have worried feelings [10, 61, 64-66], and hence LBP can also affect mental health. Individuals suffering from chronic back pain report their pain as a disability and suffer from loss of sleep or pain while asleep, loss of mobility and independence, as well as participating in less leisure

[1] The Global Burden of Disease Study 2010 (GBD 2010) is a series of papers published in *The Lancet* (2012 Dec 13; 380) from the work performed from a collaboration of seven institutions: the Institute for Health Metrics and Evaluation (IHME), the University of Queensland School of Population Health, Harvard School of Public Health, the John Hopkins Bloomberg School of Public Health, the University of Tokyo, Imperial College London, and the World Health Organization (WHO). In total, GBD 2010 had 488 co-authors from 303 institutions (Source: [60]).

and everyday activities, all of which can cause great distress and for suffering individuals to lose some enjoyment in life [61, 64].

2.2.3 The Effects of Back Pain on Society

Back pain has a large effect on the economy due to its high prevalence rates [10, 11], resulting in many work days missed. Although a precise figure is difficult to obtain due to numerous different estimations found [10, 13, 14], the high incidence rate of LBP causes large financial costs globally. In 2001 alone, it was estimated that the direct cost of LBP in Australia was AU$1.02 billion. Direct costs arise from the amount spent on interventions required for diagnosis, treatment and rehabilitation. Indirect costs for Australia in 2001 amassed AU$8.15 billion, and arise due to productivity loss caused by the disease [13]. This gives a total cost of LBP to be AU$9.17 billion in a single year, where indirect costs counted for 89% of these expenses. In the United States LBP is estimated to cost US$100-200 billion each year, with two-thirds of this price due to decreased wages and productivity [14]. These costs show that LBP is not just a burden for the affected individual but on the community as well. Workplaces are affected by the loss of productivity, costs associated with workers compensation, and the time and costs required for training new staff to compensate for the suffering individual's absence. These figures show that indirect costs far exceed direct costs, and thus the importance of addressing the disease before pain is experienced and thus reducing indirect costs. This could be accomplished either through pre-emptive treatment or use of medical devices to alert the user when they are at risk of back pain occurring, thus encouraging them to alter their posture and behaviour to reduce risk.

2.2.4 Risk Factors for Back Pain

For many suffering individuals, their back pain is idiopathic (non-specific), meaning their pain is not attributable to a known specific pathology [63]. However, there are numerous physical and psychological risk factors that increase the likelihood of back pain occurring [10, 11, 14-19], with over 100 identified possible risk factors. It is possible to manipulate exposure to physical risk factors associated with the onset of back pain [55] in order to reduce their influence on back pain [67]. This may be achieved by either altering a motion or technique, or a change of lifestyle depending on the likely source of pain. Commonly reported risk factors for back pain include, but are not limited to: poor posture, prolonged sedentary behaviour, high and low (instability) spinal load, age, height, sex, obesity, occupation, smoking, depressive and anxious moods, belief that back pain will occur, somatization tendency, individual, and organisational factors.

Of these risk factors discussed, poor posture, high spinal load, and, although some studies do not support the opinion that sitting at work is associated with LBP [68], prolonged sedentary behaviour have been frequently the focus of addressing back pain as these are considered more important when designing preventative measures [15]. Although *in vivo* spinal loads can be measured through intra-discal pressure measurements [21, 22], it is unethical as it is invasive, requires surgical intervention, costly, and can cause permanent herniation [23, 24]. Alternatively, the spinal load can be estimated using biomechanical models [16, 23, 69-76] or software such as the 3D Static Strength Prediction Program (3DSSPP) [77], Anybody Modelling System (AnyBody Technology, Aalborg, Denmark) and OpenSim (NCSRR, Stanford University, CA, USA). However, these can be inaccurate, have low practicality, are only validated for a set number of activities, or require specialised software and training [25, 74, 78, 79]. For this research, poor posture and prolonged sedentary behaviour are the main focus in terms of these risk factors and the development of biomechanical model to estimate spinal loads is outside the scope of this thesis.

Awkward static and dynamic working postures have been linked as a possible cause of back pain and are one the most commonly reported risk factors for back pain [14]. This is due to the type of work being performed, and how it is being completed with different types of workplaces influencing back and neck pain differently [80]. For example, academic staff and office workers have been shown to be at higher risk of neck pain which may be a result of extended periods of sitting and posture used [81, 82], where labourers are also at heightened risk when lifting with poor posture [10]. It has been theorised that poor posture, particularly during excessive forward flexion and/or axial rotation, exposes the spine to large compressive forces [10, 26-28] which has the potential to cause inflammation, nerve impingement, muscles fatigue, and structural damage to the vertebrae and intervertebral discs [10, 14, 83].

2.3 Measuring Spine Posture

2.3.1 Introduction to the Measurement of Spinal Posture

There are many methods used to measure the posture of an individual, in which these can generally be broken down into laboratory/clinical measurements, and real-world measurements.

Laboratory/clinical measurements are generally performed by a researcher or clinician in a laboratory or at a clinic on an individual. These measurements use highly accurate technologies and methods so clear conclusions can be made from the data. However, these devices can be highly expensive and not suitable for use outside the laboratory/clinic due to not being portable or requiring the researcher/clinician to take the measurement.

Real-world measurements of an individual's spinal posture are those taken while performing their everyday life with no restrictions in place. These measurements are usually performed using wearable sensors, which have lower accuracy and reliability than those used in laboratories and clinics but also have a lower price.

On top of accuracy and reliability of measurements and cost, there are numerous other significant characteristics that should be considered when measuring spinal posture. The spine is a complex structure consisting of many bones and joints, each of which can move in six degrees of freedom (DOF) (3× translational and 3× rotational). However, as translation is generally small, it is of greater importance that sensors measure the three rotational DOF. It is also important that sensors are able to obtain data in dynamic scenarios due to the large motion of the spine, and because the spinal loads can increase in such conditions [72]. Back pain can occur numerous environments; hence it is significant that the sensors allow for measurement in various locations and therefore need to allow portable and unrestricted data collection. Also,

having low invasiveness is vital so as not to cause harm to any users and to be ethically appropriate.

2.3.2 Laboratory & Clinical Measurements

There are numerous systems used in laboratory and clinical settings that measure an individual's posture. This section will give details on the more commonly used devices. Although devices such as tape measures and goniometers can be used to assess an individual's posture, these will not be discussed here as they require manual readings and are less advanced than other technologies.

Radiography

Radiography techniques, such as X-ray, Magnetic Resonance Imaging (MRI), and Computed Tomography (CT) scans, are considered the gold standard for measuring spinal posture due to their high accuracy. However, these radiography techniques also have numerous limitations.

Radiography is a commonly used method for identifying spine biomechanics and has been used in several studies [3, 84-86]. X-Ray analysis of ROM is highly accurate and reliable [87], with Pearcy (1984) using an X-Ray system with root mean square errors (RMSE) of 2 mm in translation and 1.5° in rotation. X-Ray analysis, however, is more accurate when using computerized image processing methods [84] and bi-planar radiography allows for 3D measurement of individual vertebrae [5].

The major limitation of radiography is that it is an invasive method [88, 89] as participants and patients are exposed to unnecessary radiation which raises ethical concerns [3]. Many radiography systems available also only allow static analysis to be performed, however, some techniques such as fluoroscopy and cineradiography allow for dynamic analysis of movement. Most of these systems are also very costly and require a licensed professional for operation [90]. It is due to the limitations of radiography, especially the exposure to radiation, that other techniques for measuring

spinal position and motion should be used in non-clinical applications such as estimating risk factors for back pain.

Optical Motion Capture

Optical motion capture is a common method used to analyse movement in a clinical or laboratory setting [91, 92]. These systems allow for accurate absolute and relative kinematic measurements of 3D dynamic movements [93] and are thus also considered a 'gold standard'. There are many optical motion capture systems available that have a variety of important characteristics including sampling frequency, marker identification process, processing time, accuracy, reliability, and cost [94].

Most optical motion capture systems have a sampling rate of at least 50 Hz but can exceed 200 Hz [93], which is adequate for capturing and analysing most human movement activities. Motion capture systems generally have a high accuracy of about 1 mm, but can be in the order of 0.1mm within a three-metre field of view according to the manufacturer's specifications [95]. One study [96] found the difference in accuracy and reliability between three optical motion capture systems: a new low cost optical tracker system (OptiTrack 3D, 2011, ~$8,000) (NaturalPoint, Inc. Corvallis, US), a new expensive system (VICON MX, 2010, ~$400,000), and an old expensive system (VICON 612, 1993, ~$240,000) (Vicon Motion Systems Ltd. UK). The largest difference in mean vector length data between OptiTrack and VICON MX was 2.2%, and for VICON 612 and VICON MX was 2.1%. In terms of repeatability, the coefficient of variation for the OptiTrack 3D, VICON 612 and VICON MX were 2.3%, 2.5%, and 0.3% respectively. This shows that the accuracy and repeatability of the new, expensive system were greater than the others.

The errors are increased when human kinematic trials are performed. When performing optical motion analysis, it is desired to measure skeletal kinematics. However, one of the most common methods is to place the optical sensors on the skin [97, 98]. The intention however is to measure the motion of the underlying bone. Therefore, markers are placed over known anatomical landmarks to construct and track body segments. Errors arise from this method via Soft tissue artefacts (STA),

which is the error introduced to optical motion analysis data due to the undesired movement of the skin, and hence skin markers, relative to the bone due to several musculoskeletal components (e.g. skin, muscle, adipose tissue). This can have a major effect on the results by reducing accuracy and reliability, particularly in the frontal and transverse planes [99]. The error can be reduced significantly using intra-cortical bone pins which fixate markers directly to the bone through incisions in the skin. However, this technique is invasive [100] and set-up is time-consuming and must be performed by a surgeon.

Limitations of optical motion capture systems are they are expensive, only allow movements in a restricted volume/environments thus only useful in a clinical or laboratory setting, and markers can be obscured leading to missing data points [101]. Optical motion capture systems are also computationally expensive [93] and marker identification and overall processing time can be extensive [102]. However, some new optical motion capture software systems such as the VICON Blade (VICON Motion Capture Systems Ltd., UK) allow for real-time results to be obtained.

Inertial Sensors

Accelerometers have been highlighted as possible sensors to measure spine orientation and motion, and have been used in a number of studies [89, 102] with static posture accuracies generally within 5°. However, accuracy and reliability were much lower in dynamic scenarios. Thus, it was recommended to combine accelerometer and gyroscope measurements to obtain more data and thus minimise dynamic error by combing the sensor signals.

Inertial Measurement Units are the combination of accelerometers and gyroscopes, typically both tri-axial used to measure linear and angular motion [103, 104]. Sometimes extra sensors such as magnetometers [105, 106] can be incorporated in IMUs to compensate for orientation drift. Separately, gyroscopes can estimate orientation through the integration of measured angular velocity but suffer from drift error in orientation results. Accelerometers and magnetometers have no drift effects, however, magnetometers have large short-term signal noise issues [107]. Hence to

obtain accurate and reliable results, IMUs typically use Kalman filters to fuse signals from gyroscopes with accelerometers and magnetometers to provide the minimum error in the orientation results [107]. The minimisation of error is performed with the knowledge that errors related to different sensors will have different spectral properties.

Inertial measurement units have varying accuracy and reliability depending on the quality and intended application of the sensor, but they can have specifications suited for posture tracking. There are many IMUs that have static and dynamic accuracies of ±0.5 to 1.0° and ±2.0 to 3.0° respectively [108-110] with prices being AU$2900 to AU$6250 [108, 111] showing that spinal tracking systems using three such IMUs could easily exceed AU$20,000.

A study focussing on the inter- and intra-tester reliability when measuring spinal orientation in the sagittal plane using the ADIS 16364 IMU [80] showed that intra-class correlation coefficients for intra- and inter-testing reliability were between 0.37-0.9 and 0.18-0.76 respectively depending on the type of movement or posture. These results show that not all positions and movements of the spine can be reliably obtained using IMUs. Increasing the experience of the tester, especially in identifying anatomical landmarks, can increase the reliability of the results obtained from IMUs [80]. In the study performed by Goodvin et al. (2006), when the IMU system was verified against a VICON optical motion analysis system, it was found that there was a maximum of 3.1° of error in the results of the IMU system for regional spinal motion [104].

The major disadvantages of IMUs are the cost, and accuracy and reliability when used in human kinematic trials. This is affected by factors such as the experience of the tester, the method of attachment, and the size of the sensor [80]. While IMUs are able to measure in 3D, when applied to the spine researchers have had varying success in reliably measuring the angular orientation of the spine [112]. A further disadvantage of IMUs is their price. IMUs can cost AU$6250 [111] but can be less for lower quality devices. An example of a lower quality IMU is the SparkFun 9DOF

Razor IMU (SparkFun, Niwot, United States) which costs approximately AU$105 [113].

Electro-Goniometer

An electro-goniometer is a tool used to measure joint orientation and allows for dynamic movement measurements to be taken in a time efficient manner, with real-time results available [93]. There are numerous types of electro-goniometers, including potentiometric and flexible electro-goniometers.

The Lumbar Motion Monitor (LMM) is a commonly used device that uses potentiometric electro-goniometers to instantaneously measure three-dimensional angular position, velocity and acceleration of the lumbar vertebrae [90, 106, 114]. When measured on a three-dimensional reference frame, this device has been found to have average deviations during dynamic movements of 0.47°, 1.71° and 0.50° for single planar movement in the sagittal, frontal and transverse planes respectively. For two dimensional coupled movement, the device was found to have average deviations of 1.13° and 1.71° in the sagittal and frontal planes respectively when coupled with transverse plane motions [114]. Thus, it has been shown to be as accurate as other clinical devices. This device, however, is very expensive, with costs exceeding US$30,000, and requires training to use [112].

The OSI CA 6000 Spine Motion Analyser is another electro-goniometer device which measures three-dimensional regional spinal movements using six potentiometers. The Spine Motion Analyser is able to record motion throughout an entire movement, however, its sampling rate is only 10 Hz [115], hence rapid motions cannot be analysed thoroughly. The intra- and inter-tester ICCs have been found to be high for all motions except flexion in human participants with and without neck pain. Intra-tester ICCs for participants with and without neck pain were all greater than 0.87 (except flexion was 0.68) and all greater than 0.85 (except flexion was 0.76) respectively. All the inter-tester ICCs for the Spine Motion Analyser were greater than 0.88 [115]. In the same study, the standard error of measurement in all planes was 3.92° or lower, being the greatest in flexion. Another study measured the difference in

obtained ROM between the Spine Motion Analyser and radiographs. The average difference in results for flexion, extension, left and right lateral bending was 13°, -2.1°, 6.2°, and 6.3° respectively [116].

Flexible electro-goniometers are generally more expensive than potentiometric electro-goniometers, however, they offer several advantages, while Flexible electro-goniometers also adapt better to the body and are not sensitive to misalignments with respect to joint axes [117, 118]. The accuracy and reliability of flexible electro-goniometers have been studied and it was found that they generally had a mean square error of less than ±3° for single plane motions, except in rotation where the error was reported to be 5° to 7° [119]. Although a price could not be obtained for this specific product used this study [119], the successor, the SG-Series (Biometrics ltd., Newport, UK), has been priced at approximately £500 (AU$920, US$710) [120].

In general, electro-goniometers are hindered by a limited range of motion due to cable connection or telemetry [106]. Electro-goniometers also have a number of other potential disadvantages, with a major one being the inability to measure absolute position or orientation with respect to a global co-ordinate system [93].

Electromagnetic Tracking Systems

Electromagnetic tracking systems allow for absolute and relative translational and orientation data to be obtained in all three dimensions. The ability of these systems to give real-time results while also having low computational costs, no line of sight problems, relatively inexpensive, and relatively small set-up time are all advantages electromagnetic tracking systems [93, 121]. Low sampling rates of electromagnetic tracking systems as compared to other types of systems mean they are not suited for rapid movements, being a major disadvantage. The field distortion caused by ferrous and conductive metals in the measurement volume can affect result accuracy and reliability, hence being another limitation of such systems [93, 95], as well as small measurement volumes [102].

Several electromagnetic tracking system devices, including the 3SPACE FASTRAK System and Liberty (Polhemus Inc., Colchester, USA), and Flock of Birds

(Ascension Technology Corp., Burlington, USA) have been used in previous biomechanical studies [121-129]. At a range of 30 inches (0.76m) the 3SPACE FASTRAK and Liberty have static accuracies of 0.03 inches (0.76mm) in translation and 0.15° in rotation according to manufacturer specifications [130, 131]. At a similar distance, the Flock of Birds device has a static accuracy of 0.07 inches (1.8mm) in translation and 0.5° in rotation [132]. However, these accuracies decline as the range increases [130, 131] which is also apparent with other electromagnetic tracking systems. In a study performed by Schuler et al. [133] using an Aurora electromagnetic tracking system (Northern Digital Inc., Waterloo, Ontario, Canada), the average static translational error was found to be 0.1±0.04mm, 0.2±0.17mm and 0.8±0.81mm when sensors were 50mm, 300mm and 500mm away from the field generator respectively. Average rotational errors for the same distances were found to be 0.4 ± 0.31°, 0.4 ± 0.21° and 0.9 ± 0.85° respectively. In a study by Mills et al. [121] using the Liberty system, they found that accuracy and reliability of results decreased in dynamic trials, becoming less reliable the faster the motion with a range of error up to 13mm.

The results of all studies discussed shows that the accuracy and reliability of electromagnetic tracking systems can be high when applied to static situations but can drop significantly when used in dynamic trials and when the distance between sensor and field generator increases. Having a limited capture volume is thus a major limitation of electromagnetic motion tracking systems [121].

Table 2.2 shows a summary of the laboratory and clinical based devices used to measure spinal posture in a number of key performance indicators. Cost has been omitted from this table as it can be appreciated that price ranges will alter for various brands and quality of the various equipment types. However, it can be seen that the cost for these clinical measurement devices can exceed AU$1000 for electro-goniometers, and much greater for other system (e.g. AU$400,000 for VICON MX), when measuring three-dimensional spinal kinematics.

Table 2.2 Key performance indicators of various kinematic measurement systems used in clinical and laboratory settings.

Device/ Method	Radiography	Optical Motion Capture	Inertial Sensors	Electro-goniometer	Electromagnetic Tracking Systems
Equipment	X-ray, Magnetic Resonance Imaging, Computed Tomography	Receiver unit (including 2 or more cameras), Retro-reflective markers	Accelerometers, gyroscopes, Inertial Measurement Units	Potentiometric, flexible	Magnetic field generator, sensor/receiver unit, control unit
Accuracy	1.5°	<1mm	1 - 3°	Various, but all studies discussed showed <13°	0.3 – 0.9°
Portable	No	No	Yes	Yes	No
Invasive	Yes	Minimal	Minimal	Minimal	Minimal
Advantages	High accuracy, gold standard	High accuracy, gold standard	Portability, wearable	Wearable	Low cost and computational time, no line of sight issues
Limitations	Invasive, radiation exposure	Soft tissue artefact, restricted volume/ environment	Reduced accuracy, prone to errors from ferrous metals	Limited range, inability to measure absolute orientation	Low sampling rates, small capture volume and prone to errors from ferrous metals

2.3.3 Real World Measurements

In the real world, devices used to measure spinal posture primarily must allow for portable, unrestricted measurements to be made. These devices are therefore commonly worn on the body such that they 'follow' the wearer during their normal activities of daily living while simultaneously collecting data. These devices are thus commonly termed wearable sensors or devices.

Wearable devices have seen an increase in popularity and development due to the advancement of sensor technology [134-137]. Wearable sensors have been used in

applications such as vital sign measurement, disease diagnosis, and activity monitoring [42, 134, 136, 138-140], as well as in the measurement of posture.

There are several commercially available wearable devices that track the posture of the user and give an alert (e.g., vibration, text message, etc.) to the user when their posture becomes 'poor' as defined by a predefined threshold in the device, to reduce the risk of the onset of back pain. This method of using sensors to give feedback on their body (in this instance, their posture) is termed bio-feedback and has been shown to have positive effects in the past [33].

Commercially available devices commonly use an inertial sensor as their measurement tool but can use other sensor types as well. Such devices include the Lumo Lift (Lumo Bodytech Inc., Palo Alto, United States), BackTone 4000 (BackTone, Australia), Upright Pro and Upright Go (UpRightTechnologies Ltd., Tel Aviv, Israel), and Alex (NAMU Inc., Seoul, Korea). These types of devices give long-term, real-time measures of spinal posture and bio-feedback to the user when poor posture is maintained. However, these devices may be limited in their potential use in research due to a lack of raw information available to the operator, such as three-dimensional orientation and other kinematic data. In addition, they have a potential low accuracy depending on the sensors used. The Lumo Lift, for example, is a device that measures upper back posture using a bi-axial accelerometer [52], whereas IMUs are able to give more robust orientation measurements [107]. The device is not able to measure the axial rotation of the spine and is limited for use with tight clothing, as the sensor itself is clipped to the clothes of the user near the upper chest; loose clothing would give significant errors in posture analysis. The other devices listed have similar limitations, in that they are aimed at the general population due to their affordable pricing, albeit with alterations in design such as sensors used and the attachment method.

All these devices only give feedback to when the user's posture is poor and is at risk of back pain. The ViMove (DorsaVi, Melbourne, Australia) and Spineangel® (Movement Metrics, Hamilton, New Zealand) are examples of a more sophisticated posture trackers. The ViMove outputs spinal posture orientation in real-time and is thus more useful for kinematic research and for use by clinicians. ViMove is a wireless

system containing two inertial units, each with one tri-axial accelerometer and single axis gyroscope [49]. The ViMove has been shown to RMSE values when compared to an OptoTrack motion capture system, of 0.5° to 2.8° and 2.1° to 6.3° for single-plane and three-dimensional movements respectively [49]. It is, therefore, suitable as a research tool due to its high accuracy [49], and the aforementioned ability to output kinematic data. However, the high cost for the device and monthly subscription to software limit its accessibility to the general population and many clinics.

The Spineangel® consists of an integrated circuit tri-axial accelerometer and data recorder and is designed to be clipped onto the belt or waistband at the lateral iliac crest [51, 53, 54]. The Spineangel® measures the tilt angle in the sagittal and coronal planes and can set into two different modes; continuous or intermittent [51, 53, 54]. In continuous mode the Spineangel® records posture in the sagittal and coronal planes at 10 Hz, whereas in intermittent mode it records the number of times a custom, pre-set postural threshold is exceeded [51, 54]. The Spineangel® has been shown to have intra-task, intra-session, and inter-day ICC values greater than 0.93 [54].

The Dorsa ViMove, Spineangel®, and all other devices listed in this section are compared in a number of key areas in Table 2.3.

Table 2.3 Commercially available devices to track posture and give feedback to the user when posture is poor.
URLs:
1 - https://www.lumobodytech.com/lumo-lift/
2 - https://www.uprightpose.com/collections/all-products/products/upright-go
3 - https://www.uprightpose.com/collections/all-products/products/upright-trainer
4 - http://www.backtone.com/backtone-posture-trainer/
5 - http://alexposture.com/
6 - [51, 53, 54]
7 - https://www.dorsavi.com/au/en/vimove/

Device	Lumo Lift [1]	UpRight Go [2] and Pro [3]	BackTone 4000 [4]	Alex [5]	Spineangel® [6]	Dorsa ViMove [7]
Sensors	Bi-axial accelerometer	Accelerometer. Additional strain gauge in Pro version	Electronic sensor (activated when pulled)	Tri-axial accelerometer, pivot sensor	Tri-axial accelerometer	2 x IMU (3D accelerometer, 1D gyroscope), 2 x surface EMG
Location	Clavicle	Go: upper back Pro: upper or lower back & shoulders	Mid-back	Cervical spine at the hairline	Lateral iliac crest at belt line level	Neck, Lower back, or Thigh
Attachment	Magnet clasp to clothing	Go: Re-usable silicon adhesive Pro: Single-use Velcro-medical tape adhesive	Shoulder/ Torso strapping	Ear hook	Clipped on belt/ waistband	Disposable application pads (double-sided tape)
Measurement	Torso tilt angle	Torso tilt angle	Threshold tension on the strapping/ electronic sensor	Head/neck tilt angle	2D tilt angle	3D spinal orientation Muscle activation voltages
Outputs	Bio-feedback, good posture hours, steps, calorie burn	Bio-feedback, posture tracking	Bio-feedback	Bio-feedback, real-time posture tracking, good posture hours, inactivity warning	Audio-feedback and 2D tilt angles or number of occurrences exceeding a posture threshold	3D Lumbar Angles
Communication	BlueTooth	BlueTooth	N/A	BlueTooth	Audible alarm	BlueTooth
Cost (US$)	$100	Go: $100 Pro: $130	$61	$49	N/A	$2000 + $149/month

2.4 Classification of Human Activity

The classification of activity has importance in numerous areas such as sport, defence, age care, and in daily living for general health. Prolonged sedentary postures have been shown to be a risk factor for increasing the likelihood of back pain. There are also numerous health issues that may arise from inactivity, with five of the major non-communicable diseases linked to inactivity, being coronary heart disease, stroke, type II diabetes, and breast and colon cancer [29]. In fact, it has been estimated that in 2013, physical inactivity was responsible for these five diseases cost health-care systems US$53.8 billion globally in 2013. On top of this, deaths related to physical inactivity cost US$13.7 billion due to lost productivity worldwide in 2013 [141]. However, the method used to obtain this estimate ensured this was an underestimate [142], thus does not portray the full issue of physical inactivity. Tracking an individual's activity would allow evaluation of that individual's physical behaviour to assess if they frequently experience events of prolonged sedentary behaviour or if they are inactive. Thus, in using activity recognition the functional decline of individuals can be monitored and interventions can be put in place for individuals who are at risk of developing or worsening health issues.

2.4.1 Inactivity and its Risks to Health

The issue of sedentary behaviour, or low activity time, goes much further than back pain, as there are numerous non-communicable diseases for which inactivity has been shown to be a risk factor. In fact, it has been estimated that physical inactivity was responsible for 5.3 million, or approximately 9%, of all premature deaths globally in 2008 [29] thus being the fourth most major cause for death [30]. It has been estimated that physical inactivity causes 6-10% of incidences of coronary heart disease, type II diabetes, and breast and colon cancer [29]. Numerous studies have shown that

individuals employed in sedentary occupations have an increased mortality risk from many health implications.

The metabolic equivalent of task (MET) is the ratio of work performed compared to resting, where one MET is the oxygen consumed (work performed) while completely at rest and is equal to 3.5 ml (O_2)/kg/min [46]. Sedentary (inactive) behaviour is any activity performed at 1 to 1.5 MET [32, 143]. Table 2.4 shows a list of common activities and sports, their approximate MET value [46-48], and time required each week to reach various MET·h/wk levels based on the first, second, third, and fourth quartiles of energy expenditure of individuals from Ekelund et al. [144], as well as 60 and 133 MET·h/wk from Kyu et al. [145].

In 2010 there were 52.8 million deaths globally, in which coronary (ischaemic) heart disease was the largest cause of death, responsible for 13.3% (7.02 million) of all deaths, as well as being the leading cause of years of life lost [146]. Morris et al. [147, 148] found an association between sedentary occupations and an increased risk of early mortality from coronary heart disease in middle-aged men. They found the risk of mortality from coronary heart disease for workers in physically '*heavy*' (active) occupations was less than half that of those in physically '*light*' (sedentary) occupations for men aged 45-64 years. Morris and Crawford [149] discovered that ischaemic myocardial fibrosis was also more common and severe in lightly active occupations as compared to heavily active occupations. It also appeared at an earlier age. Heady et al. [150] showed that drivers (sedentary group) of double-decker buses and trams had higher rates of first clinical attacks of coronary heart disease than conductors (active group) of the same type of bus and tram. The drivers also showed higher rates of '*sudden deaths*' (death within three days) from such attacks. Numerous other studies also found an association between lower levels of physical activity and the occurrence of, and deaths from, coronary heart disease and heart attacks [151-153].

Paffenbarger et al. [151] found that increasing stairs climbed, walking distance, participation in strenuous sports played (e.g., running, basketball, swimming, mountaineering, etc.), and a composite physical activity index (combination of stairs climbed, walking distance, and participation in sport as expressed in kcal/week) all

Table 2.4 Metabolic equivalent of task (MET) for common activities and sports, and the time required to reach several MET·hours/week thresholds performing each active activity or sport. (Source: [44-46]).

Activity	MET	Time (h)					
		2.5 MET·h/wk	16 MET·h/wk	30 MET·h/wk	35.5 MET·h/wk	60 MET·h/wk	133 MET·h/wk
Inactive							
Lying – Sleeping	1.0						
– Television	1.3						
Sitting – Television	1.3						
– Typing	1.5						
Standing	1.6						
Active							
Walking – 3km/h	2.0	1.3	8.0	15.0	17.8	30.0	66.5
– 5km/h	3.5	0.7	4.6	8.6	10.1	17.1	38.0
– 7km/h	6.4	0.4	2.5	4.7	5.5	9.4	20.8
– 8km/h	8.3	0.3	1.9	3.6	4.3	8.6	16.0
Walking – 8km/h, 3% gradient	9.8	0.3	1.6	3.1	3.6	6.2	13.6
Jogging – 9km/h	8.8	0.3	1.8	3.4	4.0	6.8	15.1
Running – 12.9km/h	11.8	0.2	1.4	2.5	3.0	5.0	11.3
– 16.1km/h	14.5	0.2	1.1	2.1	2.4	4.1	9.2
– 19.3km/h	19.0	0.1	0.8	1.6	1.8	3.1	6.9
– 22.5km/h	23.0	0.1	0.7	1.3	1.5	2.6	5.8
Stair Ascending	4.7	0.5	3.4	6.4	7.6	12.8	28.3
Stair Descending	3.5	0.7	4.6	8.6	10.1	17.3	38
Skipping – 66/m	9.8	0.3	1.6	3.1	3.6	6.2	13.6
– 100/m	11.0	0.2	1.5	2.7	3.2	5.4	12.1
– 145/m	12.1	0.2	1.3	2.5	2.9	5.0	11.0
Sport							
Bicycling – 15km/h	5.9	0.4	2.7	5.1	6.0	10.2	22.5
– 30km/h	9.8	0.3	1.6	3.1	3.6	6.2	13.6
Golf	4.8	0.5	3.3	6.3	7.4	12.5	27.7
Hockey – Field	7.8	0.3	2.1	3.8	4.6	7.7	17.1
– Ice	8.0	0.3	2	3.8	4.4	7.5	16.6
Soccer	10.0	0.3	1.6	3.0	3.6	6.0	13.3
Tennis	7.3	0.3	2.2	4.1	4.9	8.2	18.2
Swimming – Slow	5.8	0.4	2.8	5.2	6.1	10.3	22.9
– Fast	9.8	0.3	1.6	3.1	3.6	6.1	13.6
Canoeing – Slow	2.8	0.9	5.7	10.7	12.7	21.4	47.5
– Fast	12.5	0.2	1.3	2.4	2.8	4.8	10.6

protected against the risk of heart attack. It was found that an energy expenditure of less than 2000 kcal per week (from these activities) increased the risk of heart attack by 64%. Paffenbarger et al. [152] also found that higher participation in stair climbing, walking, and sports was associated with lower total mortality due to other cardiovascular, and respiratory causes, as well as an increase in longevity.

Stroke is a major cause of death and disability, with approximately 795,000 attacks annually in the United States (US), 610,000 of which are first attacks [154]. Stroke prevalence in the US is 2.7% and accounts for approximately 5.3% of all deaths [154]. Globally, stroke was the second leading cause of death, responsible for 5.3 million deaths (11.1%), and the third highest cause of years of life lost in 2010 [146], tending to be a larger killer in low- to middle-income countries [155].

There exist numerous risk factors for stroke, in which physical inactivity and longer sedentary duration have been identified to increase the risk of stroke over individuals who are physically active [156-166]. Soares-Miranda et al. [156] found that increased walking distance, walking pace, and walking score (combination of walk distance and pace) all lowered the risk of stroke. It was found that those who walked 49 or more blocks per week had 54% less risk of stroke compared to those who walked less than 5 blocks per week[2]. Similarly, individuals who habitually walked greater than 4.8km/h had a 53% lower risk of stroke as compared to those who commonly walked slower than 3.2km/h. Pandey et al. [158] concluded from studying the relationship between midlife cardiorespiratory fitness (CRF) and risk of stroke after the age of 65 years that a high midlife CRF was associated with a 39% lower risk when compared to a low CRF. Armstrong et al. [163] found that women who reported moderate levels of activity had reduced risk of any cerebrovascular disease (including stroke), however, reported no further reduction in risk at higher levels of activity. Aberg et al. [164] also concluded that low levels of fitness and to a lesser degree, low muscle strength, at the age of 18 were both independently associated with higher risk of stroke later in life. This goes to show that continued moderate or higher levels of activity are very important in reduced risk of stroke at any stage of life.

Other than coronary heart disease and stroke, physical inactivity is also a risk for three other major non-communicable diseases: type II diabetes, breast cancer, and colon cancer [29]. It has been found that physical activity of 10-60 MET·h/wk can reduce the risk of type II diabetes by 2-19%, with activity levels beyond this showing

[2] A block is a large building or group of houses. Although not a standard unit of measurement, it shows that a greater walking distance decreases the risk of stroke.

greater reduction in risk but at a reduced rate [145]. Compared to insufficiently active individuals, highly active people (MET·h/wk > 133) had a reduction of risk of 14% for breast cancer, 21% for colon cancer and 28% for diabetes [145]. A systematic review and meta-analysis [167] found that prolonged sedentary time (e.g., sitting, television viewing, etc.), even after adjusting for physical activity, increased the risk of diabetes incidence, cancer incidence and mortality, and all-cause mortality. This shows the importance of not only measuring physical activity but also sedentary behaviour.

Physical inactivity can also be responsible for numerous other diseases, including obesity [154], dementia [168], osteoporosis [169], anxiety and depression [170, 171], and many more, thus showing the need to perform adequate levels of physical activity.

A systematic review [144] found that individuals who sit for greater than eight hours per day and have a MET·hours per week (MET·h/wk) of less than 2.5 for physical activity were up to 59% higher risk of fatality in a 2-18 year follow-up than individuals who sit for less than 4 hours per day and have MET·h/week greater than 35.5 for physical activity. Compared to the more active group however, it was found that individuals who sit for more than 8 hours a day, but also greater than 35.5 MET·h/wk for physical activity, had no increased risk of mortality, showing that increased sitting due to factors such as occupation can be overcome with increased physical activity outside of working time. This review, however, found that physical activity did not reduce the risk of mortality in groups with a high number of hours viewing television (greater than three hours per day) except in highly active individuals with greater than 35.5 MET·h/wk for physical activity. This may be due to a lack of time to perform physical activity as too much leisure time is spent watching television instead.

These studies show the importance of tracking activity for the reduction of risk in numerous non-communicable diseases, not only for back pain; individuals can reduce their risk of these diseases by performing just a few hours of physical activity (Table 2.4) all of which would reduce the costs on the global health-care system by billions of US dollars and the number of early mortalities. It was repeatedly found that

physical inactivity increases the risk of all-cause mortality and incidence of, and mortality from, numerous non-communicable diseases. Several studies also showed that reaching recommended levels of physical activity did not completely mitigate the increased risk associated with such diseases caused by prolonged sedentary time, but still gave improvement. It is thus important to track sedentary activities, such as standing, sitting, and lying (as one would to reduce the risk of back pain for some individuals), and physical activities commonly used in everyday living and/or with high MET values, including walking, jogging, jumping, and stair ascending and descending. In addition, it would also be of benefit to have the ability to track walking on an incline due to is higher MET than flat walking, as well as transitions between activities, such that when this occurs, miss-classification does not occur.

2.4.2 Activity Classification

The classification of activity of a person can give valuable information on how active that individual is. This would, therefore, give the information required to help reduce the inactivity levels of the individual, by providing evidence to them if they reach recommended levels of activity or not. This, in turn, could thus reduce the risk of numerous diseases, as highlighted in Section 2.1.5 and Section 2.3.1. Activity tracking can also be beneficial for numerous other applications, such as in tracking the activity and functional decline of the elderly living at home, or those who suffer from Parkinson's disease.

The gold standard for classifying activity is task analysis using video capture to analyse tasks. Using this method, researchers can film participants performing their experimental task, then in post-processing assign the activity the participant is performing for each time frame. This allows for accurate, and an unlimited number of descriptors of activity, for classification of activity for each time frame. Although this method is open to human error, it has been shown to have reliability and is commonly used as a reference method for determining accuracies of other methods [34-36]. The

major limitations for video analysis of human activity for classification are that the analysis is time expensive and the activities must be performed within view of a camera. Therefore, for applications such as tracking activities of daily living, other methods are used, such as using wearable sensors.

Fitbit (Fitbit Inc., San Francisco, CA, United States) and Apple Watch (Apple Inc., Cupertino, CA, United States) are examples of popular commercially available technologies that are worn on the wrist to monitor numerous parameters, including tracking of activity. However, such devices only focus on general health and activity but are limited in their ability to monitor more complex movement patterns that can lead to pathological conditions such as back pain and other diseases.

In a clinical setting, it has been common practice to use inertial sensors, especially tri-axial accelerometers, for the classification of activity [36-42, 44, 45]. The accelerometer data is commonly split up into windows of data (approximately one to two seconds), with various parameters calculated for each interval, with the number and type of parameters altering for each study.

When using accelerometers, it is common that these parameters are calculated for each individual axis and/or magnitude of acceleration (Equation 2.1). These parameters include mean acceleration, the standard deviation of acceleration, maximum amplitude, minimum-to-maximum range, tilt angle, and energy expenditure which is estimated by the normalized signal magnitude area (SMA, Equation 2.2, r = 0.95) [39, 172]. In many instances, studies have also used filtering techniques, such as low and high pass Butterworth, and median filters to then obtain the parameters to classify activity [36-39, 44]. These parameters are generally compared to predefined thresholds or put into a developed machine learning algorithm to determine activity.

Equation 2.1

$$a_m = \sqrt{{a_x}^2 + {a_y}^2 + {a_z}^2}$$

a_m: Magnitude of Acceleration

a_x: X-axis Acceleration

a_y: Y-axis Acceleration

a_z: Z-axis Acceleration

Equation 2.2

$$EE \approx SMA = \int_{ti}^{tf} |a_x|\, dt + \int_{ti}^{tf} |a_y|\, dt + \int_{ti}^{tf} |a_z|\, dt$$

EE: Energy Expenditure

SMA: Signal magnitude area

a_x: X-axis Acceleration

a_y: Y-axis Acceleration

a_z: Z-axis Acceleration

t: Time

ti: Initial Time of Window

tf: Final Time of Window

There are numerous different types of classification learners available for developing activity classifiers using machine learning, including decision trees, K-nearest neighbour (KNN), support vector machine (SVM), logistic regression, and discriminant analysis [173, 174].

A decision tree is a type of learner which allows for multiple different response classifications, is easy to interpret, has fast prediction speeds and has low memory requirements. The accuracy of decision trees and other machine learning types can be increased using ensemble methods such as bootstrap aggregation, known as bagging. Bagging is the process where multiple weaker[3] trees are trained each using their own random subset of data. When classifying data, the final prediction is based on each of

[3] Each single tree is weaker due to not using all the data. The power of Bagging is due to their being numerous weak trees, combining to be more accurate than a single tree that uses all the data for training.

the singular trees '*voting*' for a classification; the classification with the most votes is the classification the model then chooses. To increase the accuracy further, individual trees can be trained using random subsets of data, and random features rather than all features. This creates many random trees and is therefore called *Random Forest* modelling [175, 176].

The nearest neighbour algorithm categorises data according to the classes of the data's neighbours and does so by assuming that objects near each other are similar (i.e. data is classified based on the class of neighbouring data) [173, 177]. This method generally uses multiple nearest neighbours to make a decision and thus is commonly termed K-nearest neighbour (KNN) [177]. For the classification of data can either based on a straight 'vote' of the K-nearest neighbours, or a weighting can be given to each vote based on their distance from the data in question [177, 178]. The KNN algorithm is simple to implement and intuitive [178], however, is best suited to applications where memory usage and prediction speed have little importance [173].

Support vector machine (SVM) is a machine learning algorithm which classifies data by use of a decision boundary (hyperplane). In a linear SVM, the best hyperplane in linearly separable data is one which has the largest margin between two classes. A loss function is used when data is not linearly separable to penalise points on the wrong side of the hyperplane. SVMs can also use a kernel transform function to convert nonlinearly separable data into higher dimensions where a linear decision boundary can be found [173]. The SVM kernel functions can be of numerous forms, including linear, polynomial (quadratic, cubic, etc.), Gaussian, exponential, multi-layer perception, and spline. A comparison of these various kernel functions showed no change in accuracy when used for the automatic recognition in gait changes due to ageing [179]. This study however only separated the data into two classifications, the young and the elderly and thus the choice of kernel function may be more important in the classification of data with more than two groups.

2.4.3 Previous Activity Classification Models

There have been a number of attempts in the past to create activity classifiers using wearable sensors. From a review of the literature, most commonly these classifiers will use accelerometers as the sensors but can make use of other sensors [36-42, 44, 45]. It is also common for accelerometer data used for these classifiers to be filtered to obtain the gravitational and bodily motion components of acceleration using low-pass and/or high-pass Butterworth filters with cut-off frequencies between 0.25 and 1 Hz [36, 37, 39, 44]. Of interest for this research are classifiers which have been developed to predict at least standing, sitting, lying and walking; as are fundamental activities that describe different basic bodily postures and movement.

Lugade et al. [36] developed a decision tree to classify activity from two tri-axial accelerometers placed on the right thigh and on the waistband of pants between the two anterior superior iliac spines of the pelvis. Raw accelerometer data was filtered using a median filter and low pass filter to obtain the gravitational component of acceleration. The gravitational component was subtracted from the original median filtered data to obtain bodily motion acceleration. Both were then used to classify activity using a number of features, including SMA (Equation 2.2), continuous wavelet transform scaling thresholds, and thigh and waist angles. The model can classify numerous activities, including standing, sitting, right, left, prone, and supine lying, walking, jogging, transitions and shuffling. Average positive predictive values were greater than 80% for all activities except standing and transitions which had values of 75% and 71% respectively. When fidgeting/shuffling was excluded, standing positive predictive values increased to 85%. The model was also able to predict walking activities at speeds as low as 0.1 m/s, which allows the model to be implemented in populations with low walking velocities, such as the elderly. Although this model was able to classify activity with reasonable accuracy, its performance can still be improved upon, especially for standing activity. The model also does not allow classification of some other commonly used activities, such as stair ascending and descending, therefore, being another limitation for everyday activity tracking.

Khan et al. [40] developed an activity classifier via machine learning to predict standing, sitting, lying, walking, cycling, and stair ascending and descending using a single tri-axial accelerometer. They compared several different classification algorithms and sensor placements and found the most accurate was the use of a decision tree algorithm and accelerometer placed on the upper back. The average accuracy of the best classifier was 79.43%, with accuracies for different activities ranging from 69.6% to 99.4%. Although incorporating stair ascending and descending, unlike Lugade et al. [36], the accuracies of these activities were found to be 71.0% and 69.6% respectively. The low accuracy of the model to predict to stair ascending and stair descending, along with numerous other activities, is a limitation of this model and therefore not ideal for use in everyday activity tracking.

Kwapisz et al. [41] also developed an activity classifier via machine learning and compared various learning algorithms. Their classifier was trained to classify standing, sitting, walking, jogging, stair ascending and stair descending using cell phone accelerometers at 20 Hz. From comparing different learning algorithms, they, like Khan et al. [40], also found that a decision tree had the highest average accuracy of all activities. Multilayer perceptron, however, had accuracies within ±2.2% for all activities except walking downstairs, which was 11.2% less accurate. The decision tree-based algorithm was able to classify activities with the following accuracies: standing – 93.3%, sitting – 95.7%, walking – 89.9%, jogging – 96.5%, stair ascending – 59.3%, and stair descending 55.5%. Again, like Khan et al. [40], the accuracy of the model to accurately predict stair ascending and stair descending is a major limitation which hinders its use for the tracking of these activities.

Mannini and Sabatini [42] also compared numerous machine learning classification learners to classify activity based on data collected by five body worn bi-axial accelerometers, placed at the hip, wrist, arm, thigh, and ankle. The classifiers were trained to classify standing, sitting, lying, walking, running, stair ascending, and cycling. From this analysis, they found that the most accurate single-frame learner was the nearest mean learner with an overall accuracy of 98.5%, being 5.5% more accurate than the decision tree learner. In this study, however, they used subject-specific

training, in which a distinct classifier was trained and validated for each individual. Subject-specific training is expected to increase the accuracy of each learner due to removing the variations present in the way activity is performed between subjects. Using this method, however, decreases the usefulness when applying classification models to large populations due to the time required to train a model for each individual. The model created by Mannini and Sabatini [42] also requires the data from five accelerometers, which is comparatively more than the number of accelerometers required by the activity classifiers created by Lugade et al. [36], Khan et al. [40], and Kwapisz et al. [41].

Other than activities of daily living, fall detection is another common event that classifiers have been created for using accelerometers with great success [180-185]. However, although important for certain groups that are at increased risk of fall, or for those who a fall may have a severe impact on health (e.g. the elderly [186-189]), this research focuses on activities of daily living and therefore further investigation into fall detection will not be included.

2.5 Summary of Literature

Back pain is one of the most significant disorders affecting the modern world, with 60-80% of all people expected to experience it at least once in their lifetime. Back pain has been found to be the largest contributor to disability when expressed in years lived with disability and the second most common reason for sick leave from work. Of all major musculoskeletal disorders, only severe rheumatoid arthritis has a higher disability weighting than back pain, showing the severity of the pain felt by suffering individuals, who can experience loss of mobility, sleep, and their independence.

Due to its severity and common occurrence, back pain has major cumulative costs. In 2003, back pain cost AU$9.17 billion in Australia, AU$8.15 billion of which were due to loss of productivity. In the United States, back pain is estimated to cost between US$100-200 billion annually, with two-thirds due to indirect reasons.

Over 100 risk factors have been identified for back pain, however, poor posture, prolonged sedentary behaviour, and high spinal loads are believed to be the most important when designing preventative measures [15]. Although there are numerous systems available to measure spinal posture and kinematics in the laboratory, it has been shown that wearable bio-feedback systems, that alert the user when their posture becomes poor, have been successful in re-training the user in improving their posture, and therefore potentially reducing the risk of back pain.

Although slightly different, inactivity is similar to prolonged sedentary behaviour and is thus of interest in this research. Inactivity has been linked to an increased risk of numerous non-communicable diseases, such as coronary heart disease, stroke, type II diabetes, breast and colon cancer, obesity, and dementia. In effect, inactivity was responsible for 5.3 million (9%) of premature deaths globally in 2010. Some longitudinal studies have been performed to show that adequate levels of activity, and reducing sedentary time, can significantly decrease the mortality rate.

2.6 Gaps in Previous Research

The risk factors for back pain and numerous other non-communicable diseases have been studied in the previous literature, however, there remain some gaps in this research which include;

- Limited research into inexpensive (<AU$1000), unrestricted posture tracking.
- No highly accurate activity classifier for activities including standing; sitting; prone, supine, right, and left lying; walking; jogging; stair ascending and descending; jumping; walking on an incline; and transitions.
- No all-in-one device that tracks the posture and activity of the user including the activities listed above.

The aim of this research is to address these gaps, so knowledge can be obtained and used to help decrease the prevalence of back pain and other diseases in which inactivity may be responsible for.

Chapter 3

Comparison of Sensors in Measuring Motion Simulating Spinal Kinematics

3.1 Aim

The aim of this study directly relates to the first aim listed in Section 1.3, which is to compare a number of commonly used spinal kinematic measurement systems, including a low-cost (<AU$1000) wearable sensor, in their ability to measure motion typically seen in the human spine. AU$1000 was chosen as the threshold because, as shown in Chapter 2, many all clinical based measurement devices are above, and in some cases far exceed, this threshold. The work performed in this chapter was to determine the accuracy and repeatability in single- and multi-axis ROM and random motion measurements of five different sensing technologies commonly used in human spinal kinematic testing, being: optical motion capture, an expensive IMU and an inexpensive IMU, an analogue accelerometer, and an accelerometer as part of an IMU. It is hypothesised that the inexpensive IMU will have an average accuracy lower than that of all other measurement systems. It is also hypothesised that the errors for the IMU measurements will be greater in the yaw axis than in the roll or pitch axes, as been shown in previous studies.

The sensors were compared to a Katana Robot 450 (Neuronics, Zurich) as the reference system due to its high accuracy and repeatability of motion, and its capability of moving in conditions which can simulate human spine kinematics. This research preliminary work into addressing the use of inexpensive and unrestrictive sensors for spinal kinematic measurements, being the first gap listed in Section 2.5. Although the author has taken the specific application of spinal motion to develop the movements to be analysed, the results of this study are useful to applications outside of spinal and human kinematics.

3.2 Methodology

3.2.1 Equipment and Data Collection

The measurement systems used in this study were an eight-camera OptiTrack Flex optical motion capture system (v100R2, AU$7200 N = 8 cameras, N = 2 OptiHubs), an expensive IMU (Lord MicroStrain 3DM-GX3-25, AU$2900), inexpensive IMU (SparkFun 9DOF Razor IMU SEN-10736, AU$115), analogue accelerometer (Kistler K-Beam 8393B10, AU$3450), and an accelerometer as part of an IMU (Lord MicroStrain 3DM-GX3-25 accelerometer). Both IMUs contain a tri-axial accelerometer, a tri-axial gyroscope, and a tri-axial magnetometer. The IMUs and accelerometers were chosen due to their common use in wearable posture analysis systems and covered various price ranges. The sensors were tested on a Katana Robot 450, a two degree of freedom (X and Z) robotic manipulator, which was selected due to its high accuracy (0.8 mm, < 0.105°) and repeat accuracy (< 0.1 mm, < 0.013°). The configuration and placement of sensors and reflective markers are shown in Figure 3.1. The Katana Robot 450 was programmed to move in a ZYX rotation sequence. This was the case as can be seen in Figure 3.1., a rotation in the Z-axis affects the position of the other two axes and was thus the chosen as the first rotation axis. It has also been recommended that the axis with lowest degree of rotation be chosen as second in the rotation sequence [190]. Therefore, the Y axis was selected as the second rotation axis as in this study, the Y axis will have no motion. The X axis was thus selected as the third axis in the rotation sequence, giving a ZYX rotation order.

SparkFun Razor IMU orientation data was collected in Euler angle form in a ZYX rotation sequence via Bluetooth at 50Hz using a BlueTooth Mate Gold module. A ZYX rotation order was selected to match rotation order of the Katana Robot 450. The data was collected using Tera Term v4.90 (OSDN Corporation, Japan) and upsampled to 100Hz using one-dimensional linear interpolation. MicroStrain IMU data was also collected in Euler angle form in a ZYX rotation sequence and along with

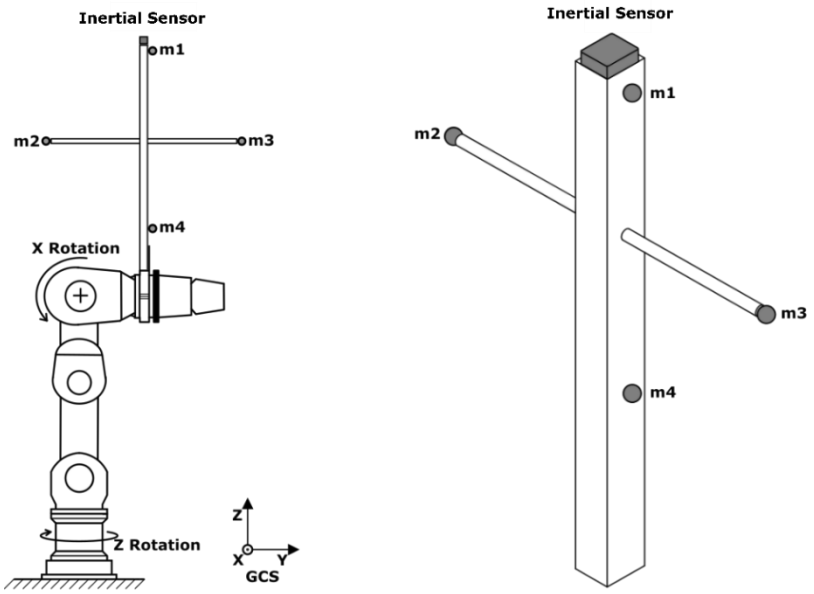

Figure 3.1 Placement of the inertial sensors (IMUs and Accelerometers) and opto-reflective markers (m1 – m4) on the Katana in its initial position. The Z axis of the global coordinate system (GCS) aligns in the opposite direction to the acceleration due to gravity. The local co-ordinate system's (LCSs) of the optical motion capture and the inertial sensors aligns with the GCS in the initial frame. Y rotation measurement testing was achieved by repositioning the sensors at a rotation of 90° around the Z axis from their original position.

the MicroStrain accelerometer data, was collected at 100 Hz using 3DM-GX3 Monitor 1.7 (Lord MicroStrain Sensing Systems, Williston, VT, USA). OptiTrack marker three-dimensional position data was collected at 100Hz via Capture2D v1.0.0.94 (C-Motion, Germantown, USA) and marker identification was performed in AMASS v2.0.0 (C-Motion, Germantown, USA). Kistler accelerometer data was collected at 100Hz via TracerDAQ v2.3.2.0 (Measurement Computing Corporation, Norton, MA, USA).

A 3rd order bi-directional low-pass Butterworth filter was applied to all measured data with a -6dB cut-off frequency of 4Hz. A cutoff frequency of 4Hz was chosen based on inspection of the spectral response of the raw data. A number of trials were re-analysed with a cut-off frequency of 10Hz to ensure that the results were not sensitive to the cut-off frequency chosen. These results showed no significant difference for any movement or sensor type. Post-processing of data was performed in MATLAB R2013a (The Mathworks Inc., Natick, MA, USA) and statistical analysis was performed using IBM SPSS Statistics v24 software (IBM Corporation, New York, US).

3.2.2 Katana 450 Robot Arm Movements

The range of motion testing compared the ability of the sensors to accurately and repeatedly measure the ROM of the Katana under various dynamic conditions. ROM testing simulated simple tests that can be performed to assist practitioners in determining the level of pain experienced by patients, or to check if rehabilitation is effective. A ROM of 120° was used to approximately replicate a degree of motion capable of the spine (Table 2.1) [1-6]. The ROM testing saw the Katana begin in a static position, then accelerate up to a maximal speed (1, 1.5 or 2 rad/s) before decelerating to 0 rad/s at 120°. The Katana then reversed direction with a return velocity profile that mirrored the original velocity profile.

Six different ROM movements were tested over three sets of ten repetitions and repeated over two sessions. The sensors were tested in their ability to measure ROM in all three measurement axes as numerous joints in the human body, including the spine, have up to three axes of rotation. Accelerometers, however, were only tested in the X-axis due to their inability to measure rotation in axes parallel to gravity. The sensors were also tested at various speeds to find the effect this has on orientation results. The speeds tested include 1 rad/s (~57°/s), 1.5 rad/s (~86°/s), and 2 rad/s (~115°/s), where 1 rad/s is approximately the self-selected speed of the lumbar spine during maximum flexion [191]. The sensors were also tested in a two-dimensional coupled motion (120° of motion in X-axis, while simultaneously moving 120° in the Z axis). 120° of motion for each axis was chosen to keep it consistent with the single axis ROM tests to ensure changes in accuracy were due to coupled axis motion rather than a change in the extent of motion.

The random motion testing was included in this testing to simulate unpredictable human motion. In random motion testing the Katana continually changed direction and speed of motion in the X and Z axes for approximately 60 seconds and was repeated 10 times. Since the Katana does not actuate around its Y axis, this was an opportunity to test sensor accuracy around an axis having an absence of motion while movement occurred in other axes.

Due to large errors obtained in Z-axis orientation measurements when the IMU was inverted with respect to gravity (i.e. when X-axis rotation greater than 90°), it was deemed necessary to perform secondary random motion testing on the SparkFun Razor IMU. This testing saw the Katana move in the same ROM in all three axes as the primary testing, with an initial orientation altered by an offset of -60° in the X-axis to ensure the IMU remained upright throughout the entire random motion trial. Parameters on all the test motions can be found in Table 3.1.

3.2.3 Determination of Rotations

All sensors were placed on the Katana via a custom clamp and rigid wooden beam, which was placed on the last moving segment from the base of the Katana as seen in Figure 3.1. This allowed flat sensors to be attached to the circular cross-section of the

Table 3.1 Summary of the various motions the Katana performed during experimentation and of which were measured by the various sensors.

Motion	Number of Axes	Spinal Motion Equivalent	Speed	Range of Motion	Repetitions
ROM X axis slow	1	Flexion/Extension	1 rad/s	120°	60
ROM X axis medium	1	Flexion/Extension	1.5 rad/s	120°	60
ROM X axis fast	1	Flexion/Extension	2 rad/s	120°	60
ROM Y axis medium	1	Lateral Bending	1.5 rad/s	120°	60
ROM Z axis medium	1	Axial Rotation	1.5 rad/s	120°	60
ROM coupled axis medium	2	Coupled Flexion/Extension & Axial Rotation	1.5 rad/s	X: 120° Z: 120°	60
Random motion	2	Coupled Flexion/Extension & Axial Rotation	X: 0.220 rad/s (avg), 2.64 rad/s (max) Z: 0.135 rad/s (avg), 1.07 rad/s (max)	X: 171° Z: 184°	10
Random motion - 60° X	2	Coupled Flexion/Extension & Axial Rotation	X: 0.220 rad/s (avg), 2.64 rad/s (max) Z: 0.135 rad/s (avg), 1.07 rad/s (max)	X: 171° Z: 184°	10

Katana, and to increase the distance between the sensors and the Katana to reduce electromagnetic disturbances from the Katana affecting IMU magnetometer readings.

Four opto-reflective markers (m1 – m4) were placed on the rigid beam such that they could be tracked by the OptiTrack system and a local coordinate system (LCS) could be created. The LCS was created as follows:

Y-axis: Y′ = The line running from m2 to m3.
X-axis: X′ = Cross product of the Y-axis, and the line running from m2 to m4.
Z-axis: Z′ = Cross product of X and Y axes, pointing up.
Origin = m2.

Orientations from the OptiTrack system were then determined by creating a rotation matrix from the LCS with respect to the global coordinate system (GCS) using Equation 3.1. Euler angles were extracted in a ZYX rotation sequence to match the Katana rotation sequence using Equations 3.2 and 3.3.

Equation 3.1

$$R = \begin{bmatrix} X' \cdot X & Y' \cdot X & Z' \cdot X \\ X' \cdot Y & Y' \cdot Y & Z' \cdot Y \\ X' \cdot Z & Y' \cdot Z & Z' \cdot Z \end{bmatrix}$$

X, Y, Z: Axes of the global co-ordinate system
X', Y', Z': Axes of the Katana local co-ordinate system from OptiTrack markers

Equation 3.2

$$R_{Z'Y'X'} = \begin{bmatrix} r_{11} & r_{21} & r_{31} \\ r_{12} & r_{22} & r_{32} \\ r_{13} & r_{23} & r_{33} \end{bmatrix} = \begin{bmatrix} c\alpha c\beta & c\alpha s\beta s\gamma - s\alpha c\gamma & c\alpha s\beta c\gamma + s\alpha s\gamma \\ s\alpha c\beta & -s\alpha s\beta s\gamma + c\alpha c\gamma & -s\alpha s\beta c\gamma - c\alpha s\gamma \\ -s\beta & c\beta s\gamma & c\beta c\gamma \end{bmatrix}$$

c: cosine
s: sine
α: 1st axis of rotation
β: 2nd axis of rotation
γ: 3rd axis of rotation

Equation 3.3

$$Z\ axis\ rotation = \alpha = \tan^{-1}\left(\frac{r_{12}}{r_{11}}\right)$$

$$Y\ axis\ rotation = \beta = -\sin^{-1}(r_{13})$$

$$X\ axis\ rotation = \gamma = \tan^{-1}\left(\frac{r_{23}}{r_{33}}\right)$$

The IMUs and accelerometers were placed at the end of the rigid beam such that their initial LCS aligned with the GCS. Both IMUs directly output Euler angles in a ZYX rotation sequence using the Direction Cosine Matrix algorithm.

To obtain angles from the accelerometers, the tilt angles were calculated using the acceleration outputs [192]. This method, however, did not allow for rotations about the axis parallel to gravity, Z, to be calculated. Therefore, only X-axis rotation was calculated for the accelerometers using Equation 3.6.

Equation 3.6

$$X\ axis\ rotation = \gamma = \tan^{-1}\left(\frac{a_X}{\sqrt{{a_Y}^2 + {a_Z}^2}}\right)$$

To test sensors in the Y-axis of rotation, they were rotated 90° about the Z-axis such that Katana movement in the X-axis was measured as Y-axis motion by the sensors. All rotations were taken as a relative rotation about the initial frame of each trial.

3.2.4 Data Analysis

The range of motion measurements was taken to be the maximum Euler/tilt angle value recorded per cycle minus the average Euler/tilt angle value recorded before motion commenced for that cycle, shown graphically in Figure 3.2. The ROM results (Table 3.2) are the average ROM measured over the 30 cycles in the same session. Intra-session RMSEs were used to determine the accuracy of each sensor during ROM

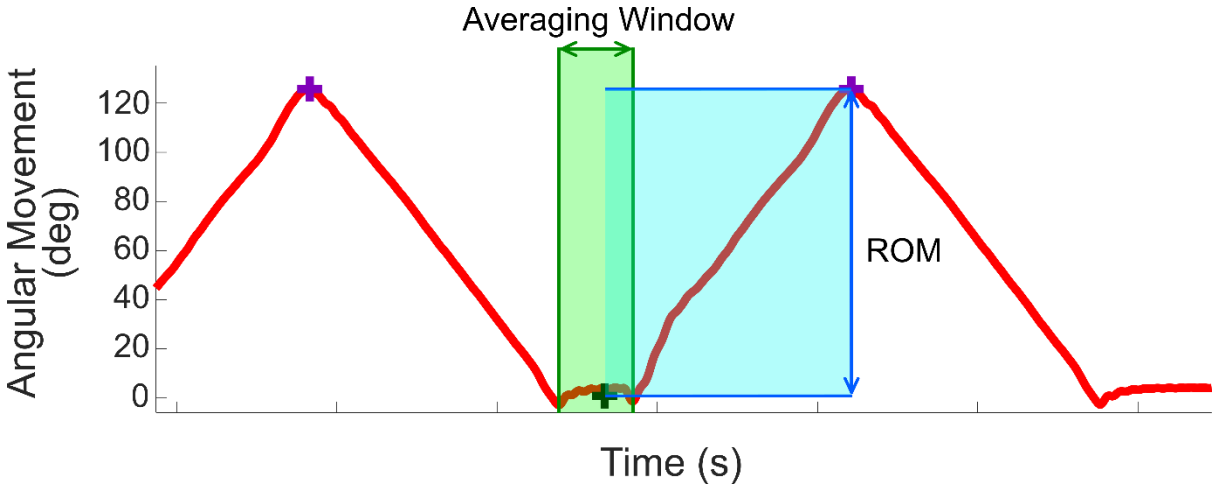

Figure 3.2 Graphical representation of the range of motion (ROM) measured by the sensors.

- **Orientation-time trace of sensor.**
- **Initial and final times of averaging window, taken to be time in which the two local minima occurred.**
- **Movement repetition orientation maxima.**
- **Movement repetition orientation minima; average orientation value within the averaging window.**
- **ROM minima and maxima, ROM = maxima – minima.**

testing, where a lower value indicates a more accurate result. This was calculated for both sessions using the 30 measured ROM values compared to the actual ROM of the Katana of 120°. RMSE of the ROM results taken in the two sessions were used to determine the inter-session repeatability of the sensors, where a lower value indicates better repeatability. Standard deviation (SD) of measured ROM values were used to determine the intra-session repeatability of the sensors during ROM testing, in which a lower SD indicates a more repeatable sensor. One sample t-test was used to test for a significant difference ($p < 0.05$) between ROM test sessions.

In random motion testing, the average motion profile detected by each sensor over the 10 repetitions was determined. The average motion profile was compared to the motion of the Katana to calculate RMSE values to assess the accuracy of each sensor. Intraclass correlation coefficients (ICC) type (2, k) [193] were used to show the agreement between the measured motion of the sensors and the actual motion of the Katana.

3.3 Results

The average ROM, SD, intra-session RMSE, inter-session RMSE, and one sample t-test indicators for each ROM test condition, session, and sensor are shown in Table 3.2.

Table 3.2 Range of motion (ROM) results averaged over all repetitions and standard deviation (SD) for each session for various speeds and planes of motion. Inter-sensor intra-session root-mean-square error (RMSE) and intra-sensor inter-session root-mean-square error (Inter-Session RMSE) are also shown. S – Slow: maximum speed of 1 rad/s, M – Medium: maximum speed of 1.5 rad/s, F – Fast: maximum speed of 2 rad/s.
*** Significant difference between sessions ($p < 0.05$).**
 # No significant difference in results between sessions, however, a Bland-Altman analysis shows a linear trend between mean results and the difference between session ($p < 0.05$).
- No significant difference in results between sessions ($p < 0.05$).

Sensor	Motion		Session 1 ROM (SD) (°)	RMSE (°)	Session 2 ROM (SD) (°)	RMSE (°)	Inter-Session RMSE (°)
OptiTrack Flex	X-axis (S)	*	121.80 (0.07)	1.80	121.59 (0.06)	1.59	0.23
	X-axis (M)	#	121.98 (0.04)	1.98	121.95 (0.13)	1.96	0.13
	X-axis (F)	*	122.43 (0.06)	2.43	122.20 (0.15)	2.21	0.27
	Y-axis (M)	*	122.02 (0.04)	2.02	121.58 (0.06)	1.58	0.45
	Z-axis (M)	*	117.87 (0.18)	2.14	118.25 (0.27)	1.77	0.52
	Coupled: X (M)	*	120.38 (0.04)	0.38	120.60 (0.10)	0.61	0.18
	Z (M)	*	118.52 (0.07)	1.48	116.49 (0.17)	3.52	2.26
	Mean		120.71 (0.07)	1.75	120.38 (0.13)	1.89	0.58
MicroStrain IMU	X-axis (S)	*	121.46 (0.04)	1.46	121.34 (0.05)	1.34	0.15
	X-axis (M)	*	121.62 (0.05)	1.62	121.64 (0.04)	1.64	0.07
	X-axis (F)	*	122.12 (0.10)	2.12	122.06 (0.04)	2.06	0.13
	Y-axis (M)	*	118.76 (0.05)	1.24	118.52 (0.07)	1.48	0.26
	Z-axis (M)	*	119.87 (0.08)	0.15	119.53 (0.04)	0.47	0.36
	Coupled: X (M)	-	120.77 (0.07)	0.77	120.77 (0.08)	0.78	0.11
	Z (M)	*	118.21 (0.10)	1.80	118.97 (0.11)	1.04	0.77
	Mean		120.40 (0.07)	1.31	120.40 (0.06)	1.26	0.26
SparkFun Razor IMU	X-axis (S)	-	122.16 (0.57)	2.24	122.24 (0.55)	2.31	0.81
	X-axis (M)	*	124.39 (0.22)	4.39	124.58 (0.27)	4.58	0.43
	X-axis (F)	*	129.04 (0.29)	9.04	129.33 (0.41)	9.34	0.60
	Y-axis (M)	*	119.39 (0.27)	0.67	119.65 (0.32)	0.47	0.42
	Z-axis (M)	*	115.28 (0.24)	4.73	116.84 (0.54)	3.20	1.67
	Coupled: X (M)	-	121.90 (0.42)	1.95	121.98 (0.29)	2.00	0.54
	Z (M)	*	134.38 (0.37)	14.38	135.23 (0.46)	15.23	1.03
	Mean		123.79 (0.34)	5.34	124.26 (0.41)	5.30	0.79
Kistler Accelerometer	X-axis (S)	*	119.42 (1.35)	1.45	124.83 (1.37)	5.02	5.67
	X-axis (M)	*	120.74 (1.77)	1.89	124.27 (2.24)	4.80	4.62
	X-axis (F)	-	122.10 (2.75)	3.42	125.86 (2.32)	6.29	5.42
MicroStrain Accelerometer	X-axis (S)	-	117.86 (0.23)	2.15	117.52 (0.06)	2.48	0.41
	X-axis (M)	*	118.89 (0.18)	1.13	118.23 (0.08)	1.72	0.64
	X-axis (F)	*	119.02 (0.40)	1.06	118.68 (0.12)	1.33	0.55

Of the sensors that were tested in all three axes, the MicroStrain IMU had the lowest average intra-session RMSE, inter-session RMSE, and SD of the three sensors, indicating that it has the greatest accuracy, inter-session, and intra-session repeatability. The OptiTrack was second in all these metrics, and the SparkFun Razor IMU was third. Results from statistical testing show that only six of 27 tests had no significant difference between sessions. The MicroStrain accelerometer average intra-session RMSE, average inter-session RMSE, and SD were found to be lower than the Kistler accelerometer, and thus more accurate and repeatable.

Random motion testing results are shown in Figure 3.3, with the absolute orientation of the sensors (left) and their relative difference to the orientation of the Katana (right). Results are shown as averages over the ten cycles, for each axis.

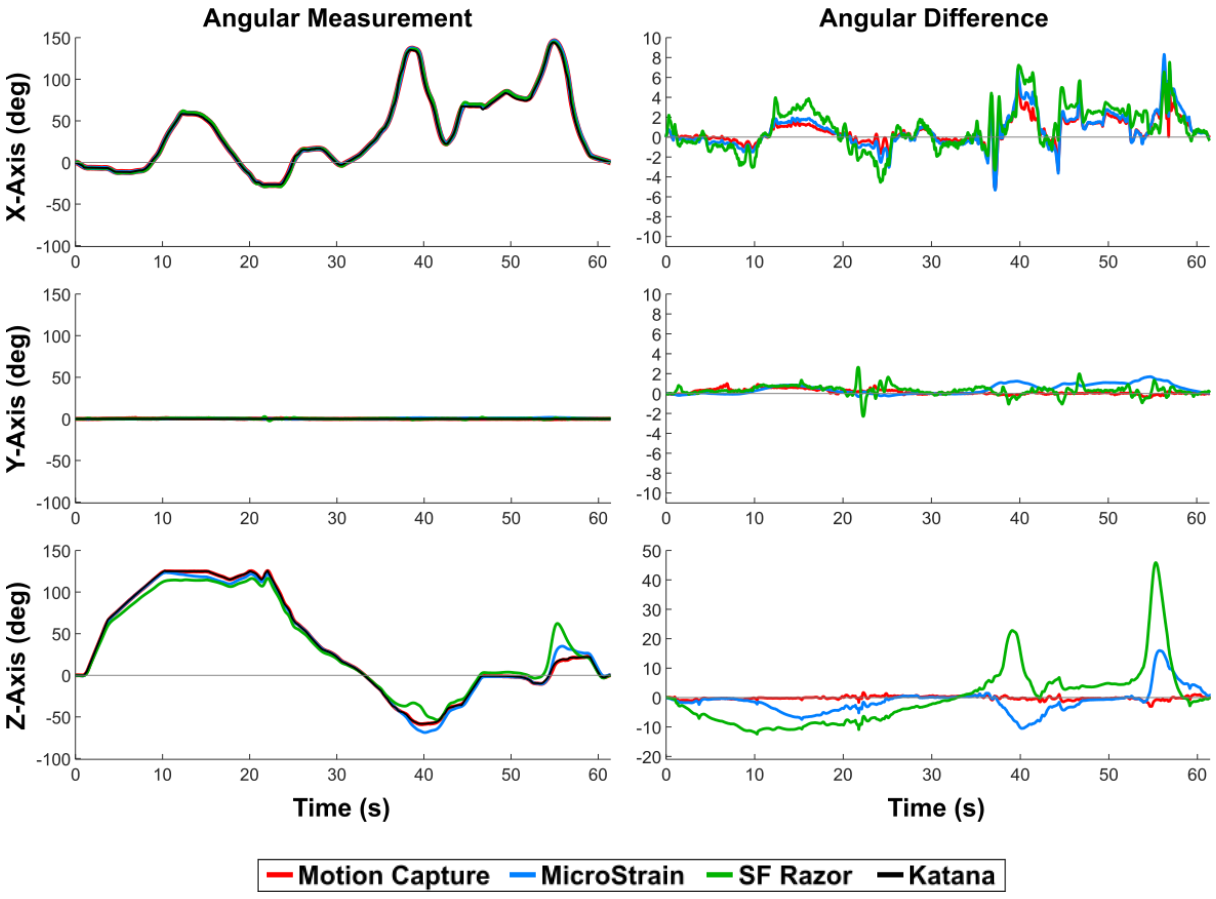

Figure 3.3 The results from random motion testing. The left-hand column of graphs shows the motion of the Katana (black) in the X, Y, and Z Euler angles in a ZYX rotation sequence, as well as the measured rotations in these axes by OptiTrack motion capture (red), MicroStrain IMU (blue), and SparkFun Razor IMU (green). The right-hand column shows the difference between the Katana motion and the measured rotations by the sensors.

The averaged RMSE in the X, Y and Z axes and ICC values in the X and Z axes for the three sensors during random motion are shown in Table 3.3. These results show the OptiTrack to be the most accurate with the lowest average RMSE of 0.81°, compared to the average RMSE for the MicroStrain IMU of 2.31° and SparkFun Razor IMU of 4.37°. All ICC values are 0.992 or higher, showing excellent agreement between sensors and Katana motion. Due to the secondary testing required for the SparkFun Razor IMU, as explained previously, Table 3.3 also shows these results, and Figure 3.4 shows the orientation-time data received in this testing. Secondary testing saw the SparkFun Razor IMU average RMSE decrease to 2.97° while keeping ICC values of 0.997 or higher.

Table 3.3 RMSE and ICC (95% Confidence Interval (CI)) values in the three measurement axes, X, Y and Z, for all sensors used during random motion testing. As there was no variance in the Katana Y motion, the Y-axis ICC values could not be calculated. Also shown is the RMSE values obtain during secondary testing of the SparkFun Razor IMU.

Sensor	X Axis RMSE (°)	X Axis ICC (95% CI)	Y Axis RMSE (°)	Z Axis RMSE (°)	Z Axis ICC (95% CI)
OptiTrack Flex Motion Capture	1.48	1.000 (1.000 – 1.000)	0.32	0.62	1.000 (1.000 – 1.000)
MicroStrain IMU	1.82	1.000 (0.999 – 1.000)	0.68	3.80	0.999 (0.998 – 0.999)
SparkFun Razor IMU	2.34	0.999 (0.999 – 1.000)	0.63	9.53	0.992 (0.991 – 0.993)
SparkFun Razor IMU – 60° X	1.67	1.000 (0.998 – 1.000)	1.36	5.88	0.997 (0.997 – 0.998)

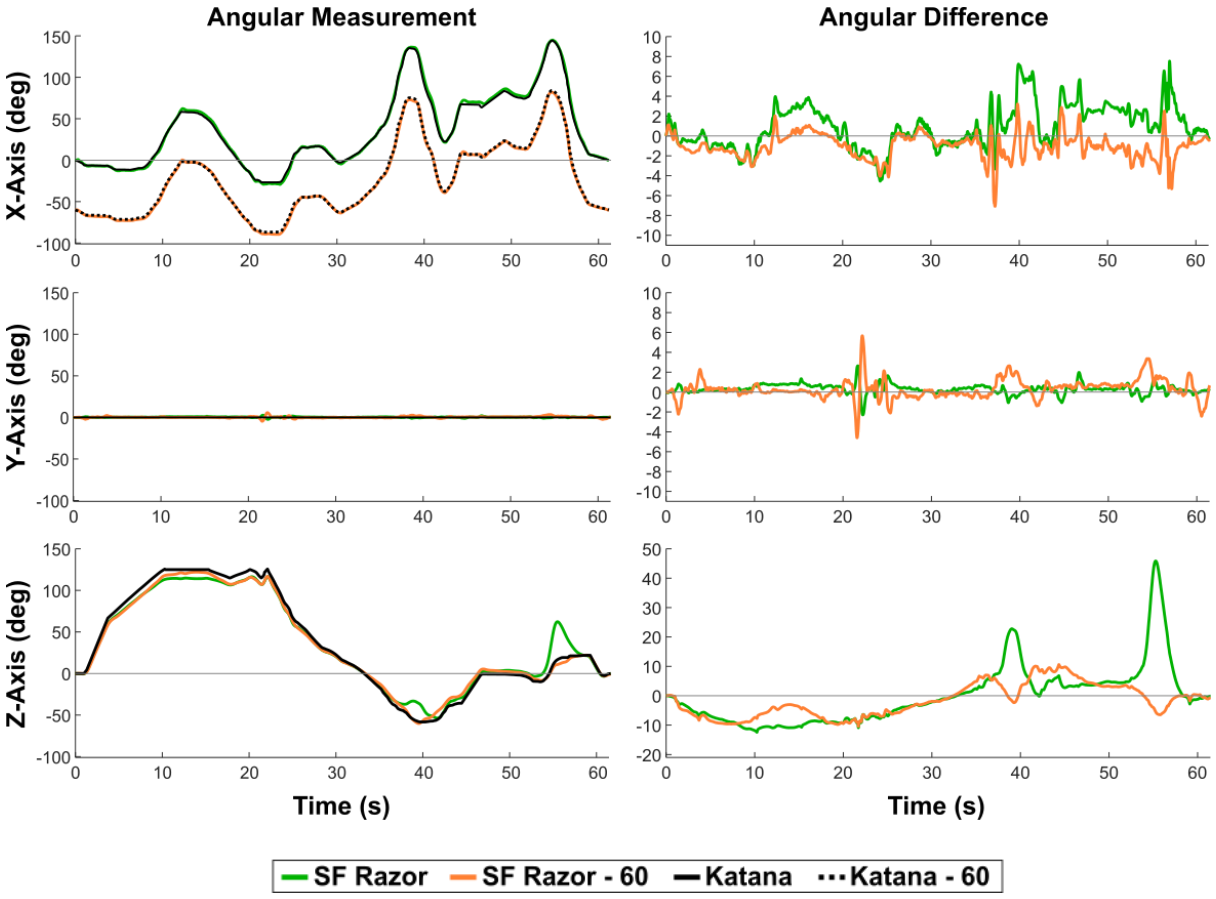

Figure 3.4 Secondary random motion testing with the Katana following the same range of motion as the original random motion tests, however now starting at -60° in the X axis (black dashed) while the other two axes were the same as the original test. The left-hand column of graphs shows the motion of Katana and measured motion by the SparkFun Razor IMU for both test sessions. The right-hand column shows the difference between the Katana motion and the measured rotations by the SparkFun Razor IMU for both sessions.

3.4 Discussion

3.4.1 Range of Motion Testing

In the range of motion testing, only six of the 27 results had no significant difference between sessions, indicating that absolute accuracy between sessions is difficult to achieve, with causes for systematic error including calibration and sensor placement. However, this difference is likely to be less than 1° in this set up as the average inter-session RMSE was 0.58°, 0.26°, 0.79°, and 0.53° for the OptiTrack, MicroStrain IMU, SparkFun Razor IMU, and MicroStrain accelerometer respectively. The average inter-session RMSE for the Kistler accelerometer, however, was greater at 5.24°. This shows the Kistler accelerometer is less reliable under such movement conditions than the other measurement systems. When applied to human participants, the error associated with all measurement systems is likely to increase due to the greater difficulty in the placement of sensors, and from soft tissue artefacts.

As speed increased the measured ROM by all measurement systems increased. This meant the accuracy of all sensors except for the MicroStrain accelerometer decreased, as shown by the increase in intra-session RMSE (Table 3.2). The results show that as speed increased from 1–2 rad/s, while the MicroStrain accelerometer and IMU had the lowest average RMSEs of 1.65° and 1.71° respectively, while the OptiTrack had the smallest change in measured ROM (0.61°–0.63°) and the SparkFun Razor had the greatest change (6.88°–7.09°). This shows that inertial effects will increase the transient response of the inertial sensors as they change direction, potentially decreasing accuracy as speeds increase. No trend can be found for the inter-session and intra-session repeatability of the sensors when altering speed. Over the three different speeds tested, the average inter-session RMSE is 0.21°, 0.12°, 0.61°, 5.24°, and 0.53° for the OptiTrack, MicroStrain IMU, SparkFun Razor IMU, Kistler accelerometer, and MicroStrain accelerometer respectively. These results show the MicroStrain IMU to have the greatest repeatability at the speeds tested.

For single plane motion and at the medium speed (1.5 rad/s), the MicroStrain IMU had average intra-session RMSE, and inter-session RMSE of 1.10° and 0.06° respectively. The average intra-session RMSE and inter-session RMSE values were 1.91° and 0.12° for OptiTrack, and 3.00° and 0.31° for the SparkFun Razor IMU. These results again show the MicroStrain IMU to have the greatest accuracy, inter-session repeatability, and intra-session repeatability.

For coupled motion testing, the OptiTrack and MicroStrain IMU are similar in accuracy and intra-session repeatability, however, the lower inter-session RMSE of the MicroStrain IMU indicates that it has greater inter-session repeatability. The results for the SparkFun Razor show considerable errors when measuring the coupled motion used in this study, with intra-session RMSEs of 14.38° to 15.23° for Z-axis measurement, which is unlikely to be acceptable for numerous applications in human kinematic measurement and other areas. The cause of such error may be explained by the fact that in the Z axes, the IMU only uses the gyroscope and magnetometer to estimate orientation. An increased error is also seen in the coupled motion Z-axis measurement for the MicroStrain IMU, however, this may not be as large due to the higher quality sensors and internal filters used in the MicroStrain data collection. These high errors are also seen in the results obtained during random motion testing, however, were able to be reduced by altering the kinematics of the system as discussed in the following section.

The results presented are the averaged results of all 30 repetitions per session, however, in a clinical situation, a practitioner is likely to only have a patient perform a ROM test once due to pain experienced. Using only the first repetition of each set of 10 repetitions, the RMSEs, on average, reduced by 0.04°. This shows the sensors to be consistent with their accuracy when used for single and multiple repetitions of ROM testing.

3.4.2 Random Motion Testing

Random motion testing results have shown all sensors to have an excellent absolute agreement in Katana motion measurements, with ICC values equal to or above 0.992 (Table 3.3). The OptiTrack was the most accurate for measuring this motion as demonstrated by the lower RMSE values. The results in the axes perpendicular to gravity (X and Y) for both IMUs are comparable to those obtained by OptiTrack. However, the RMSEs in the axis parallel to gravity (Z) are much higher for the MicroStrain and SparkFun Razor IMUs. The range of error observed during random motion testing for each measurement system (Table 3.4) show the MicroStrain and SparkFun Razor IMUs have largest single errors of 16° and 45.9° respectively in the Z axis. Both of these are much greater than the largest single error observed by the OptiTrack in this axis (-3°) and both occurring at approximately 56s, the time when the X-axis rotation is the greatest. The increase in Z-axis errors can be explained by the large differences evident, centred at times 39s and 56s in the Z-axis angular difference plot (Figure 3.3). These errors occur at the same time in which there is rotation in the X-axis greater than 90°. Under such conditions, the IMU has become inverted with respect to its starting position, which could be causing large errors in magnetometer readings used to estimate orientation around the gravitational axis.

The errors seen might be addressed by better use of Kalman filters and altering the rotation sequence of the IMUs to XYZ, as the first rotation should be about the primary axis of motion. However, due to the nature of the Katana moving in a ZYX

Table 3.4 Maximum single error (negative, positive) recorded during random motion testing.

Sensor	X-Axis (°)	Y-Axis (°)	Z-Axis (°)
OptiTrack Flex Motion Capture	-5.2, 7.3	-0.4, 1.0	-3.0, 1.7
MicroStrain IMU	-5.3, 8.3	-0.3, 1.7	-10.4, 16.0
SparkFun Razor IMU	-4.5, 7.5	-2.3, 2.6	-12.4, 45.9
SparkFun Razor IMU – 60° X	-7.1, 3.2	-4.6, 5.7	-10.4, 10.6

sequence, this could not be performed. Therefore, secondary testing was performed with the SparkFun Razor IMU as described in the methods section. The secondary testing involved the same kinematic profile as the original testing, however, with a rotational off-set of -60° with respect to the initial tests (Figure 3.4). The tracking of the Katana by the SparkFun Razor IMU under the original and new kinematic conditions can be seen in Figure 3.4 which, along with Tables 3.3 and 3.4, show the IMU to be more accurate in the Z axis under these conditions. The RMSE values reduce by 4.27° (42%) and maximum single error reduces by 35.3° in the Z axis. The reduction in RMSE and maximum single error may be due to the IMU never becoming inverted. It is, however, important to note that other factors play a role in the inaccuracies of Z-axis measurement for IMUs, such as not being able to use accelerometer data to help estimate orientation changes in this axis. Further testing was not undertaken with the MicroStrain IMU as the mechanism for error was the same for both sensors.

3.4.3 Limitations

As testing was performed on a Katana Robot 450 common sources of error in human kinematic testing was not considered in the results. It is likely that the accuracy of these sensors for estimating segment orientations would decrease on human participants due to the relative motion of skin to the underlying bone, known as soft tissue artefact. Also, when using human participants, misalignment of sensors axes to body joint axes is more likely to occur. This would cause greater inaccuracies in measurements and reduce inter-session repeatability.

A further limitation was the inability to recreate human motion profiles for angular velocity, acceleration, and jerk, which could affect the results for human kinematics contexts. Although a limitation, it was considered important to perform testing on a robot arm to obtain a higher repeatability and control of motion than what can be obtained by human participants.

Further limitations of this study include the time in which the tests were completed over, being approximately one minute per trial. While this allowed for the accuracy of the sensors to be obtained, it did not allow for a study of the effects of drift, which is an issue for gyroscopes in orientation measurements. Although IMUs typically have drift compensation capabilities, the effect of these was not tested and may be of interest for long-term data collection. While the magnetometers in the IMUs used in this study were calibrated before every session to account for nearby ferromagnetic objects, if IMUs are used in wearable systems in which the user is free to move, then the magnetic fields can change significantly between locations, which should also be taken into consideration for using IMUs containing magnetometers.

3.5 Summary

The results from this research were used to fulfil the first aim of this Ph.D. (Section 1.3). The results from ROM testing show the MicroStrain IMU to have the greatest accuracy, and intra- and inter-session repeatability. However, the OptiTrack results are comparable in ROM testing, but more accurate in the random motion testing, particularly in the Z-axis. Along with other significant advantages, this alludes to optical motion capture remaining the gold standard for human kinematic testing in laboratory conditions. The MicroStrain IMU has shown to be a suitable alternative for use in the clinic or laboratory when optical motion capture is not practical, such as when wearable sensors are required. Although the SparkFun Razor IMU experiences larger RMSE and maximum single error during complex motions, which was hypothesised, it has shown to be a viable option for inexpensive data acquisition during single axis motion such as that seen in ROM testing. The results also show that for IMUs, except in single plane ROM testing for the MicroStrain IMU, the greatest errors generally occurred in the yaw axis which was also hypothesised. The results also indicate that for ROM measurements, accelerometers can be as accurate as optical motion capture and IMUs, particularly during lower velocity movements. However, their fundamental inability to measure rotations around the axis parallel to gravity renders them unusable in three-dimensional orientation tracking of the spine.

Chapter 4

Classification of Common Activities of Daily Living

4.1 Aim

This chapter highlights the creation and validation of a novel activity classification algorithm which uses data from the two tri-axial accelerometers and directly relates to the second and fifth aims in Section 1.3. The classifier was aimed to predict activity with greater resolution (i.e., a greater number of distinct activities) than currently available devices used to track activity. Therefore, the classifier does not predict just the sedentary and active time, but various activities including standing, sitting, lying, walking, jogging, jumping, stair ascending and descending, walking on an incline, and transitions between activities. In this way, the activity classifier is not only able to track sedentary behaviour but the time in which users are active, and what activity they are performing. This is important as each activity has its own energy expenditure rating (Table 2.4) and this information is beneficial in estimating total energy expenditure of an individual throughout daily living. This would help individuals reach various weekly energy expenditure goals, which can be set to reduce the risk of numerous non-communicable diseases. To measure this aim, it was a goal to have an average prediction accuracy for standing, sitting, lying, and walking of 90%, such that its accuracy was similar to previous research and to allow for some miss-classifications in activity transition zones. An extension to this goal was to predict all activities with 90% success rate such that it classified more activities than previous activity classifiers while still maintaining high accuracy. It is hypothesised that the activity classifier will have a higher average accuracy when measuring static postures than when predicting dynamic activities due to the simplicity of the tasks. It is also hypothesised that the accuracy of the classifier to predict walking will be higher for faster walking than slower walking due to higher magnitudes of acceleration expected for higher speed walking.

4.2 Methodology

4.2.1 Participants

Twelve healthy participants performed the experiment (N = 6 females, 6 males) with mean and standard deviation age, mass, height and BMI of 25.5 ± 5.4 years, 68.4kg ± 10.3kg, 1.74m ± 0.08m and 22.5kg/m^2 ± 2.0kg/m^2 respectively. The study attained ethics approval from the Human Research Ethics Committee at the University of Adelaide. The inclusion criteria for this study included male's and female's aged between 18 and 55 years old, inclusive. The exclusion criteria included individuals who had experienced an episode of back pain in last 12 months, and individuals who have a history of spinal surgery.

4.2.2 Experimental Protocol

Participants were asked to complete five different experimental protocols which included:

1. Eight minutes of various tasks performed for approximately 15 seconds each with a total of 12 different tasks, each performed twice and in a random order. A random order was achieved by assigning each activity an individual number, then using a random number generator to create the order. The activities to be completed include standing, sitting with a straight/normal posture, sitting with a pronounced forward lean, sitting with a pronounced back lean, supine, prone, right and left side lying, sit and reach (one × hold forward position, one × continually reach and return to normal posture), walking, jogging, and jumping.

2. Ten × 10 m walking and jogging at various non-specific speeds, in which instructions were given by the researchers to go faster or slower than the previous trial. The first trial of each participant was instructed to be their normal self-selected walking pace, and it was ensured that at least one trial was of slower and faster than normal walking pace, and one was jogging.

3. 5 × stair walking (4 steps), ascending and descending.

4. Standing while: twisting, front bending, side bending, and a combination of these three motions. Each of these motions consisted of 15 repetitions, and two speeds being 1 repetition every two seconds, and 1 repetition every six seconds.

5. Flat treadmill walking at three different speeds selected to be similar to the speeds used in protocol two of this section during the same testing session and were slow, medium, and fast for 30 seconds each. The medium speed was repeated at 10% and 20% inclines. The speed was held constant for the entire 30 seconds as recording began after the treadmill reached the test speed and ceased before the treadmill was turned off.

Each participant was asked to perform a repeat session which involved the same experimental protocol as session one and within four weeks of the original test session. The first completed session was assigned the number one, and the second completed session was assigned the number 2. Then using a random number generator, one of the sessions for each participant was then randomly selected using to be a training session, where data was used to train the activity classifier, and the other used as a validation session to test the accuracy of the classifier. All participants completed the follow-up session giving a total of 12 sessions of each for training and validation.

4.2.3 Activities of Interest

From the activities performed as part of the experimental task, a set of 13 different activities were chosen to have the classifier predict, which include standing, sitting, supine, prone, right, and left lying, walking, jogging, jumping, stair ascending and descending, incline walking, and transitions. The three static activities, standing, sitting, and the various positions of lying were chosen as they describe a complete set of common stationary positions undertaken by people, and prolonged static activities have been linked to the increased risk of back pain and other non-communicable diseases. Tracking the different poses of lying in the elderly and bedridden individuals due to health reasons also has importance as it can aid in the prevention of pressure ulcers (bed sores). These are injuries to skin and underlying tissue caused by prolonged pressure on the same area of skin which can become very painful, as well as develop into more serious conditions such as infections to the skin, soft tissue, bones, and joints, and may even lead to cancer [194]. The dynamic activities of walking, stair ascending, and stair descending were selected due to their common use in day-to-day living. Other dynamic activities including jogging, jumping, and walking on an incline were selected for use in the activity classifier as they are common activities used during physical workouts and sport and have higher MET values than walking, as shown in Table 2.4. Finally, transitions were also incorporated into the classifier to identify the change of activity rather than incorrectly classifying this time. The classifier was trained to predict these activities as per Table 4.1 using data from only the training sessions.

4.2.4 Data Collection

Two ±16g tri-axial accelerometers (Adafruit ADXL326) were used in this study to collect acceleration data at two different body locations. One accelerometer was placed on the side of the left thigh approximately halfway along its longitudinal axis and the

Table 4.1 The sections within each experimental protocol in which data for each activity of the classifier was used for training.

Classifier Activity	Experimental Protocol Number (Section 4.2.2)	Activities Used for Training
Standing	1, 2, 3	Any time considered standing
	4	All Activities
Sitting	1	Sitting with a straight/normal posture, sitting with a pronounced forward or back lean, and sit and reach.
Prone Lying	1	Prone Lying
Supine Lying	1	Supine Lying
Right Lying	1	Right Lying
Left Lying	1	Left Lying
Walking	1, 2	Any time considered walking
	5	Slow, medium, and fast speed trials. Incline tests not included
Jogging	1, 2	Any time considered jogging
Jumping	1	Any time considered jumping
Stair Ascending	3	Any time considered ascending stairs
Stair Descending	3	Any time considered descending stairs
Transitions	1	Any time considered transitioning between various activities. Transitions not included: from one upright activity (standing, walking, jogging, and jumping) to another, or from one sitting activity to another.
Walking Incline	5	Medium speed trials at 10% and 20% incline

other was placed on the upper thoracic region of the spine as shown in Figure 4.1. These locations were chosen so acceleration measurements can be made superiorly and inferiorly to the hips, to help ascertain between various static poses. The local co-ordinate systems of the accelerometers were aligned by eye-judgement as close as possible to that shown in Figure 4.1.

Accelerometers with ±16g dynamic range have been suggested as suitable to obtain accelerations of most bodily motions [195]. The accelerometers were connected to the analogue pins of an Arduino Mega, which in-turn had a BlueTooth module (SparkFun BlueTooth Mate Gold) attached for wireless transfer of data. Data was collected wirelessly using Tera Term v4.93 (OSDN Corporation, Japan) software at a sampling rate of 50 Hz. This frequency was considered adequate as the majority of human motions occur at 18 Hz and below [195]. A GoPro (Hero4 Black, GoPro Inc., United States) video camera captured all actions performed by the participants at 50

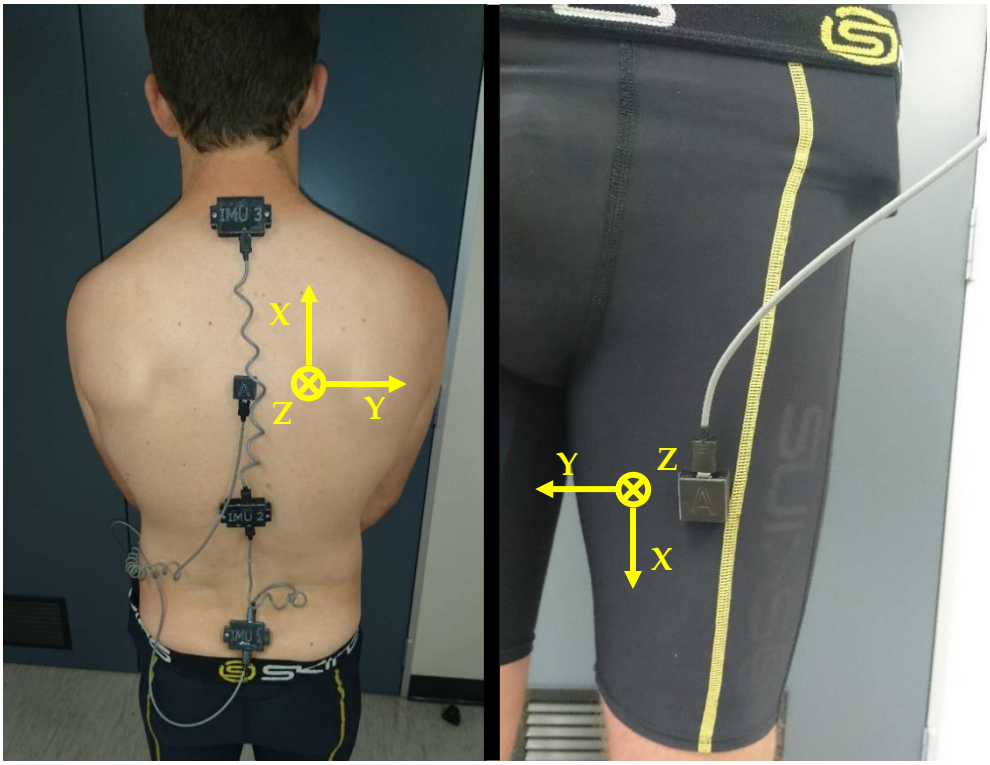

Figure 4.1 Placement of the two accelerometers on the upper thoracic region of the back, and mid anterior left thigh, with the local coordinate system of each accelerometer pictured (yellow). Also visible are the three spinal IMUs which were not used in this activity classifier but were used in later chapters of this research.

fps, to match the collection rate of the accelerometers. Video capture was used as the reference analysis in this study, as was used in previous studies [34-36].

During experimental protocol 2, participants were asked to walk or jog at various self-selected speeds over 10 m, a total of ten times per session. Each trial was timed using Kinematic Measurement Systems timing gates (Innervations, Muncie, United States), with this time used to calculate the average speed of the participants over the 10m.

4.2.5 Data Analysis

Testing sessions from each participant were randomly selected to be either a training session or a validation session. The training session data was used to create the activity classifier, and the validation session data was used to test the accuracy of the

developed classifier. All accelerometer data collected was then synchronised to video data collected for each session. Video analysis was performed in Kinovea – 0.8.15 (Kinovea Org, Copyright Joan Charmant and Contributors) to classify the activity being performed for each time frame throughout the testing, which was assigned at the discretion. Accelerometer data analysis was performed in MATLAB R2017b (The MathWorks Inc., Natick, MA, USA). Training session data was divided up according to the activity which was being performed as per video analysis data. However, in machine learning, raw data is not used for the training or as an input to a trained classifier. Instead, various parameters calculated from sub-sets of the data are used as inputs. The data for each activity was therefore further divided into one-second intervals with 50% cross-over.

The one-second intervals were used to calculate numerous parameters of the raw acceleration data for each sensor and axis. These parameters consisted of mean, standard deviation, and the maximum amplitude of the acceleration data in the time domain, and the dominant frequency and relative amplitude of the dominant frequency in the frequency domain calculated using Fourier Transforms. All these parameters were determined for each of the three axes on both accelerometers. Other parameters were also used in the activity classifier including the magnitude of acceleration (Chapter 2 equation 2.1) and signal magnitude area (SMA) (Chapter 2 equation 2.2) for each accelerometer, totalling 17 parameters on raw data for each accelerometer (Table 4.2).

It is common to filter accelerometer data with a low- and high- pass filter in order to obtain the acceleration due to gravity and acceleration due to bodily motion respectively, with these filters are generally applied with a cut-off frequency of 0.25 to 1 Hz [36, 37, 39, 44]. In this study, low- and high- pass filters were therefore also applied to raw data; however, different cut-off frequencies were also used to investigate which gave the highest accuracy. The low- and high- pass filters applied to raw data were fourth order Butterworth filters with -6 dB cut-off frequencies of 0.25, 0.5, 1, 2, 3, 4, 5, and 6 Hz. After applying the filters to the raw data, there was a total

Table 4.2 Each of the 17 parameters of acceleration calculated for each one-second interval of data and their respective definitions.

Parameter	Definition
Mean	Mean acceleration over the 1-second interval. Calculated for the X, Y, and Z axes of each accelerometer, giving 3 parameters in total.
Standard Deviation	Standard deviation of acceleration over the 1-second interval. Calculated for the X, Y, and Z axes of each accelerometer, giving 3 parameters in total.
Maximum Amplitude	Maximum acceleration recorded during the 1-second interval. Calculated for the X, Y, and Z axes of each accelerometer, giving 3 parameters in total.
Dominant Frequency	The most dominant frequency of acceleration during the 1-second interval when data is in frequency domain via Fourier transforms. Calculated for the X, Y, and Z axes of each accelerometer, giving 3 parameters in total.
Relative Amplitude of Dominant Frequency	The amplitude of the most dominant frequency of acceleration during the 1-second interval when data is in frequency domain via Fourier transforms. Calculated for the X, Y, and Z axes of each accelerometer, giving 3 parameters in total.
Magnitude of Acceleration	Calculated as the square-root of the sum of the acceleration squared in each axis over the 1-second interval as shown in equation 2.1. Calculated for each accelerometer.
Signal Magnitude Area	Calculated as the sum of the integral of acceleration with respect to time of each axis over the 1-second interval as shown in equation 2.2. Calculated for each accelerometer.

of 102 [4] parameters used for each version of the activity classifier, where each version was made using a different cut-off frequency for the filters. It is recommended that the ratio between the number of instances available for training the model and the number of features used in the model, should be at least 10 [196]. As 102 parameters were selected for use in the algorithm, then at least 1020 windows of data were required for training of the classifier.

Decision trees, KNNs, SVMs, and other machine learning approaches have been used in previous research. The algorithms have been compared in their accuracy in classifying various human activities of daily living with varying results depending on the activity of interest [40, 41, 174, 197-199]. MATLAB's inbuilt Classification Learner application was thus used to train 56 activity classifiers each using a different filter cut-off frequency and algorithm for comparison. The different algorithms used for evaluation were decision tree, KNN, weighted KNN (using distance weighting), linear support vector machine (SVM), quadratic SVM, cubic SVM, and an ensemble bagged trees model, which implements the Random Forest algorithm. All models

[4] (17 raw data parameters + 17 low-pass filtered data parameters + 17 high-pass filtered data parameters) × 2 accelerometers = 102 parameters

were trained using 0% holdout (i.e. 100% of training data was used) and the 102 parameters calculated from the training session data of each participant to predict activities based on the experimental tasks performed, which include: standing, sitting, prone, supine, right-sided, and left-sided lying, walking, jogging, jumping, stair ascending, stair descending, walking on an incline, and transitions between stances. Each of these activities were trained for based on data collected during the various experimental protocols as per Table 4.1.

All 56 models were exported from the Classification Learner and tested for their activity prediction accuracy using the randomly selected validation sessions for each participant, ensuring the same data was not used for both training and validation. Each algorithm type was also compared in their average classification speed. The classification algorithm which is considered the most suitable for activity classification in this research will be based on the combination of high prediction accuracy and speed. Difference in means tests ($p<0.05$) were conducted between the algorithm of highest accuracy to all other algorithm types. If an algorithm type showed no significant difference in accuracy to the algorithm of highest accuracy, then the algorithm with highest prediction speed was selected as the chosen algorithm in this research.

During validation of the activity classifiers, each frame of data was assigned an activity by the classifier by creating a one-second interval to calculate the parameters needed by each classifier. The one-second intervals consisted of a half-second window of accelerometer data either side of the frame in question. Therefore, when using this method in real-time, there will exist a half-second lag for classification at each frame as data from half a second into the future is required. Using a half-second either side of the frame in question, however, will allow for a more accurate estimation by the classifier especially in transition zones. This is because the average acceleration data is more likely to be representative of what activity is being performed. In Figure 4.2, a graphical comparison between using a half-second window either side of the frame of interest (FOI) and a one-second window immediately before the FOI is shown. It can clearly be seen that using the acceleration window of 0.5 s either side of the FOI gives

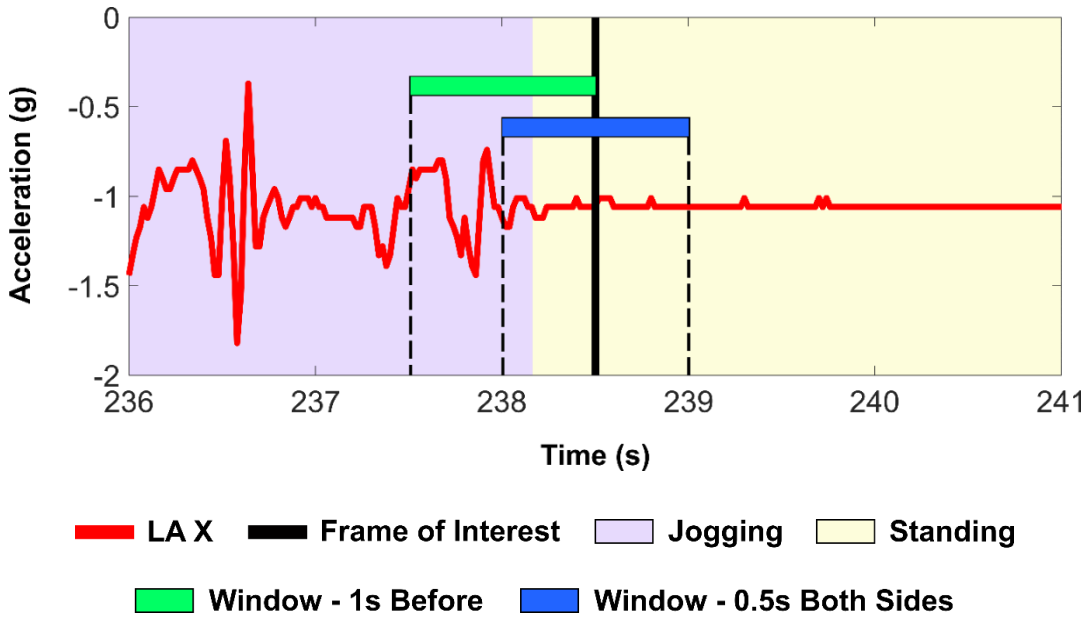

Figure 4.2 Two different methods for obtaining the input acceleration windows, being; a window of acceleration using data of 1s before the frame of interest, and a window of acceleration using 0.5s either side of the frame of interest. Clearly shown is the advantage of using a window of 0.5s either side of the frame of interest during transition zones, in that the window will consist of more data points that belong to the same activity as that seen in the frame of interest. LA X: Acceleration in the X-axis of the leg accelerometer.

an acceleration signal more alike the acceleration at the FOI than using the window of acceleration 1 s before-hand. Therefore, using the 0.5 s of acceleration either side of the FOI as the input window to the activity classifier is more likely to produce an accurate prediction, particularly during the transition between activities zones. An advantage of a window which uses the acceleration signal of 1 s before the FOI is there is no lag in activity prediction as there is with using 0.5 s either side which requires '*future*' data.

Further analysis was performed on the activity classification algorithm with the highest average accuracy across all filter cut-off frequencies. This analysis featured an activity-by-activity comparison of accuracy across all filter cut-off frequencies. Further analysis also comprised of the generation of a confusion matrix for the algorithm types and filter cut-off frequency which produced the highest overall accuracy. The confusion matrix, which shows positive predictive rates of each activity as well as the misclassification rates, was developed by removing outliers from the results. These rates were calculated by comparing the activity classifier output to that determined

by video analysis for each frame of data. In this research, outliers were calculated for each activity from each of the participants results and then removed to calculate the new accuracy of the classifier for each activity (i.e. if the accuracy of the classifier for an activity for one of the participants was outside the threshold when compared to all other participants for that activity, it was removed from the results). Outliers were calculated by first finding the median accuracy of each activity, then upper and lower quartiles, and the inter-quartile range (upper quartile minus lower quartile). The inter-quartile range was then multiplied by 1.5, where this value was added to the upper quartile and subtracted from the lower quartile to create a range in which values outside of would be considered an outlier.

4.3 Results

In total, 35695 seconds of data from all twelve participants were used for training the model when 50% cross-over of one-second intervals was implemented. This exceeds the recommended 1020 instances required for a 10:1 ratio of training instances to parameters [196] when using all the parameters outlined in Section 4.2.5. From the validation sessions, 17445 seconds of data was collected to test the accuracy of the model. The data for participant 2 validation session experimental protocol 2 and 3 was discarded from the results as video capture was unsuccessful. Prone and supine lying for participant 6 in their validation session was also removed as these activities were not correctly performed.

Figure 4.3 shows an example of the acceleration trace of each activity performed in this study and for each of the three orthogonal axes of the accelerometers. It can be seen that there are clear differences between activities. Figure 4.4 shows an example of this data in the frequency domain to illustrate the differences in the various activities in the frequency domain. The data presented are from a) spine accelerometer during standing, b) thigh accelerometer during standing, c) spine accelerometer during walking, and d) thigh accelerometer while walking. Examples of the data in the frequency domain for both accelerometers and for all activities can be found in Appendix A, which shows the distinct differences between various static and dynamic activities.

From the analysis, it was found that a quadratic support vector machine (SVM) model gave the greatest overall accuracy as opposed to other models such as single decision trees, linear SVM, and KNN classifiers (Table 4.3). The ensemble bagged trees (random forest) and cubic SVM models, however, showed no significant difference in their mean accuracies in activity classification across all filtering frequencies. The quadratic and cubic SVM models had similar classification frequencies (predictions per second) of 1810 Hz and 1690 Hz. The ensemble bagged trees model, however, had an average classification frequency of 4960 Hz, being 274% of the prediction speed of the

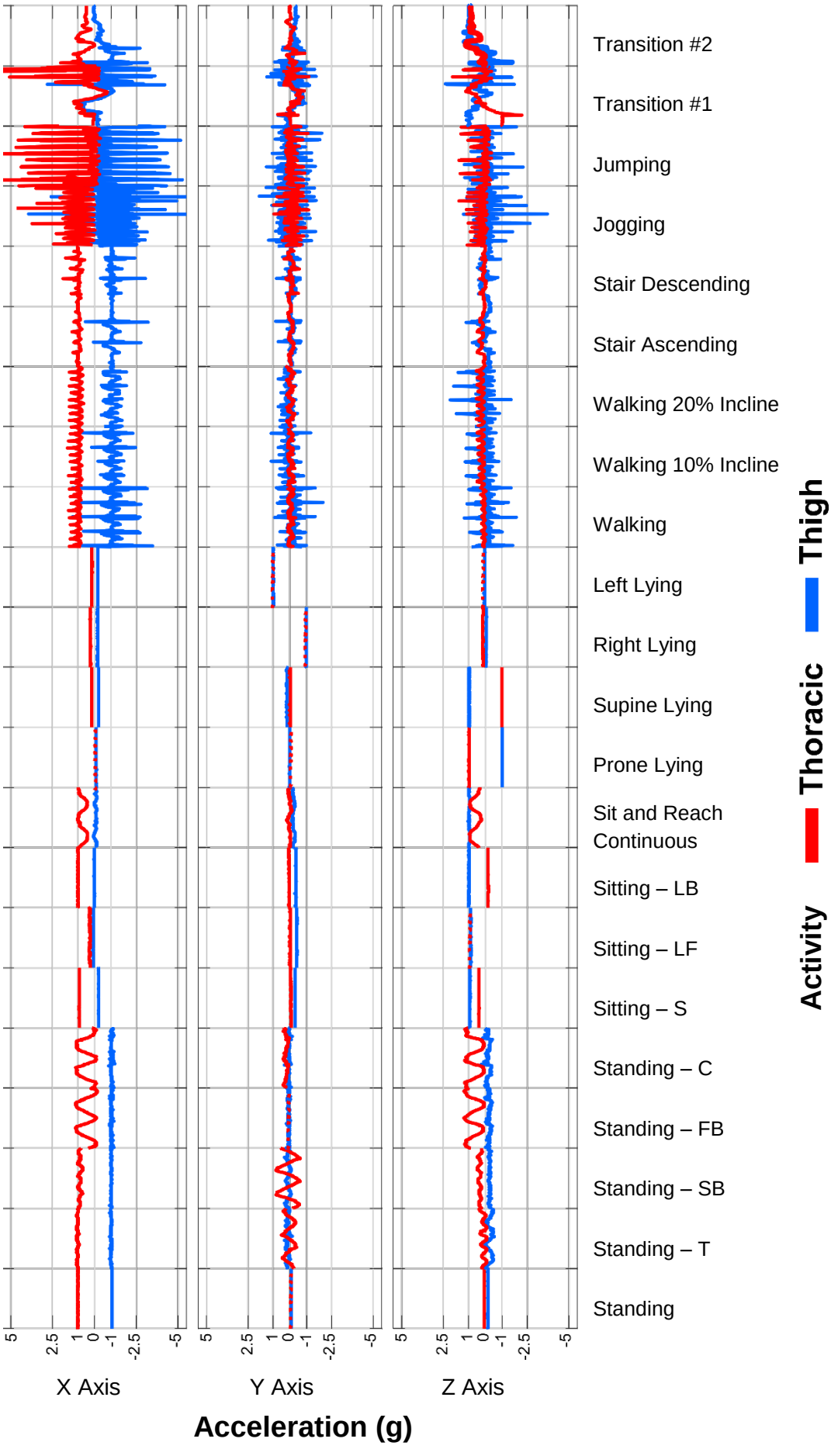

Figure 4.3 Example acceleration traces of five seconds for each unique activity performed in this study. Note: T – Twisting, SB – Side Bending, FB – Front Bending, C – Coupled Motion, S – Straight Back, LF – Leaning Forward, LB – Leaning Back, Transition #1 – Lying to Upright, Transition #2 – Upright to Sitting.

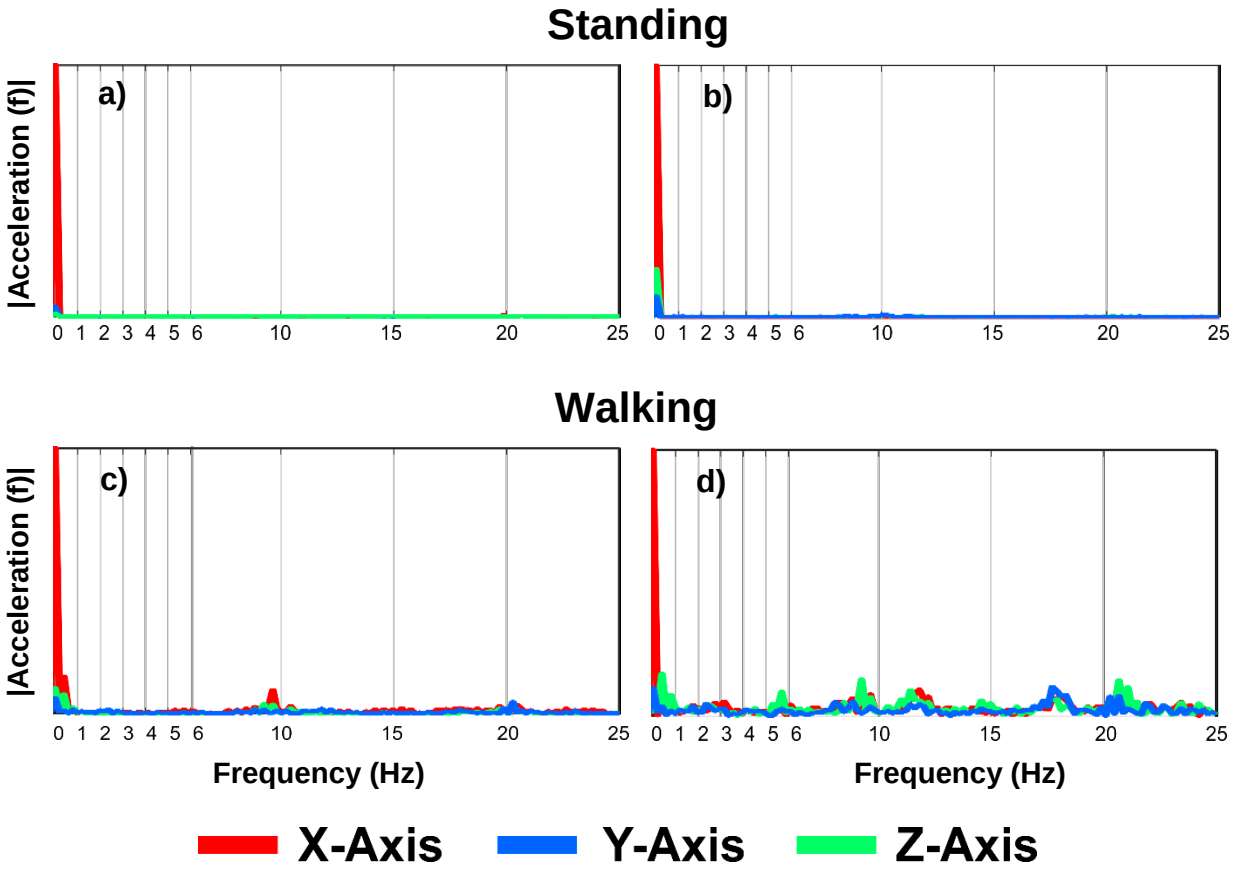

Figure 4.4 An example frequency domain of data collected from a) spine accelerometer during standing, b) thigh accelerometer during standing, c) spine accelerometer during walking, and d) thigh accelerometer during walking.

Table 4.3 Accuracy of the various classification algorithms used in this study with various cut-off frequencies applied to the low- and high- pass Butterworth filters. Also shown is the mean frequency in which each algorithm classified activities in predictions per second. Bold indices indicate highest accuracy cut-off frequency for each algorithm type.
* Significant difference ($p<0.05$) in mean accuracy to the algorithm with the highest accuracy (denoted by #).

Algorithm	0.25 Hz (%)	0.5 Hz (%)	1 Hz (%)	2 Hz (%)	3 Hz (%)	4 Hz (%)	5 Hz (%)	6 Hz (%)	Mean (SD) (%)	Frequency (Hz)
Decision Tree	79.7	80.2	80.5	81.0	81.2	81.7	81.3	**82.4**	81.0 (0.9) *	312000
Ensembled Bagged Trees	86.4	87.0	86.7	87.5	87.8	88.2	**88.4**	87.4	87.4 (0.7)	4960
K-Nearest Neighbour	80.7	79.9	81.1	81.9	81.8	**82.4**	82.2	79.3	81.2 (1.1) *	316
Weighted K-Nearest Neighbour	79.8	79.4	80.8	81.4	81.5	82.5	**82.7**	79.6	81.0 (1.3) *	308
Linear Support Vector Machine	84.8	84.9	85.4	**86.8**	86.4	86.7	86.3	82.8	85.5 (1.3) *	3950
Quadratic Support Vector Machine	87.7	87.1	87.8	88.5	**88.6**	88.4	**88.6**	85.5	87.8 (1.1) #	1810
Cubic Support Vector Machine	87.7	87.1	87.5	88.1	**88.4**	88.0	88.0	84.8	87.5 (1.1)	1690

quadratic SVM. The ensemble bagged trees model algorithm is therefore considered the best algorithm for the classification of activity in this research due to the combination of high accuracy and prediction speed.

Table 4.4 shows the accuracy of the different ensemble bagged trees models using the different cut-off frequencies, as outlined in Section 4.2.5, for the low- and high- pass filters within the model. The cut-off frequency used within the model that gave the greatest mean accuracy in determining the activities of interest was 5 Hz. The ensemble bagged trees model using a 5 Hz cut-off frequency will, therefore, be the chosen activity classifier for this research.

A confusion matrix showing the positive prediction and misclassification rates of the chosen activity classifier for each activity, after outliers have been removed, is

Table 4.4 Accuracy of the activity classifier to predict the various activities used in this study with various cut-off frequencies applied to the low- and high- pass Butterworth filters used to obtain numerous model parameters.

Activity	0.25 Hz (%)	0.5 Hz (%)	1 Hz (%)	2 Hz (%)	3 Hz (%)	4 Hz (%)	5 Hz (%)	6 Hz (%)
Standing	93.7	93.6	93.8	**94.0**	93.9	93.8	93.8	93.8
Sitting	95.0	95.2	95.2	95.3	95.4	95.3	**95.6**	95.5
Prone Lying	96.0	96.3	95.8	**96.1**	95.4	96.0	96.0	94.8
Supine Lying	**95.6**	95.4	95.1	95.3	94.8	95.0	95.2	95.0
Right Lying	94.4	94.3	94.0	**94.5**	94.3	94.2	94.1	**94.5**
Left Lying	96.2	96.4	**96.8**	96.3	96.7	96.3	96.6	96.4
Walking	86.9	87.1	87.2	87.4	**87.5**	87.4	87.2	87.1
Jogging	92.3	92.1	92.4	91.7	92.9	**93.1**	92.9	**93.1**
Jumping	94.7	93.9	94.1	93.6	94.6	**94.8**	**94.8**	94.6
Stair Ascend	66.3	68.1	71.1	74.2	75.1	76.5	**77.6**	75.9
Stair Descend	46.2	47.3	50.6	54.1	56.6	58.6	**58.9**	55.7
Transition	**84.7**	84.4	84.2	83.8	83.6	84.0	83.7	83.7
Walking 10% Incline	67.3	67.8	66.5	68.2	68.9	70.0	**70.6**	67.3
Walking 20% Incline	91.0	91.7	90.6	**92.9**	91.6	92.0	92.2	91.6
Standing While Moving	99.5	**99.7**	99.5	99.6	99.5	99.5	99.5	99.4
Treadmill Walking	97.8	95.7	98.4	98.6	98.5	98.7	98.4	**98.9**
Mean	87.4	87.4	87.8	88.5	88.7	89.1	**89.2**	88.6

shown in Table 4.5. This table shows the true activity class as determined by video analysis along the vertical axis, the predicted class along the horizontal axis, and the predictive rates of trained model filling the table for each activity. An example of how to read this table, is when the video analysis showed the participants to be standing, 93.7% of the time the model predicted the users to be standing, and for them to be sitting, walking, stair ascending, and stair descending 0.1%, 5.6%, 0.3%, and 0.1% of the time respectively. From this table, it can be calculated that the average accuracy for static activity classification (standing, sitting, and laying) is 96.0% and the average accuracy for predicting dynamic activities is 85.4%. The activity classifier is therefore more accurate in predicting static activities, as hypothesised.

The accuracy of the chosen activity classifier to predict slow walking is presented in Table 4.6. In this table is the slowest average walking speed over 10 m, as well as the average walking speed, used by each participant during experimental task 2 for both sessions. This table shows the accuracy of the classifier to predict the slowest average walking speed over 10m and the accuracy during each of the walking trials during the validation session.

The slow, medium, and fast walking speeds used for treadmill walking (experimental protocol 5) for both testing sessions for each participant is shown in Table 4.7. Also shown in this table are the average slow, medium, and fast walking speeds for each session. Upon performing a difference in means test, it was found there was no significant difference in the mean speeds for either slow, medium, or fast walking speeds between testing sessions.

Table 4.5 Positive predictive and mis-classification rates given as a percentage (standard deviation) by the activity classifier for each of the activities it's capable of predicting for the purpose of this table, outliers have been removed from use in calculation of the prediction rates and standard deviations.

Activity	Standing	Sitting	Prone Lying	Supine Lying	Right Lying	Left Lying	Walking	Jogging	Jumping	Stair Ascend	Stair Descend	Transition	Walking Incline
Standing	**93.7 (3.5)**	0.1 (0.2)	0 (0)	0 (0)	0 (0)	0 (0)	5.6 (3.3)	0 (0.1)	0 (0.1)	0.3 (0.3)	0.1 (0.2)	0 (0.1)	0 (0)
Sitting	0 (0)	**97.0 (1.8)**	0 (0)	0 (0)	0 (0)	0 (0)	0 (0.1)	0 (0)	0 (0)	0 (0)	0 (0)	3.0 (1.7)	0 (0)
Prone Lying	0 (0)	0 (0)	**96.0 (3.5)**	0 (0)	0 (0)	0 (0)	0 (0)	0 (0)	0 (0)	0 (0)	0 (0)	4.0 (3.5)	0 (0)
Supine Lying	0.1 (0.4)	0 (0)	0 (0)	**95.1 (2.5)**	0 (0)	0 (0)	0 (0)	0 (0)	0 (0)	0 (0)	0 (0)	4.8 (2.4)	0 (0)
Right Lying	0 (0)	0 (0)	0 (0)	0 (0)	**94.9 (1.7)**	0 (0)	0 (0)	0 (0)	0 (0)	0 (0)	0 (0)	5.1 (1.7)	0 (0)
Left Lying	0 (0)	0 (0)	0 (0)	0 (0)	0 (0)	**96.4 (2.8)**	0 (0)	0 (0)	0 (0)	0 (0)	0 (0)	3.6 (2.8)	0 (0)
Walking	4.9 (2.6)	0 (0)	0 (0)	0 (0)	0 (0)	0 (0)	**87.3 (2.7)**	0.4 (0.3)	0.2 (0.2)	0.7 (0.8)	0.6 (0.6)	3.8 (1.3)	2.0 (2.3)
Jogging	0.6 (0.8)	0 (0)	0 (0)	0 (0)	0 (0)	0 (0)	2.7 (1.7)	**93.5 (2.2)**	0.1 (0.6)	0.7 (0.6)	0.1 (0.1)	1.3 (1.3)	0.9 (1.0)
Jumping	0.2 (0.5)	0 (0)	0 (0)	0 (0)	0 (0)	0 (0)	0.3 (0.4)	2.1 (2.7)	**96.6 (3.5)**	0 (0)	0.2 (0.6)	0.5 (0.9)	0.1 (0.1)
Stair Ascend	6.0 (5.5)	0 (0)	0 (0)	0 (0)	0 (0)	0 (0)	9.5 (7.4)	0 (0)	0 (0)	**79.9 (8.0)**	0.4 (0.7)	0.5 (1.5)	3.7 (6.7)
Stair Descend	3.2 (2.7)	0 (0)	0 (0)	0 (0)	0 (0)	0 (0)	32.0 (11.8)	0 (0)	0 (0)	2.8 (3.6)	**61.9 (10.4)**	0 (0)	0.2 (0.3)
Transition	0.9 (1.8)	5.2 (4.7)	1.2 (1.1)	1.1 (1.5)	1.2 (1.8)	1.5 (2.0)	3.0 (3.6)	0.5 (0.6)	0.7 (0.9)	0.2 (0.3)	0.1 (0.2)	**83.7 (11.0)**	0.7 (0.6)
Walking 10% Incline	0 (0)	0 (0)	0 (0)	0 (0)	0 (0)	0 (0)	18.6 (15.4)	0 (0)	0 (0)	0.8 (1.6)	0.2 (0.5)	0 (0)	**80.5 (16.0)**
Walking 20% Incline	0 (0)	0 (0)	0 (0)	0 (0)	0 (0)	0 (0)	0.8 (1.7)	0 (0)	0 (0)	0.7 (1.2)	0 (0.1)	0.5 (1.2)	**98.2 (2.6)**
Standing While Moving	**99.9 (0.1)**	0 (0)	0 (0)	0 (0)	0 (0)	0 (0)	0 (0.1)	0 (0)	0 (0)	0 (0)	0 (0)	0 (0)	0 (0)
Treadmill	0.2 (0.5)	0 (0)	0 (0)	0 (0)	0 (0)	0 (0)	**99.0 (1.5)**	0 (0)	0 (0)	0.1 (0.2)	0.2 (0.5)	0.1 (0.2)	0.4 (1.0)

Table 4.6 Lowest average speed of 10m and the mean average speed over 10m during experimental protocol 2 for both training and validation sessions, as well positive predictive rates of the trained activity classifier to classify walking during experiment task 2 in the validation session.
 # Calculated without using participant 2's data.

Participant	Training		Validation			
	Lowest Speed (m/s)	Average (SD) (m/s)	Lowest Speed (m/s)	Accuracy (%)	Average (SD) (m/s)	Accuracy (%)
1	0.35	1.16 (0.53)	0.38	86.9	1.32 (0.63)	91.1
2	0.21	1.21 (0.54)	0.06	9.0	0.96 (0.52)	N/A
3	0.62	1.17 (0.46)	0.49	88.7	1.20 (0.48)	90.3
4	0.50	1.19 (0.46)	0.57	91.9	1.22 (0.44)	94.0
5	0.51	1.47 (0.59)	0.81	96.8	1.40 (0.48)	84.3
6	0.97	1.40 (0.32)	0.69	87.5	1.17 (0.30)	91.0
7	0.82	1.21 (0.27)	0.89	92.7	1.16 (0.25)	88.7
8	0.89	1.23 (0.25)	0.78	93.9	1.22 (0.29)	92.7
9	1.07	1.43 (0.23)	1.02	99.7	1.26 (0.18)	93.6
10	0.72	1.15 (0.27)	0.89	99.7	1.17 (0.25)	91.6
11	0.77	1.19 (0.30)	0.98	93.8	1.37 (0.30)	93.0
12	0.82	1.28 (0.25)	0.99	99.7	1.31 (0.24)	88.8
Average	0.69	1.26	0.77#	93.8#	1.25#	90.8#

Table 4.7 slow, medium, and fast speeds used for treadmill testing (experimental protocol 5) during the testing and validation sessions of all participants.

Participant	Training			Validation		
	Slow (m/s)	Medium (m/s)	Fast (m/s)	Slow (m/s)	Medium (m/s)	Fast (m/s)
1	0.44	1.02	1.67	0.42	1.06	1.90
2	0.78	1.22	1.84	0.75	1.15	1.79
3	0.62	1.15	1.74	0.70	1.12	1.72
4	0.78	1.12	1.60	0.57	1.05	1.67
5	0.51	1.34	1.86	0.81	1.33	1.68
6	0.97	1.25	1.55	0.69	1.10	1.39
7	0.82	1.25	1.56	0.89	1.28	1.60
8	0.89	1.29	1.58	0.78	1.30	1.68
9	1.07	1.36	1.71	1.02	1.30	1.46
10	0.92	1.19	1.56	0.93	1.22	1.49
11	0.98	1.21	1.54	0.98	1.27	1.76
12	1.07	1.25	1.50	0.82	1.29	1.52
Mean (SD)	0.82 (0.21)	1.22 (0.09)	1.64 (0.12)	0.78 (0.17)	1.21 (0.10)	1.64 (0.15)

4.4 Discussion

The model that was developed in this research can classify 13 distinct activities with an average accuracy of 90.3%. The activity classifier also introduces two activities that, to the best of the authors knowledge, have previously not been included in activity classification models, being jumping and incline walking. The average accuracy of the model increases to 95.6% when only interested in standing, sitting, lying, and walking.

From inspection of the example acceleration outputs in the time domain (Figure 4.3), most distinct motions performed in this study have acceleration traces that differ from all other activity outputs. The same is true about the acceleration data in the frequency domain. From the frequency domain figures (Figure 4.4, Appendix A) it can be seen that for all the static activities the frequency of the data primarily occurs at 0 Hz, where the amplitude is dependent of the pose of the participant, and thus the orientation of the accelerometer. The data in the frequency domain of the dynamic activities is vastly different from that of the static activities, in that there exist numerous peaks away from 0 Hz. The more vigorous activities, such as jogging and jumping have higher amplitudes at the frequencies away from 0 Hz than the less intense dynamic activities such as walking and stair ascending/descending as expected. From the distinct differences in the acceleration plots in both the time-domain and frequency-domain, it is clear that parameters calculated from both these will help the activity classifier differentiate between activities.

There are a few exceptions to this, however, especially in activities that are biomechanically similar such as walking and walking on an incline. Walking on an incline, particularly at a 10% incline, is very similar to walking in the acceleration trace in both the time-domain and frequency-domain due to their biomechanical similarities. As the accelerometer traces are very similar, then so are the 102 calculated parameters used within in the activity classifier, which thus explains why when the activity classifier incorrectly classified walking incline activity, it generally classed it as walking instead (Table 4.5).

It is common in the creation of activity classifiers to not only use raw data when calculating features of the acceleration for use within the model but to also apply filters to this data. Often, low- and high- pass Butterworth filters are used to separate the acceleration into a gravity component (low-pass filtered data) and a bodily motion component (high-pass filtered data) and it is common to apply a cut-off frequency of between 0.25 and 1 Hz [36, 37, 39, 44]. However, when comparing various other cut-off frequencies, as in Table 4.3 and Table 4.4, cut-off frequencies between 2 and 6 Hz offer greater accuracy in activity classification for all algorithm types tested in this research.

In this research both accuracy and prediction speed of the activity classifier are important. Upon comparison of the various algorithm types used in this research, it was discovered the ensemble bagged trees algorithm was best for this research. This conclusion was made from the high accuracy, showing to have no significant difference to that of the quadratic SVM, as well as the high prediction speed. The decision tree had a prediction speed that far exceeded all other algorithms, however, had a lower prediction accuracy than the ensemble bagged trees and SVM models and was therefore not considered for selection as the best activity classifier. Both the KNN and weighted KNN models were also not considered as both had low prediction accuracy and speed in comparison to all other models.

As the preferred algorithm for activity classification, the ensemble bagged trees models using each of the different cut-off frequencies was compared in their ability to estimate each of the activities. Of the cut-off frequencies used in this research, it was discovered they all had an average estimation accuracy of within 1.8% of each other (Table 4.4). This comparison shows that a cut-off frequency of 5 Hz gave the greatest mean accuracy of all cut-off frequencies for the ensemble bagged trees model. Table 4.4 also shows that the static motions (standing, sitting, and lying activities) were all predicted with the highest accuracies with cut-off frequencies of 2 Hz or lower. In regard to the dynamic activities, in general, these were predicted with the greatest accuracies when cut-off frequencies were between 3 and 6 Hz, with the exception of transitions, standing with movement involved, and walking on a 20% incline which

had highest accuracies at 0.25, 1, and 2 Hz respectively. Of all the dynamic motions, transitions and standing with movement generally involved lower intensity motion. These results may, therefore, highlight the usefulness of cut-off frequencies for predicting varying activities, where the low-intensity actions (static and low intensity dynamic) are best predicted with lower cut-off frequencies. Similarly, higher intensity dynamic actions are more accurately predicted with higher cut-off frequencies. The differences in accuracy, however, were generally only a small, commonly being below 4.1%. However, for stair ascending and stair descending, which in the past have been difficult to accurately predict [36, 40, 41], the differences between cut-off frequencies is much greater, being 11.3% and 12.7% for stair ascending and stair descending respectively. This shows that for the majority of activities the choice in cut-off frequency does not have a large effect. However, when trying to predict activities that are higher in complexity, and commonly experience low positive predictive rates, then a cut-off frequency of 5 Hz can increase the accuracy of the classifier greatly as compared to the commonly used cut-off frequencies of 0.25 to 1 Hz.

Most activities were able to be classified with accuracies of 80% or above, with many being above 90% (Table 4.5). The activities that were predicted with accuracies below 90% were walking (87.3%), stair ascending (79.9%), stair descending (61.9%), transitions (83.7%), and walking on an incline when at a 10% incline (80.5%). Stair ascending, stair descending, and walking on an incline are all variations on walking and therefore can have similarities in accelerometer signals. This may explain why when these activities were misclassified, the majority of the time they were classified as walking or as one of the other variations of walking.

Another common misclassification for stair ascending and descending, as well as walking, was standing. Although these two activities are dissimilar due to standing being static and walking being dynamic, there may be some confusion between the two activities when very slow walking is occurring as both have similar pose with the thigh and spine being upright. However, as seen in Table 4.6, the classifier could predict slow walking down to 0.38 m/s with similar accuracies as the average accuracy of all walking events (Table 4.5).

A more likely explanation of the misclassifications is due to 'fuzzy' border effects during the transition zones between standing and walking or between standing and stair ascending or stair descending. This is evident by the accuracy for walking while on the treadmill being much higher than the accuracy when walking in the other experimental protocols. Due to the nature of experimental protocol 5, in which the participants walk on a treadmill for 30 s, accelerometer recording only commenced once a steady state speed had been achieved on the treadmill, hence there was no standing-to-walking transition. This contrasts with non-treadmill walking where every walking event was preceded and succeeded by another activity, frequently being standing, hence there exists fuzzy border effects. Although these transition zone times may be small, the one-second interval used to create parameters means there is at least 0.5 s of overlap between activities (Figure 4.2). Although the transition zone times are only small, there are numerous walking events which only last a few (approximately three) seconds or less during experimental protocol 1, as participants were required to change from one activity to another in a different position within the laboratory (e.g. from laying down on a mat to sitting in a chair required walking between the mat and chair). This, therefore, creates numerous walking events in which a transition zone of approximately 0.5 s is a large portion of the entire walking event, and if misclassified as standing, thus reduces the accuracy of walking classifications. These 'fuzzy' border effects are experienced between any of the activities that the classifier can predict, therefore the reverse of this situation is also possible, where standing can be misclassified as walking. This is highlighted by the increase in accuracy of predicting standing when there are no fuzzy border effects, such as in experimental protocol 4 where the accuracy increases to 99.9%, even while upper body motion occurs.

A similar statement is true for the stair ascending and descending experimental protocol, in which due to the limited number of steps (four), each stair ascending and descending trial would last approximately 2.5 to 5 s and each was preceded and succeeded by standing. Thus, there was a proportionally high overlap of activities compared to total stair ascending/descending time, therefore reducing accuracy.

Transitions are another activity with an accuracy below 90%. Transition most likely had reduced accuracy due to the high proportion in time between the one-second window overlap of different activities and the time spent performing transitions. Another possible reason is the difficulty in defining when a transition both commences and concludes in video analysis. Both explain why transitions were misclassified as all other activities.

Although direct comparisons cannot be made due to the varying experimental protocols for validation and a different number of activities capable of being predicted, the activity classifier presented in this study has been shown to have similar or greater accuracies to other accelerometer-based activity classifiers reported in previous work [36, 37, 40, 41]. Similar to this research however, previous activity classifiers were validated in lab-based studies [36, 37, 40, 41]. The presented classifier can predict a total of 13 distinct activities, while previously reported classifiers range from five to eight distinct activities [36, 37, 40, 41]. Although predicting a greater number of activities leads to a higher resolution on classified activity data, it can cause confusion in the model when activities are similar (e.g., walking and walking on an incline) and thus reduce accuracy.

The accuracy of previously reported classifiers have a range of 81.3 to 91.9% for standing, 84.1 to 95.0% for sitting, 94.0 to 99.4% for lying, 70.3 to 95.9% for walking, 76.8 to 98.3% for jogging/running, 61.5 to 71.0% for stair ascending, and 44.3 to 69.6% for stair descending [36, 37, 40, 41]. This shows the presented activity classifier to be the most accurate in predicting standing, sitting, and stair ascending, whilst having similar accuracies for lying, walking, jogging, and stair descending.

The classifier presented by Lugade et al. [36] could also predict transitions with an accuracy of 85% when fidgeting was excluded. The classifier presented in this research could predict transitions with an accuracy of 83.7%, being very similar in accuracy to the classifier by Lugade et al. [20]; however, in the training and validation sessions, participants were not given any instruction on not being able to fidget.

To the best of the author's knowledge, this is the first time a classifier has been reported to predict when jumping and walking on an incline occur. Jumping was

classified correctly 96.6% of the time, being the most accurate dynamic activity when transitions were present (i.e. not including treadmill walking). This is likely due to the unique biomechanical action of jumping compared to the other activities which can all show similarities (e.g. walking, stair ascending, stair ascending, and walking on an incline are all forms of two-foot support locomotion and as such accelerometer signals can be similar).

Walking on an incline has not been previously included in activity recognition models. It was included in this research however as it has an increased energy expenditure over flat-level walking (Table 2.4) and could, therefore, reduce the time required to reach daily energy expenditure goals. Upon validation, the activity classifier developed in this research successfully predict incline walking 80.5% to 98.2% of the time, depending on the degree of incline, where the 20% gradient incline was more likely to be predicted correctly. The likely reasoning for this is that walking on a 20% gradient is more unique from level walking than walking on a 10% gradient.

Similar to the analysis performed by Lugade et al. [36], the activity classifier created in this research was also tested in its ability to determine walking when participants were walking slowly, as instructed to do so in experimental protocol 2. Predicting slow walking has importance when tracking the activity of the elderly, where it has been found that there is a 12 to 16% decline in walking speed every decade after 62 years of age [200]. Slow walking has also been identified as a risk factor for some non-communicable diseases [156]. For example, those who walk habitually faster than 4.8 km/h (1.33 m/s) have 53% lower risk of stroke compared to those who walk less than 3.2 km/h (0.89 m/s) [156]. As seen in Table 4.6, when using the activity classifier to classify the walking trials, it was on average more accurate when classifying the slowest walking trial for each participant. This is a surprising result as it was hypothesised to be less accurate during slow walking, instead being predicted as standing. However, this result is due to a lower proportion of the time in transition zones as when walking slower, it takes longer to walk the required 10 m. From Table 4.6, it can also be seen the classifier is highly valid to be able to predict walking at speeds as low as 0.38 m/s with an accuracy of 86.9%. One participant was instructed

to walk very slow, averaging a speed of 0.06 m/s over the 10 m. As can be seen in Table 4.6, the activity classifier struggled to accurately predict such slow walking, with an accuracy of only 9.0%. However, a walking speed as low as 0.06 m/s is very unlikely to occur. The results of this analysis show that although the activity classifier can predict slow walking, there is a lower limit in which it performs this to a suitable accuracy.

This suggests there needs to be separate models for different groups of varying physical ability. For example, there is no reason in training an activity classifier model for slow walking individuals with high walking speeds, or with activities they cannot perform due to certain health problems, such as jumping and jogging in patients with severe osteoarthritis. Similarly, there is no purpose in training an activity classifier for use in the non-elderly population with very slow walking speeds, such as speeds below 0.8 m/s. The exception for this, however, is for individuals with health issues that cause them to walk slower such as those suffering from obesity, injury, or from musculoskeletal conditions. Therefore, the activity classifier presented in this research is aimed for use with the healthy, non-elderly population due to the health status and age of participants, as well as the activities used in training and validating the model. This is a key limitation of the activity classifier presented in this research as it can not be used universally. However, the methods used to create this classifier could be applied in similar ways to various groups of people (children, the elderly, physically impaired etc.) to produce numerous group specific activity classifiers.

The average classification accuracy for the slow, medium, and fast treadmill walking speeds is 98.3%, 98.1%, and 98.9% respectively (Table 4.7) therefore proving to be consistent in accuracy in predicting walking across numerous treadmill walking speeds. This increase in accuracy over those shown in Table 4.6, even when at lower speeds, is due to the non-existence of transition zones between activities in the treadmill trials (experimental protocol 5). In combination with all the other results discussed, this shows that the accuracy of the activity classifier created in this research is largely dependent on the type and duration of activity of the user. For instance, the accuracy of the activity classifier to predict walking during a single one-hour event of

walking is very likely to be higher than the accuracy during multiple walking events that have a total duration of one-hour, which can be seen when comparing accuracies obtained from experimental protocol 2 (short walking bouts) and experimental protocol 5 (simulating long walking bouts).

Limitations with the current activity classifier include the low positive prediction rates of stair descending, being 61.9%. The small number of steps (four) on the staircase is another limitation. If the number of steps in the staircase was increased, the accuracy of the classifier would likely increase due to a lower proportion of fuzzy border effects. A greater number of steps in the staircase would also lead to more training data available for stair ascending and descending, which could also increase the accuracy of the activity classifier in these activities.

Subject related factors, such as age and mass may affect the accuracy of the classifier presented in this research. As discussed previously, this activity classifier was produced using healthy, non-elderly participants. As such, errors may arise in positive prediction rates of classifier when used with elderly participants due to different movement patterns. A similar statement is true unhealthy individuals, such as the obese, which could experience significantly greater soft tissue movement relative to underlying bone and therefore affecting accelerometer readings.

Another limitation of the current study is the difficulty in what activity to label turning on the spot by participants during experimental protocols one to three. In this study, turning on the spot was classified as walking, as participants generally lifted their feet one at a time, similar to walking. However, this was commonly performed at a far lower intensity than walking and thus accelerometer signals were similar to standing, and therefore turns could often be classified as standing.

In future work, turning on the spot may be identified as a separate task. This may be introduced into the activity classifier via the use of gyroscopes, which measure angular velocity. Additional future work on the activity classifier would be the inclusion of a tilt angle parameter, calculated using accelerometer measurements in each axis (equation 3.6). The inclusion of this parameter may decrease the confusion between walking and walking on an incline.

4.5 Summary

This chapter details the creation and validation of a new activity classifier which can predict 13 distinct activities. The activity classifier was created using machine learning and trained using 102 parameters from data collected by two triple-axis accelerometers, which were placed on the anterior thigh and upper thoracic region of the spine.

From this research, there were a number of key findings. Firstly, there was no significant difference in accuracies of the ensemble bagged trees, quadratic support vector machine, and cubic support vector machine models in classifying activity. Of these models, however, the ensemble bagged trees model had a significantly faster prediction speed and was hence chosen as the most suitable model for use in this research. When comparing cut-off frequencies, it was found that a cut-off frequency of 5 Hz for the low- and high- pass Butterworth filters gives the greatest accuracy for the classification of the 13 distinct activities used in this research. This is contrary to the commonly used cut-off frequencies of between 0.25 Hz and 1 Hz. However, for the majority of these various cut-off frequencies, the average positive prediction rates were within 2% accuracy of the 5 Hz model. Based on these results, an ensemble bagged trees model utilising a cut-off frequency of 5 Hz for low- and high- pass filtering was, therefore, the chosen activity classifier for further use in this research.

The activity classifier created could predict the 13 distinct motions with an average accuracy of 90.3% when using the experimental protocol outlined in Section 4.2.2. There are some activities, however, including stair descending, that have low accuracies and need further work before these can be predicted with confidence. The average accuracy of the classifier increases to 95.6% when only the tasks of standing, sitting, lying, and walking are considered, and therefore meeting the primary aim set out in Section 1.3 while also narrowly meeting the extended aim. The results also indicate that the activity classifier can predict slower than average walking pace with high accuracy, with speeds of 0.38 m/s classified with an accuracy of 86.9%, just slightly below the overall average accuracy of walking. The results from this study

also indicate that the classification of activity accuracy increases as the length of time in which an activity is performed is extended, as shown by the accuracy of the activity classifier during treadmill testing as the ability to accurately predict walking increases from 87.3% to 99%.

Chapter 5

The Spinal Motion Measurement Device

5.1 Aim

The aim of this part of the research was to create an inexpensive sensor system capable of measuring three-axis angular orientation and angular velocity (flexion-extension, lateral bending, and axial rotation) of multiple positions along the spine. Although angular velocity has been shown to be a better predictor and measurement parameter for back pain than the range of motion and hence more able to monitor respective rehabilitation [201], many commercially-available devices do not measure this. Finally, it has been shown that prolonged sedentary postures not only increase the risk of back pain occurring but are also proved to have harmful effects on general human health and increases the risk of numerous non-communicable diseases. Numerous studies have been conducted that have shown that an increased risk of death and chronic diseases such as coronary heart diseases, stroke, diabetes, some cancers, and obesity exists for individuals that commonly experience extended episodes of sedentary behaviour and inactivity as discussed in Section 2.3.1. Therefore, a further aim of the SMM was to have the ability to monitor static and dynamic activities. Further design aims of the device include being lightweight and portable, so it does not affect the natural motions of daily living. Although not completely fulfilling it, the aim of this chapter directly relates to aim 3 detailed in Section 1.3. The method for activity classification will not be discussed in this chapter as it has been conversed in previous chapters.

5.2 Device Design

5.2.1 Hardware

It was a requirement that the sensors of the SMM device (Figure 5.1) be capable of measuring flexion-extension, lateral bending, and axial rotation angles of the spine, as well as the speed of these movements. Inertial measurement units (IMUs) are the combination of accelerometers and gyroscopes used to measure linear and angular motion [103] and extra sensors such as magnetometers [104-106] can be included to compensate for orientation drift. IMUs have been used in the past for numerous applications including trunk inclination measurement [202, 203], 3D spine kinematic measurement of participants with and without back pain [204, 205], identification of low back pain [205], estimating spinal moments, and estimating ground reaction forces [206]. Therefore, IMUs were selected to be the spinal kinematic measurement sensors as they are also lightweight and portable, and thus have a minimal affect the

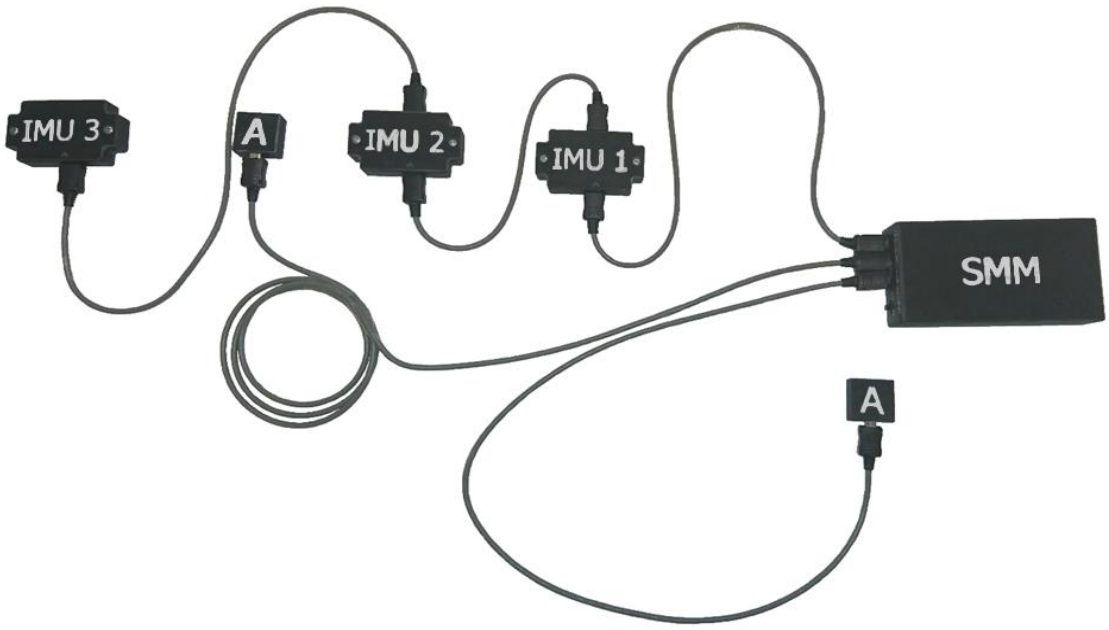

Figure 5.1 The Spinal Motion Measurement device (SMM), showing the 3 inertial measurement units (IMUs) connected in series, 2 accelerometers (A), and control and power box (with SMM label) consisting of the Arduino Mega, BlueTooth module, battery and charger all enclosed in 3D printed cases for protection.

natural movements of the user. SparkFun Razor 9DOF IMUs were chosen as these sensors have been shown to be accurate in measuring motions at, and above, self-selected spinal motion speeds as discovered by the research discussed earlier in Chapter 3. These sensors are also inexpensive, costing AU$115, and thus keeping to the aim of this research in developing a low-cost device (Section 1.3).

For monitoring the activity of the user, the SMM device uses two Adafruit (New York, United States) tri-axial ADXL326 accelerometers with ±16g measurement range, which are placed on the thigh and spinal sections of the human body, where the spine accelerometer can also aid in spinal posture measurements through the use of tilt angles. The use of tri-axial accelerometers allows for a more complete depiction of the activity over single-axis or bi-axis accelerometers. A ±16g measurement range of the accelerometer was selected in order to measure the dynamic range of all daily physical activities, where running typically has the greatest magnitude of acceleration of up to 12g [195]. The accelerometers will also collect data at 50 Hz as is adequate to measure human movement, as the majority of human motion occurs below 18 Hz [195].

The SMM was designed to be portable and have the minimal restriction of motion, which were achieved by allowing wireless data acquisition. This was accomplished using an onboard battery (2400 mAh Lithium Polymer) and charger for power, and BlueTooth (SparkFun BlueTooth Mate Gold WRL-12580) for data transmission.

An Arduino Mega was selected to collect and collate data from each sensor and chosen over competitors due to its low cost, popular use, and comparatively high number of serial ports (N = 4) allowing up to three IMUs (as BlueTooth requires the fourth port) to measure spinal kinematics, as well as numerous analogue devices to be incorporated via the analogue pins. For the purpose of the SMM, two analogue accelerometers were included for activity recognition, giving a total of five inertial sensors. A simplified schematic of the component connections of the SMM device can be seen in Figure 5.2, showing the accelerometers are connected directly to the

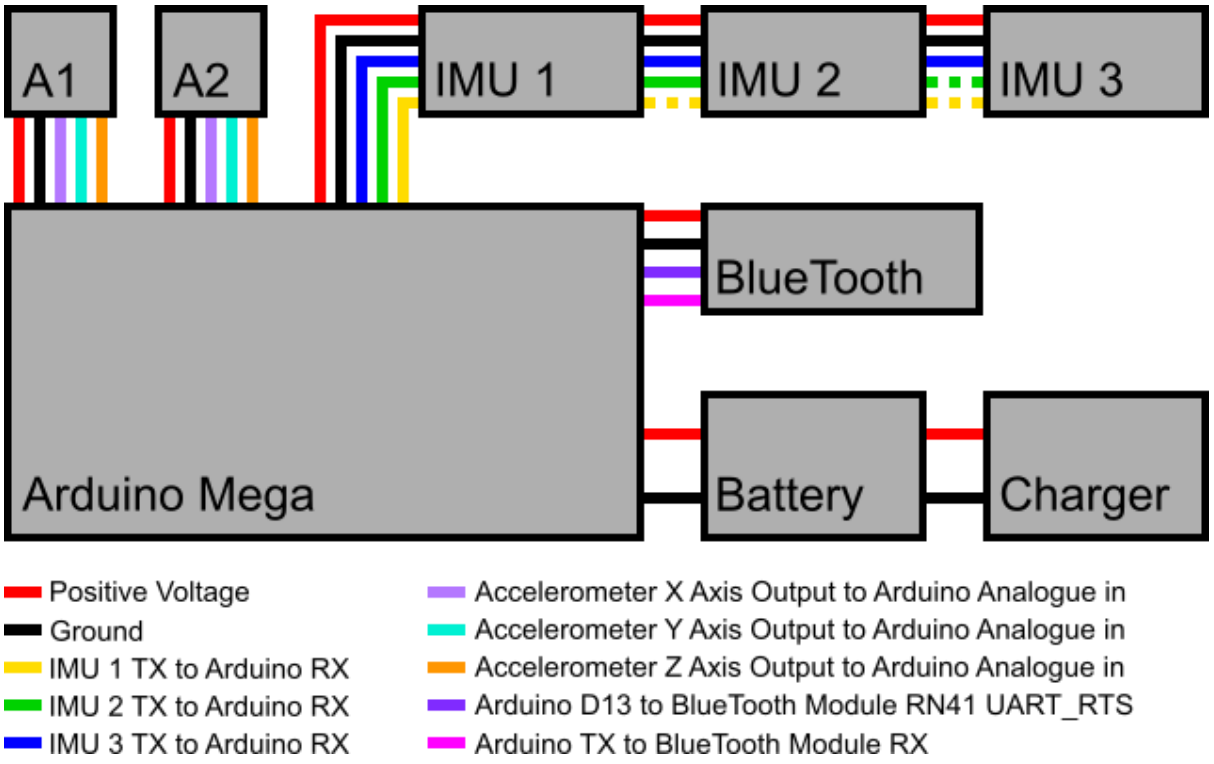

Figure 5.2 Simplified circuit diagram of the Spinal Motion Measurement device (SMM) showing how the inertial measurement units (IMU), Accelerometers (A1, A2), Arduino Mega, BlueTooth module, battery and charger are connected. It should be noted that TX is the transfer pin, RX is the receive pin, and the dashed yellow and green lines indicate that these connections exist but are not utilised in this configuration, allowing any number of IMUs (maximum 3) to be used and in any order. E.g. Can be used with just one IMU, and that IMU can be any of the IMUs.

analogue pins of the Arduino Mega, whereas the IMUs are connected in series to their own serial port, allowing data to be collected by each of the three IMUs at 48Hz.

All sensors are coupled via micro-USB cables, which allow IMUs and accelerometers to be connected or disconnected. The device is also completely reprogrammable as the users have direct access to the USB input on the Arduino Mega and, via an FTDI (Future Technology Devices International) basic breakout, to the FTDI connectors on the IMUs, allowing researchers to alter the device to their specific application. Including all hardware, the SMM had a build cost of AU$630 (US$500).

5.2.2 Software

The SMM operates using three main pieces of software for each individual IMU control, entire SMM control, and data collection. Each IMU includes an Arduino Pro on board such that the function of the IMU can be reprogrammed. The IMU software has a number of tasks to be performed as part of the SMM device. The software, which is modified from Razor AHRS Firmware v1.4.2 (released under GNU General Public License v3.0, Copyright © 2013 Peter Bartz), has several inbuilt functions which include:

1. Initialisation

   The initialisation aspect of the code has several roles to perform such as defining baud rate, the frequency of data collection, initialising the accelerometer, gyroscope and magnetometer sensors within the IMU, and resetting the sensor fusion required to obtain accurate orientation data from the fusion of accelerometer, gyroscope, and magnetometer data.

2. Sensor reading

   Raw values of accelerometer, gyroscope, and magnetometer measurements are read from each of the tri-axial sensors. Calibration factors are then applied to the raw data obtained.

3. Data Conversion

   Calibrated data is converted into orientations in a rotation matrix form via algorithms and sensor fusion.

4. Drift Correction

   Drift correction is primarily performed to data collected by the gyroscope due to large errors associated with obtaining orientation from the integration of angular velocity.

5. Euler Angles

   Euler angles are calculated from the drift corrected rotation matrix in a Yaw-Pitch-Roll rotation sequence. The SMM was designed such that yaw, pitch, and roll equate to axial rotation, lateral bending, and flexion/extension movements of the human spine respectively, as depicted in Figure 5.3. This rotation sequence was based on recommendations that the largest rotation axis is the first in the sequence, the smallest rotation axis is second in the sequence, and the remaining axis is the third in the rotation sequence [190]. From these recommendations and data in Table 2.1 that shows the ROM of the spine, lateral bending of the spine experiences the least degree of rotation of the three-movement axes and thus was chosen as second in the rotation order. Flexion/extension, however, has the highest ROM of all 3 axes but was not chosen as the first rotation in the rotation order as IMUs cannot tell the difference between axial rotation of the spine, and when an individual is turning around (Figure 5.3), thus effectively giving a 360° ROM in this axis. Although the human body can have a complete 360° of motion in all three axes, it is more likely an individual will turn around while standing upright than turning over their head in either of the other two axes; hence why axial rotation was chosen as the first rotation axis in the order of rotations.

6. Data Output

   The control software is uploaded to the Arduino Mega and is primarily used to collate data to be sent via BlueTooth to a receiver. The software allows the SMM device to read data from each IMU when the IMU is ready to send each data packet, thus keeping the data collection frequency to a maximum of 48 Hz. Collected data from the IMUs is organised into a text string consisting of an identifier (A, B, or C); roll, pitch, and yaw Euler angles; X, Y, and Z axis angular velocities; time in milliseconds since power on; and, an ending character to express that all data has been collected for this data packet. The software reads data collected from both accelerometers at 50Hz, approximately the same frequency as the IMUs, where these frequencies are adequate for measuring human motion [195]. The data collected by the IMU is then sent to the Arduino

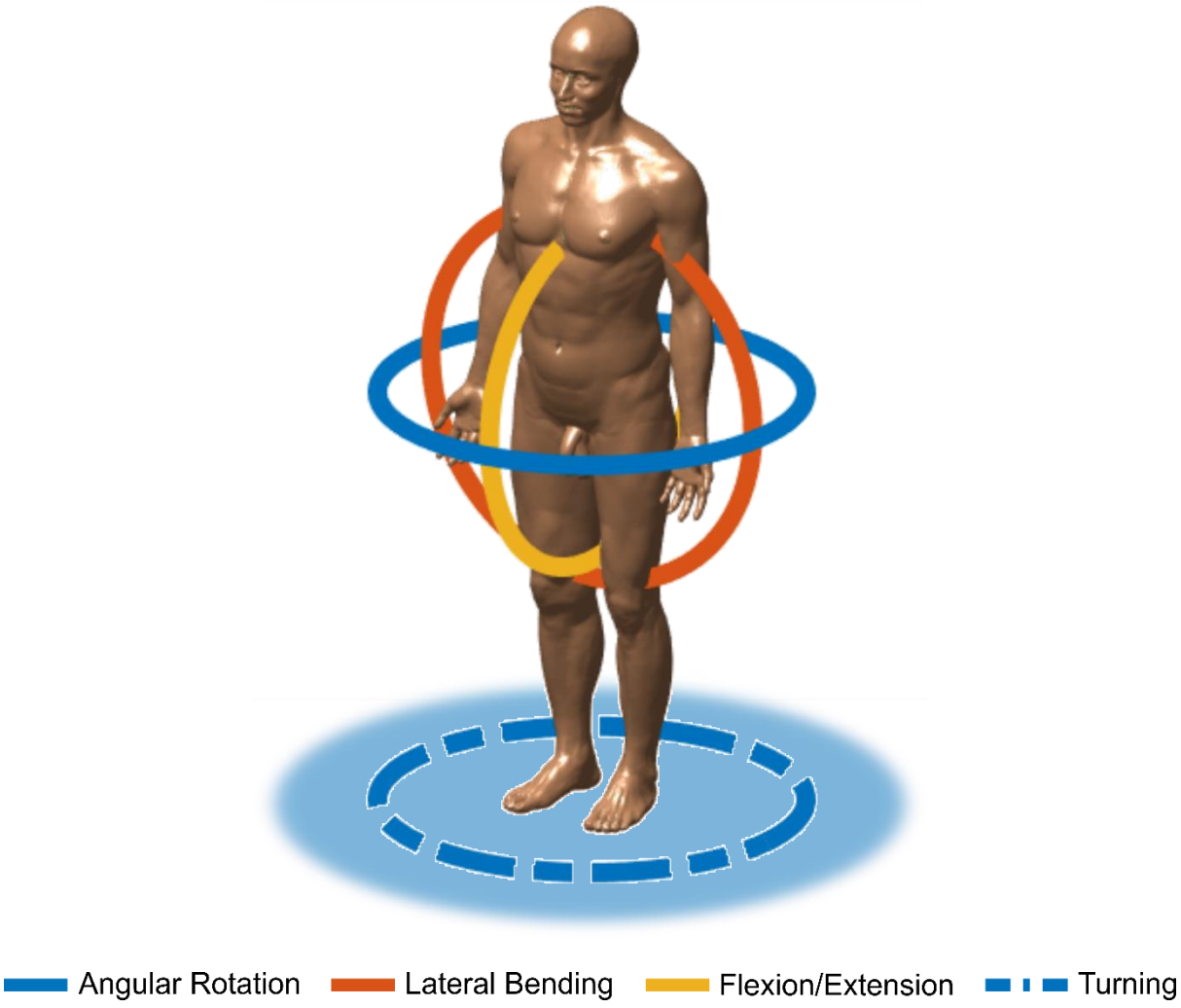

Figure 5.3 Axes of motion of the spine; angular rotation (AR), lateral bending (LB), and flexion/extension (FE) and of the whole body, turning, which occurs in the same axis as angular rotation of the spine due to the AR-LB-FE rotation order selected for the inertial measurement units (IMUs) of the Spinal Motion Measurement device (SMM).

Mega. Collected data from the accelerometers is arranged such that each data packet consists of an identifier (L or S); X, Y, and Z axis accelerations; time in milliseconds since power on; and, an ending character to express that all data has been collected for this data packet. The collected data is then sent via BlueTooth to a data logger, with an example of how the data appears in Figure 5.4. The code also incorporates a fail-safe by ensuring the BlueTooth module is not overloaded with data from the sensors; which can cause the connection between the SMM and data acquisition apparatus to be broken and thus data collection to cease.

Data collection can be performed using any software which can acquire data from serial ports. For instance, the SMM device has been successfully tested

```
A 64.42,-0.81,175.86,-0.92,-1.97,-0.32,15644@@
B 55.83,-2.54,172.02,-0.18,1.47,0.98, 15644@@
C 108.02,-1.45,162.52,0.40,-0.97,0.05,15644@@
S 1.07,0.24,0.12,16256@
L -1.01,0.12,-0.11,16256@
A 64.45,-0.86,175.85,-1.13,-1.76,-0.19,15665@@
B 55.86,-2.50,172.04,0.10,1.26,1.12, 15665@@
C 108.05,-1.50,162.52,0.33,-0.41,0.33,15665@@
S 1.01,0.19,0.12,16276@
L -1.01,0.12,-0.11,16276@
A 64.40,-0.89,175.83,-1.55,-1.27,-0.25,15685@@
B 55.84,-2.45,172.07,0.31,1.47,0.91, 15685@@
C 108.06,-1.50,162.51,0.33,-0.62,0.26,15685@@
S 1.01,0.19,0.12,16296@
L -1.01,0.12,-0.11,16296@
```

Figure 5.4 An example of how data sent from the SMM appears when collected by the data logger.

using Tera Term v4.93 (OSDN Corporation, Japan) and a purpose-built graphical user interface (GUI) created in MATLAB R2016b (The MathWorks Inc., Natick, MA, USA).

The SMM device is able to determine the activity of the user through the use of algorithms applied to the accelerometer data. A model has been created in this research that can determine if the user is standing, sitting, lying, walking, jogging, jumping, stair ascending and descending, walking on an incline, and transitions between activities. This model was created in MATLAB's in-built Classification Learner application, using data obtained from twelve participants performing the numerous activities over extended periods of time to train the classifier. The model has been shown to have an average accuracy of 90.3% when all activities are considered.

5.3 Discussion

Compared to other similar devices such as the Lumo Lift and ViMove that only use one and two sensors respectively to track spinal posture, the SMM device uses up to four sensors (3 IMUs and the spinal accelerometer) and thus estimates spine posture with greater fidelity. To measure whole spine posture with the SMM, it is recommended to place the spinal accelerometer on the spinous process of one of the upper thoracic vertebrae (T1-T6) as this region experiences lower levels of motion than the cervical and lumbar segments [1-6, 207, 208] which is where the more accurate IMUs should be placed. One of the IMUs should be placed on the sacrum for a body reference frame. The sacrum was chosen as is part of the pelvic region, the region between the thorax/abdomen (the main part of the body) and the lower limbs and is thus commonly chosen for the body reference frame. The remaining IMUs can be placed along the spine at any spinal level as chosen by the user/researcher. In the future, pre-defined locations of the remaining IMUs would need to be set for the SMM to become a commercial device such that IMU outputs can be compared to predefined postural thresholds for poor posture. The IMU sensors are placed such that the roll axis of measurement aligns with flexion-extension, pitch aligns with lateral bending and yaw aligns with angular rotation. To ensure accuracy and repeatability at different levels of the spine, users of the SMM should take care in their mounting procedures of each sensor on the spinous processes. That is, placing the sensors on the spine as seen in Figure 5.5, in that the sensors are placed flush on the back, and the long edge of the case travels in a pure mediolateral direction.

When compared to other IMUs, the SparkFun Razor IMU has comparable accuracy to the MicroStrain 3DM-GX3-25 in numerous types of motion while being far less expensive (AU$115 vs AU$2900), and thus were suitable choice to implement into the SMM. With approximate costs of AU$630, the full SMM device is still far less expensive than the MicroStrain 3DM-GX3-25 IMU but allows for more information to be obtained. Further, it can transfer this data wirelessly via BlueTooth to a data logger. The advantage of the MicroStrain IMU, however, is in its precision accuracy,

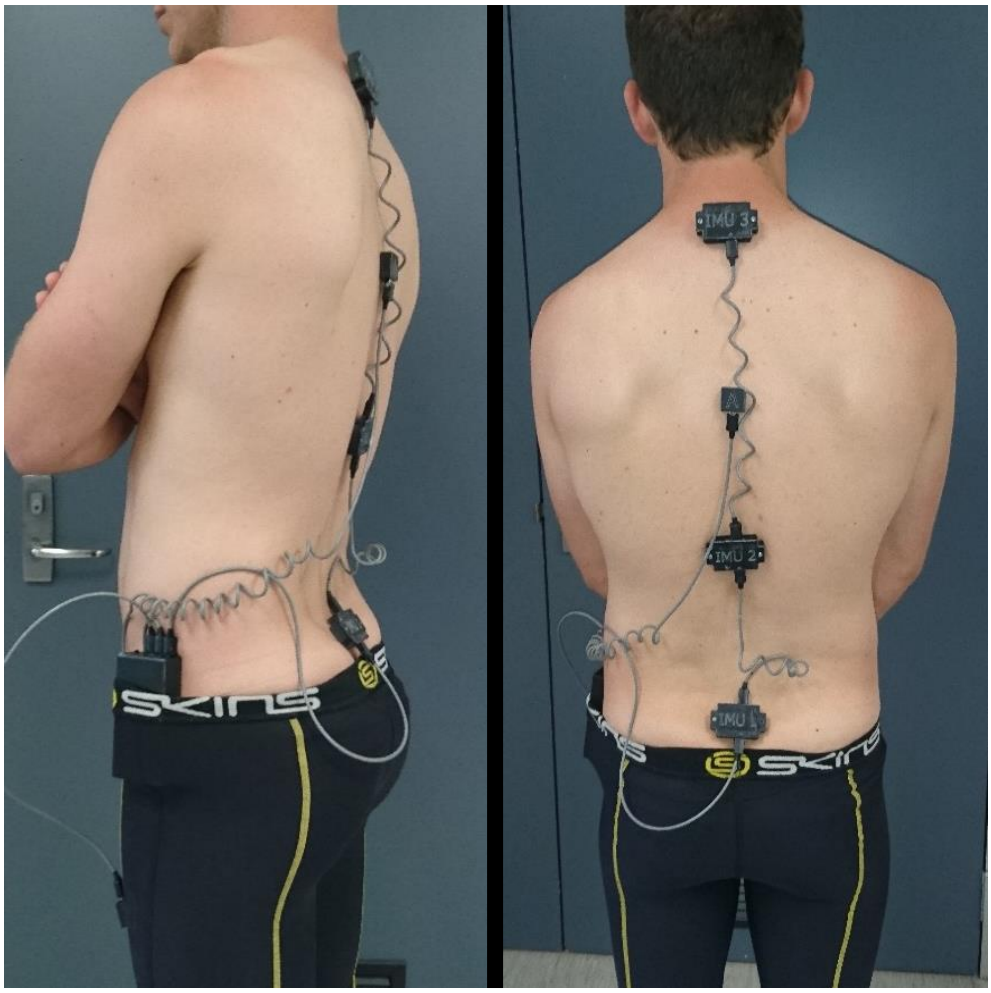

Figure 5.5 The Spinal Motion Measurement device applied to a human's back, showing three IMUs placed such that the long edge of the case runs purely left-to-right, and accelerometers placed on the thigh and thoracic spine such that the case edges run left-to-right and superiorly-to-inferiorly, and cable connects to the under-edge.

especially during faster motions, ease of calibration, higher data collection rates and ease of altering the parameters collected through dedicated software.

The SMM has a number of advantages and disadvantages when comparing to other devices in terms of outputs given. Although the other devices listed in Table 2.3 can give posture information, including bio-feedback when poor posture is maintained and inactivity warnings, only the SMM and ViMove allow for kinematic data to be recorded. This is important for a more thorough kinematic analysis than what the others can provide for use in research or by clinicians. When applying the classification algorithms developed in Chapter 4, the SMM can also predict numerous standard activities of daily living, rather than just activity and inactivity.

Another important comparison between devices is their method of obtaining data for posture analysis, including the sensors used and processes applied to the raw sensor data. The majority of the devices in Table 2.3 use an accelerometer to determine the tilt angle of the spine and compare this to a predefined threshold to determine if an unsafe posture is reached. However, accelerometers are not as accurate or robust as IMUs in determining orientation, and they also lack the ability to measure rotations around the gravitational axis. Some of the devices, such as Alex and UpRight Pro have included additional sensors to help increase accuracy. The BackTone 4000 is a device that uses an electronic sensor, which when triggered will emit a noise to tell the user to adjust their posture. The triggering of this device is through applying tension to an attached strap, which occurs when the user bends forward. This limits the device in that it can only be used to give an indication on poor posture compared to a predetermined threshold, not a severity or duration of good and poor posture, and thus giving no quantitative assessment of posture over time. The ViMove and SMM use IMUs, which have been shown to be more accurate in measuring orientation than using accelerometers alone, and they also have the ability to measure rotations around the gravitational axis and are therefore a better option for measuring spinal kinematics than accelerometers.

Ease of use is one area in which the commercial products have an advantage over the SMM, particularly the Lumo Lift which simply clips onto the user's shirt, has one push-button operation, and connects with BlueTooth to a smartphone app. The ViMove, UpRight Pro and UpRight Go require the user to place the units on their posterior, which may make alignment difficult without the aid of another person. The SMM also requires placement of several inertial sensors on the posterior side of the body and so its level of difficulty of use is similar to that of the similar placed devices, but higher than Lumo Lift and the devices worn on the head such as Alex. Currently the SMM requires computer software to be used to its full potential, including data acquisition of three-dimensional orientation and angular velocities and the classification of activity, whereas numerous other devices connect straight to a smartphone App and are thus easier to use in day-to-day living. This is a limitation of

the SMM, however, the ease of use of the SMM can be addressed in the future but is outside the scope of this thesis.

A further limitation of the SMM device is the frequency with which it can collect data, being 48Hz per IMU. This is lower than other technologies used in human kinematic testing such as VICON motion capture camera systems and Biometrics movement analysis systems including electro-goniometers and accelerometers (Biometrics Ltd. Newport, UK). The data logging rate of the SMM device, however, is still high enough to track the motion of the spine based on recommendations made by Mathie et al. [195].

Further development of the SMM would see the SparkFun Razor 9DOF IMU replaced by its successor, the Razor 9DOF IMU M0, which is 40% less expensive than the original, cutting costs of the overall SMM device by approximately AU$150. This IMU also has the potential for a greater accuracy in orientation data, higher data collection rates and is smaller in size. Further to this, the SMMs software should be developed into a smartphone app to allow for greater usability away from a computer, however, is outside the scope of this thesis.

5.4 Summary

The SMM device developed had a major emphasis on being inexpensive while also not lacking quality in accuracy and usability, and therefore addressing the third aim of this Ph.D. The device features interchangeable sensors, allowing between one and five inertial sensors (up to three IMUs and two accelerometers) to be used at any one time. The device not only tracks spinal posture but has the capability to monitor user activity as both have been linked to the increased risk of back pain and other non-communicable diseases. A major limitation of the SMM in its current state is its ease of use which should be addressed before it is able to be used by the general population. Other limiting factors of the device include its size, and the comfort of the device, particularly during prolonged use. Once these limitations are addressed, the device should then be an attractive option for use by researchers and the wider community to obtain spinal kinematic measurements, the classification of activity, and to reduce the incidence of back pain.

Chapter 6

Posture Measurement and Tracking: A Validation Study

6.1 Aim

The aim of this section of the research was to validate the spinal sensors of the Spinal Motion Measurement device (SMM), the SparkFun Razor IMUs, in their ability to track human spinal posture/orientation on human participants. This aim directly relates to the fourth aim explain in Section 1.3, where the goal is to validate the SMM to have an accuracy within ±5° for spine kinematic measurements in all three dimensions, therefore offering similar accuracies to the Dorsa ViMove, albeit being less expensive. This range of accuracy would also be sufficient to show the SMM to not have clinical significant difference to the reference measurement, which is desired to show the validity of the SMM. The ±5° threshold can be seen to be within the 10% threshold for clinical significance by comparing it to 10% ROM typically seen in the spine (Table 2.1), in which the tightest threshold is ±7.7° (10% of lateral bending ROM). The accuracy of the IMUs was compared to the tracked motions by a VICON MX Vantage V8 (Vicon Motion Systems Ltd., Oxford, United Kingdom) optical motion capture system, which is the gold standard in human kinematic testing. The comparisons occurred at three distinct regions of the spine to investigate possible differences in accuracies at the varying body locations. It is hypothesised that the SMM will have an average accuracy of within ±5° for all axes over all motions, due to evidence obtained in Chapter 3. It is also hypothesised that the SMM will have greater errors when measuring yaw, which has commonly been indicated in previous literature, as well as when measuring motion on superior regions of the spine due to greater ranges of motion and angular velocities with respect to the global coordinate system.

6.2 Methodology

6.2.1 Participants

The investigation included six healthy participants (N = 3 females, 3 males) with a mean ± standard deviation age, mass, height and BMI of 27.6 ± 5.4 y, 67.5 ± 9.2 kg, 1.71 ± 0.09 m and 22.9 ± 1.3 $kg \cdot m^{-2}$ respectively. All participants had the experimental protocol explained to them and gave written consent to participate. The study gained ethics approval from the Human Research Ethics Committee at the University of Adelaide. The inclusion criteria for this study included male's and female's aged between 18 and 55 years old, inclusive. The exclusion criteria included individuals who had experienced an episode of back pain in last 12 months, and individuals who have a history of spinal surgery.

6.2.2 Experimental Task

Each participant performed 15 repetitions of four different movements at a fast and slow speed. The fast speed required each repetition to be completed in two-second intervals, while the slow speed allowed six seconds per repetition. Each half repetition was kept in time with a metronome. Three movements were considered simple motion: twisting, side bending, and front bending. These motions were chosen to have the majority of movement occurring in a single axis of spinal motion, being angular rotation (AR), lateral bending (LB) and flexion-extension (FE) respectively. The fourth movement was a coupled motion (CM) task, which saw the participant touch a stool placed at a constant, comfortable distance in front and to the left of the participant's left foot. All participants completed a follow-up session within four weeks of the original testing.

6.2.3 Equipment and Data Collection

Three IMUs (SparkFun 9 Degrees of Freedom Razor IMU SEN-10736) were assembled into a single measurement system. This device also consisted of an Arduino Mega, BlueTooth module (SparkFun BlueTooth Mate Gold WRL-12580), and a 2400mAh Lithium Polymer battery, allowing data to be collected wirelessly and portably. The IMU measurement system called the Spinal Motion Measurement device (SMM) was tested for accuracy against a 12 camera VICON MX V8 (Vicon Motion Systems Ltd. UK) system at three different spinal levels.

Three-dimensional Euler angle data from the IMUs of the SMM was collected wirelessly at a sampling rate of 48 Hz using Tera Term v4.93 (OSDN Corporation, Japan) and was later upsampled to 100 Hz using one-dimensional linear interpolation in post-processing after filtering. Three-dimensional position data from the VICON system was collected at 100 Hz using Nexus v2.5 (Vicon Motion Systems Ltd. UK). A 3rd order bi-directional low-pass Butterworth filter was applied to all measured data with a -6dB cut-off frequency of 6Hz. The same filter was applied to orientation (IMUs) and position (VICON) data as both are of the same dynamic order.

6.2.4 Sensor Placement

The three IMUs of the SMM were placed on the skin superficial to the spinous processes of the seventh cervical vertebrae (C7), twelfth thoracic vertebrae (T12), and sacrum (S) mid-way between the right and left posterior superior iliac spine (PSIS) using double-sided tape. Rigid clusters of four reflective optical markers with a diameter of 9.5 mm were then placed on each of the IMUs (Figure 6.1).

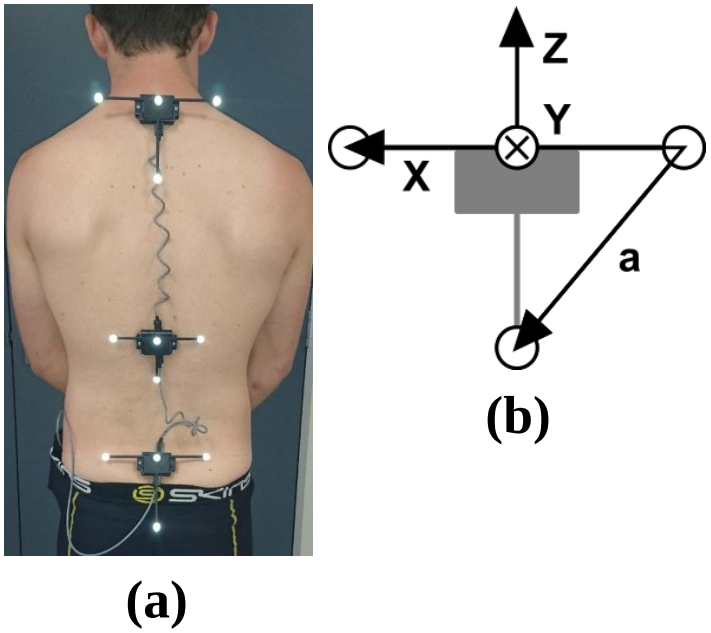

Figure 6.1 (a) Rigid marker clusters on top of the IMUs of the SMM placed on the seventh cervical vertebrae, twelfth thoracic vertebrae, and sacrum of the spine. (b) Local co-ordinate system defined for the VICON measurements, in which the 'X' and 'a' vectors are produced directly from marker locations. The Y axis is denoted by a central cross to indicate it is pointing anteriorly, and is the cross product of X and a. The Z axis is the cross product of X and Y and is pointing superiorly.

6.2.5 Orientation Calculation

Euler angles were obtained directly from the IMUs in a yaw-pitch-roll rotation sequence. In this validation study, yaw, pitch, and roll align with the angular rotation, lateral bending, and flexion/extension axes of the spine and thus the rotation sequence of the IMUs could be considered as AR-LB-FE. Euler angles were calculated from VICON data by using each rigid cluster to create a local coordinate system. The local coordinate system (Figure 6.1b) was created as follows: The **X**-axis was created by the line running from the right marker to the left marker at that level. Axis **a** is the line running from the right marker to the middle, lower marker. The **Y** axis is defined as the cross product of **a** and **X** pointing anteriorly and the **Z** axis was defined as the cross product of **Y** and **X** pointing superiorly. With these definitions, the AR, LB, and FE occur around the Z, Y, and X axes respectively. A rotation matrix with respect to the global coordinate system was created for each data frame and Euler angles were

then extracted in a **Z-Y-X** (AR-LB-FE) rotation sequence. To allow comparison in outputs of the two systems, the yaw orientation values for both systems were zeroed to account for coordinate system misalignments between VICON and the IMUs. The roll and pitch axis outputs for both systems were not zeroed, and hence absolute values were used for comparisons in these axes, and ROM for the yaw axis. Orientations were also not calculated relative to the sacrum IMU in this study, rather their position and orientation with respect to the global co-ordinate system. This methodology was chosen such that the absolute accuracy of the SMM sensors could be obtained.

6.2.6 Data Analysis

The root-mean-square error was calculated by using the difference in the time matched output of the IMUs and VICON for each time point across each trial. The standard deviation of the difference between the two measurement systems was calculated to give an indication of the variability of the SparkFun Razor IMUs.

A paired-samples t-test (95% confidence level) statistical analysis was performed (IBM SPSS Statistics v24, New York, United States) to determine if there was a significant difference in RMSE results between sessions, between speed pairs (fast and slow), and location pairs (Sacrum and T12, Sacrum and C7, and T12 and C7). Speed pairs were defined as the pairs of motions in which motion type, the location of sensors, and the axis of measurement were kept constant and speed was altered e.g. fast angular rotation sacrum roll and slow angular rotation sacrum roll. Location pairs were defined as the pairs of motions in which motion type, the speed of motion, and the axis of measurement were kept constant and analysis was performed between the different sensor locations e.g. fast angular rotation C7 roll and fast angular rotation T12 roll.

A Bland-Altman (BA) analysis was used on the simple motion trials to determine any bias in the orientation values in each of the three axes. For this analysis,

combined session data was used when no statistical difference was observed between sessions. To reduce the amount of data contained in each plot, only data from the middle three cycles of the 15 (cycles 7, 8 and 9) from each motion were used to create the BA plots.

Intra-class correlation coefficients (ICC (2, k)) [193] were determined to show the rate of absolute agreement in measurements between the IMUs and VICON systems. The ICC values were determined using the maxima and minima of the main axis of motion for each cycle. A similar method was used for coupled motion results, although ICC values were obtained for all three measurement axes. The minima and maxima points were chosen as they show the largest discrepancies between systems as determined graphically from orientation-time plots and BA plots. This gave the lower limit of agreement between the two systems. The ICC values were determined for the T12 and C7 locations only, due to the small motion of the sacrum not allowing the maxima and minima per cycle to be easily detected.

The percentage of time the IMU errors were within ±10% of the ROM of the VICON measurements ($ET_{10\%ROM}$) was another measure of performance used in this study. The threshold of ±10% was chosen as is the recommended threshold to show clinical difference in means [50]. This was calculated for each trial using two different thresholds for 10% ROM. Threshold 1 was determined using each individual trials relative ROM between the thoracic and sacrum IMUs, and cervical and sacrum IMUs. This threshold was calculated only for the main axis of motion for the simple motions, and for all axes in coupled motion. Threshold 2 was determined using the maximum relative ROM between the thoracic and sacrum IMUs, and cervical and sacrum IMUs for each axis observed for each participant over the two sessions. Thresholds in the second thresholding condition were therefore always greater than, or equal to, the thresholds used in the threshold 1 condition. For this performance measure, a value of 100% indicates that for 100% of the time the IMU has errors of less than ±10% ROM and value of 0% indicates that the error was never within ±10% ROM for that motion type. A graphical representation of this parameter using the same motion trial in both plots, but with the different threshold conditions can be seen in Figure 6.2. The figure

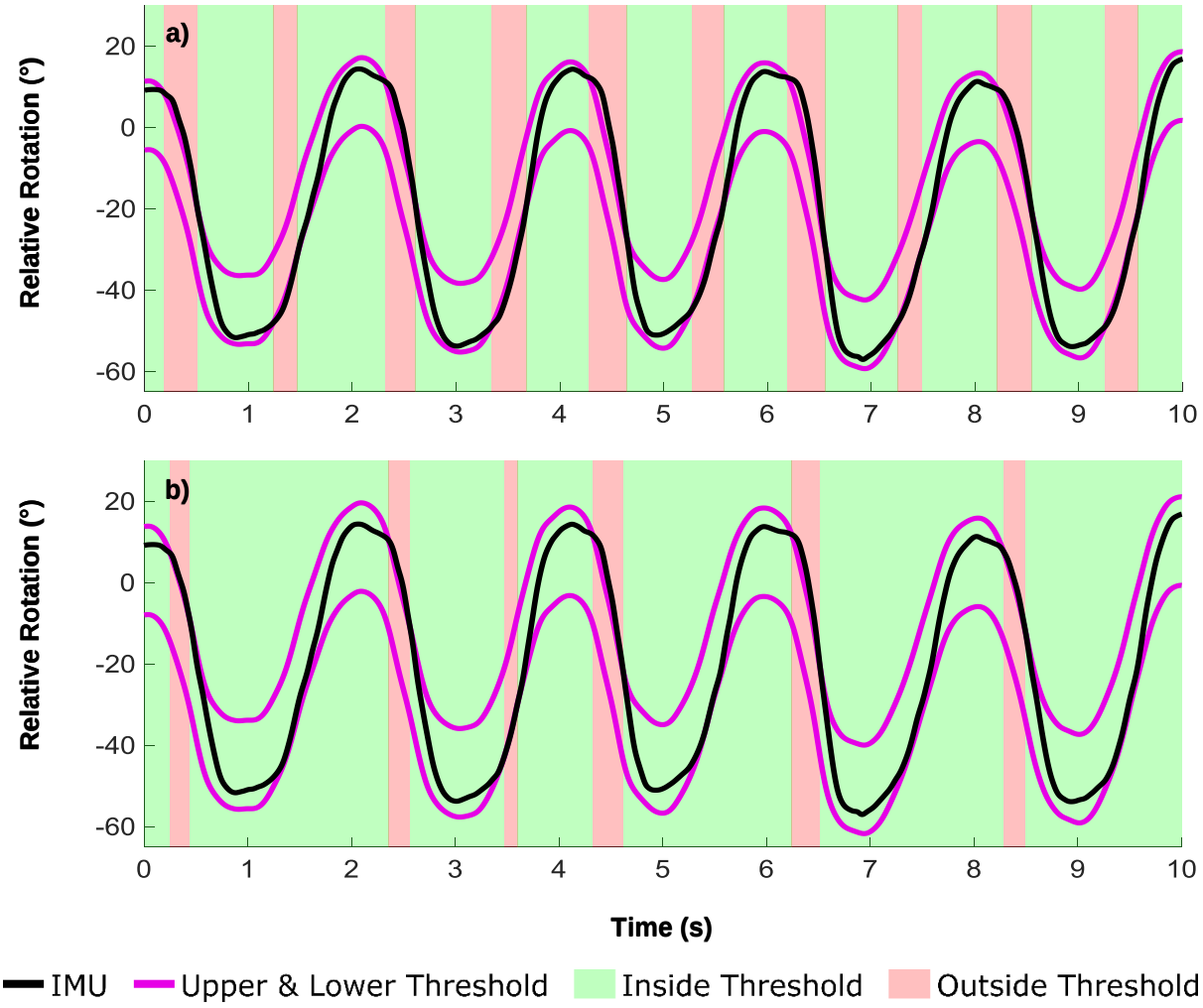

Figure 6.2 A graphical representation of the percentage of time an IMU errors were within ±10% of the ROM of the VICON measurements (ET10%ROM) for the T12 IMU roll axis from one participant during the first 10 seconds of the fast-coupled motion trial. Green represents the time when the IMU is within ±10% of the VICON measurement and red represents the time when the IMU is outside ±10% of the VICON measurement. Both plots represent the same trial, however, with different threshold values where thresholds for a) 10% of the range of motion experienced in the roll axis during the fast-coupled motion trial performed by this participant and b) 10% of the maximum range of motion experienced in the roll axis during all motion trials by this participant.

shows the roll axis for the fast-coupled motion trial performed by participant 4 during their first testing session. As can be seen, the $ET_{10\%ROM}$ is lower when the ROM is taken from the motion trial the parameter is focusing on (a), rather than the max ROM measured in the axis by the participant over both test sessions (b). The $ET_{10\%ROM}$ for (a) will always be less than, or equal to, the $ET_{10\%ROM}$ for (b).

All analyses performed in this chapter used all 15 repetitions of the various motions performed by the participants. Some plots created however used a subset of the collected data for ease of viewing.

6.3 Results

The orientation outputs from the Razor IMU and VICON measurement systems were compared in all axes (Figure 6.3). This figure shows an example of the tracking of the spine kinematics at the C7 level for the slow variation of each motion and is representative of all other results obtained, which show similar trends when comparing the IMUs and VICON except for some forward bending results which show larger discrepancies in yaw measurements at the end range of motion for each cycle.

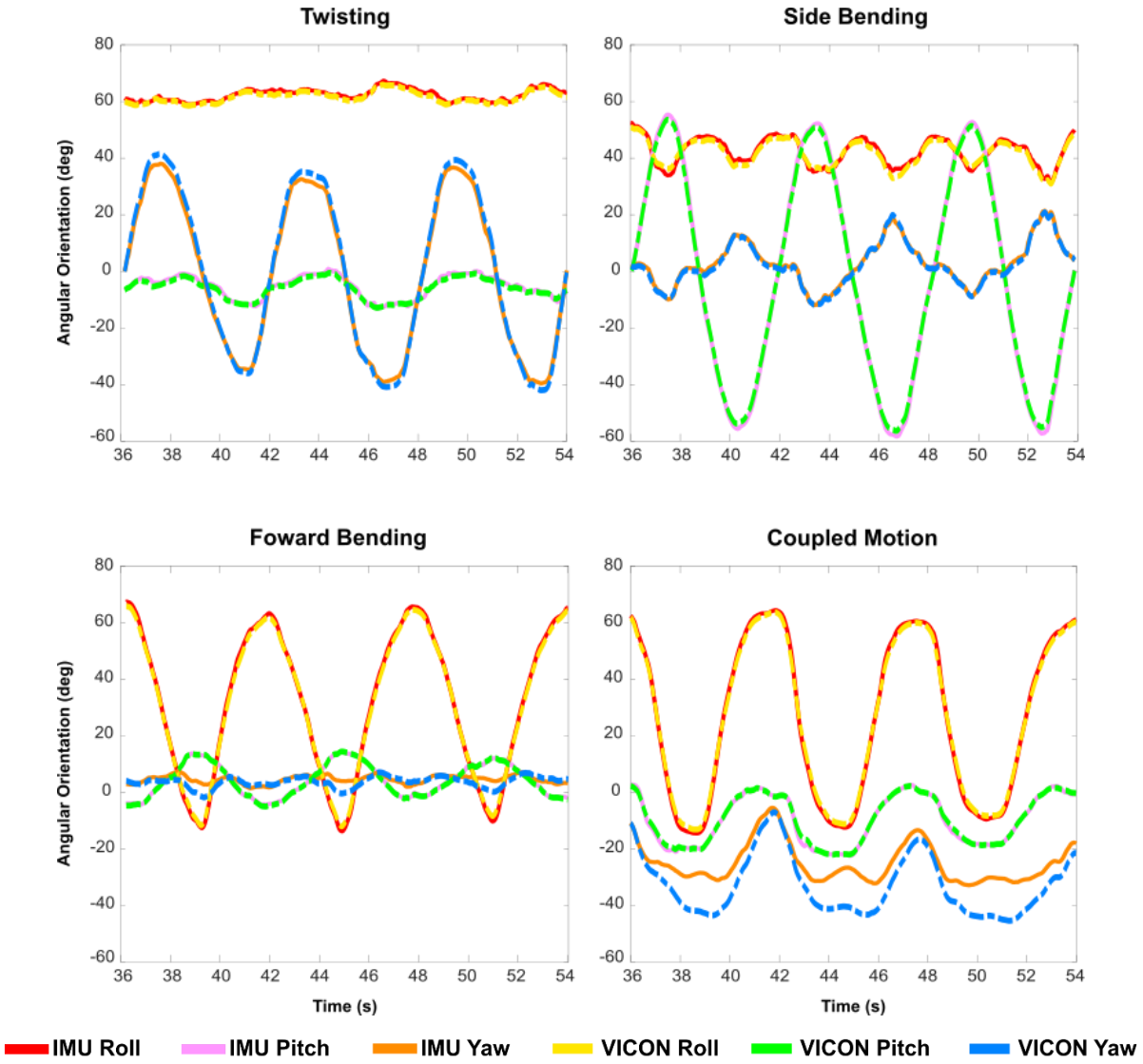

Figure 6.3 Outputs obtained from the IMUs and VICON systems. This example shows the seventh, eighth, and ninth cycle of the slow variation of each of the movement types used in this study at the seventh cervical vertebrae level.

Only 7% (5 of 72) of measurements had a significant difference in RMSE results between sessions (Table 6.1). This table also shows the RMSE and SD of the difference between the two measuring systems for each movement type and spine location, with average RMSEs in the roll, pitch, and yaw axes of 1.98°, 1.78°, and 3.86° respectively. As only 7% of the measurements showed a significant difference between sessions, the RMSE and SD were calculated by combining the results from the two sessions except for the 7% of measurements where a significant difference was observed. In this case, the higher RMSE session data is reported.

Table 6.1 Root-mean-square errors (standard deviation) of SparkFun Razor IMU.
*** Indicates a significant difference in results between sessions ($p < 0.05$).**
T12 – Twelfth thoracic vertebrae, C7 – Seventh cervical vertebrae.
AR – Angular rotation, LB – Lateral bending, FE – Flexion/Extension, CM – Coupled motion.
s – Slow speed, f – Fast speed

Motion	Sacrum			T12			C7		
	Roll	**Pitch**	**Yaw**	**Roll**	**Pitch**	**Yaw**	**Roll**	**Pitch**	**Yaw**
AR-f	1.64 (0.89)	2.46 (2.14)	2.04 (1.44)	2.55 (1.64)	3.41 (3.18)	2.14 (1.79)	3.22 (1.62)	3.56 (3.47)	3.17 (2.57)
AR-s	0.75 (0.44)	**1.33 * (0.64)**	3.71 (2.70)	0.87 (0.75)	1.00 (0.83)	5.67 (3.31)	0.97 (0.56)	1.04 (0.80)	4.33 (3.23)
LB-f	0.75 (0.52)	**1.59 * (1.07)**	1.09 (0.51)	0.78 (0.68)	1.18 (0.96)	1.38 (0.88)	**1.54 * (1.26)**	**4.31 * (4.20)**	2.01 (1.63)
LB-s	0.66 (0.28)	0.96 (0.39)	0.81 (0.51)	0.68 (0.53)	0.91 (0.60)	1.57 (1.03)	1.01 (0.85)	1.64 (1.46)	1.56 (0.84)
FE-f	2.62 (2.42)	0.88 (0.51)	1.93 (1.32)	1.77 (1.69)	0.68 (0.46)	4.45 (2.57)	4.00 (3.85)	0.66 (0.53)	6.66 (4.01)
FE-s	0.90 (0.66)	0.85 (0.37)	1.87 (1.05)	0.99 (0.90)	0.66 (0.32)	6.58 (3.49)	1.40 (1.34)	0.58 (0.45)	5.26 (3.25)
CM-f	2.34 (2.17)	2.34 (1.99)	1.93 (1.39)	2.21 (2.06)	1.82 (1.61)	3.48 (2.36)	4.56 (4.41)	2.29 (1.21)	**6.26 * (4.74)**
CM-s	0.86 (0.62)	0.90 (0.56)	4.11 (2.59)	1.57 (1.27)	0.79 (0.52)	2.57 (1.77)	1.67 (1.61)	0.85 (0.70)	6.74 (4.55)
Mean	1.50 (1.00)	1.48 (0.96)	2.44 (1.44)	1.57 (1.19)	1.57 (1.06)	3.92 (2.15)	2.64 (1.91)	2.21 (1.56)	4.79 (3.09)

Statistical analysis showed that 44% of speed pairs (16 of 36) had a significant difference in RMSE results. There is no trend in which spine location or axis of measurement contributes to the number of significantly different speed pairs. For instance, when looking at the spine location, 4/16 significantly different pairs were from the sacrum, and 6/16 were from both the T12 and C7 locations. When looking at

the axis of measurement, 5/16 significantly different pairs were in the roll axis, 7/16 in the pitch axis and 4/16 in the yaw axis. Motion type was the only variable that showed a trend towards single axis motions having more significantly different speed pairs, with 5/16 significantly different pairs coming from each of the simple motion tasks, and only 1/16 coming from the coupled motion task.

Statistical analysis of location pairs showed that 29% (21 of 72) had a significant difference in RMSE results. There appeared to be no trend in which location pair contributed the most to this result, with the S-T12, S-C7 and T12-C7 pairs contributing 8/21, 6/21 and 7/21 respectively.

The Bland-Altman (BA) plots (Appendix A) either showed a trend that the error of the IMUs increased as the participant moved towards their end ROM, or no trend in error and orientation, depending on the motion, spine location, and measurement axis being analysed. An example of the BA plots is shown in Figure 6.4.

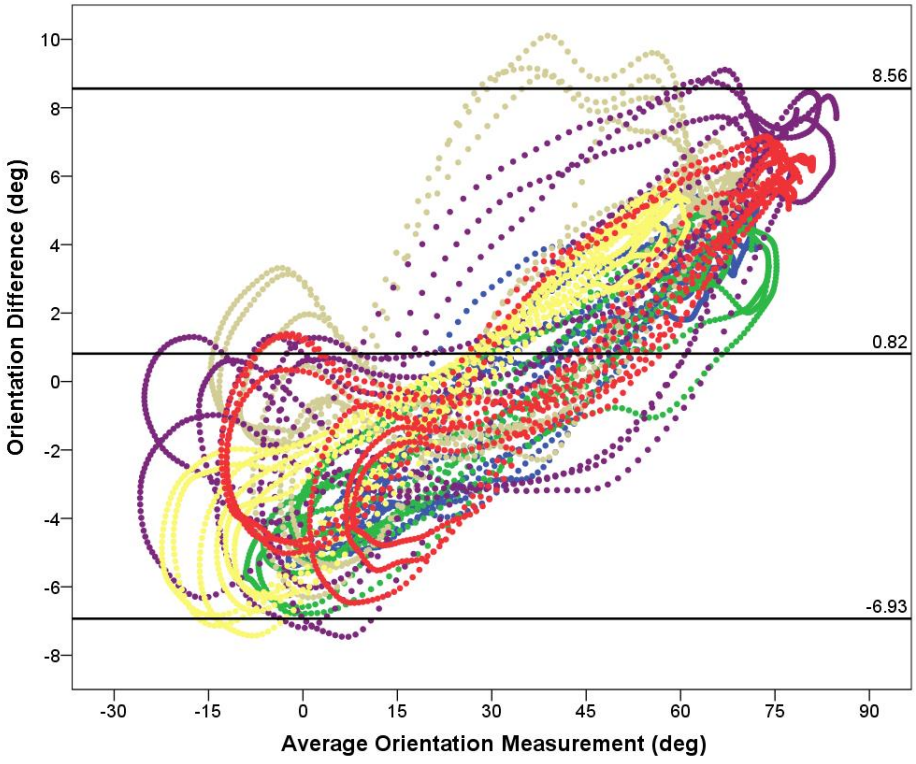

Figure 6.4 Example Bland Altman (BA) plot created using obtained data, for the thoracic IMU during the fast variation of Flexion-Extension. The BA plot shows average orientation measurement on the horizontal axis and difference between the IMU and VICON on the vertical axis. All six participants, with session data combined when no significant difference occurred, are plotted per BA plot using the seventh, eighth, and ninth cycles of each movement type. The graph also features the average orientation difference line at 0.82°, and average orientation difference ± 1.96 SD at -6.93° and 8.56° on the vertical axis.

ICC values indicate that the SparkFun Razor IMU can reliably measure motion when compared to the VICON measurement system (Table 6.2). The ICC values in this table have ranges of 0.775 – 1.00 (average: 0.954, SD: 0.065) and 0.777 – 0.999 (average: 0.957, SD: 0.064) for minima and maxima values respectively. The average ICC values for flexion-extension, lateral bending, and axial rotation are 0.962 ± 0.060, 0.951 ± 0.067, and 0.951 ± 0.067 respectively.

Table 6.2 Intraclass Correlation Coefficients (ICCs) of the SparkFun Razor IMU measurements.

Motion	Minima Lumbar	Minima Thoracic	Maxima Lumbar	Maxima Thoracic	Mean
FE-f	0.998	0.933	0.992	0.796	0.945
FE-s	1.000	0.996	0.997	0.991	0.996
LB-f	0.994	0.829	0.992	0.777	0.898
LB-s	0.993	0.966	0.999	0.976	0.984
AR-f	0.995	0.996	0.998	0.999	0.997
AR-s	0.990	0.985	0.944	0.991	0.978
C-f Roll	0.981	0.886	0.993	0.867	0.932
C-s Roll	0.996	0.977	0.994	0.989	0.989
C-f Pitch	0.970	0.975	0.937	0.869	0.938
C-s Pitch	0.995	0.999	0.995	0.953	0.986
C-f Yaw	0.897	0.813	0.981	0.942	0.908
C-s Yaw	0.996	0.775	0.974	0.971	0.922
Mean	0.981	0.928	0.983	0.927	0.956

It is evident that the ROM in the primary motion axis for simple motion is greater than the ROM experienced by the corresponding axis in the coupled motion tasks which can be seen in Table 6.3. From these results, it was concluded necessary to use two different thresholds for determining $ET_{10\%ROM}$ as presented in Table 6.4. As evident in Table 6.4, the IMUs of the SMM are within the ±10% ROM threshold for the majority of the time, with average $ET_{10\%ROM}$ values of 92.5% and 98.8% for the two different threshold conditions (Trial ROM and Max ROM Observed) respectively.

Table 6.3 Average range of motion of the T12 and C7 IMUs used during each of the motions tested. The range of motion was determined by the VICON system. The values for uniaxial motion is composed of the range of motion experience during Flexion-Extension (Roll), Lateral Bending (Pitch), and Axial Rotation (Yaw) trials. The values for the coupled motion are the ranges of motion experience in the three-movement axes during the couple motion trials.

Speed	Axis	T12		C7	
		Uniaxial (°)	Coupled (°)	Uniaxial (°)	Coupled (°)
Slow	Roll	90.5	73.1	98.3	71.5
	Pitch	58.3	21.0	100.7	34.1
	Yaw	96.0	60.6	151.7	78.2
Fast	Roll	79.8	79.1	84.9	79.9
	Pitch	48.0	19.0	84.5	29.6
	Yaw	87.6	57.1	142.8	70.8

Table 6.4 The average percentage time (%) the SMM IMUs error was between the two ± 10% ROM thresholds ($ET_{10\%ROM}$).

Motion	Axis	Threshold 1 10% Trial ROM (%)		Threshold 2 10% Max ROM Observed (%)	
		Sacrum-T12	Sacrum-C7	Sacrum-T12	Sacrum-C7
FE-f	Roll	100	87.0	100	94.3
FE-s	Roll	100	100	100	100
LB-f	Pitch	99.8	95.7	100	99.2
LB-s	Pitch	100	100	100	100
AR-f	Yaw	100	100	100	100
AR-s	Yaw	83.1	100	89.4	100
C-f	Roll	99.7	72.2	99.9	91.6
C-f	Pitch	79.0	62.4	100	100
C-f	Yaw	91.1	82.4	97.9	99.9
C-s	Roll	99.9	100	100	100
C-s	Pitch	92.2	98.3	100	100
C-s	Yaw	85.7	92.5	100	100
Mean	All	94.2	90.9	98.9	98.8

6.4 Discussion

The purpose of this study was to validate the Spinal Motion Measurement device's spinal sensors (SparkFun Razor IMU) for use in human kinematic testing when applied to the spine. Statistical analysis of RMSE results revealed that only 7% (5 of 72) of orientation measurements showed a significant difference between different sessions. This indicates the selected IMUs for use in the SMM to be repeatable in its accuracy across different days. One factor that may have contributed to the 7% of significantly different data is slight misalignments or adjustments in the placement of sensors between sessions due to inconsistencies between the local coordinate systems of the SMM and VICON, rather than inconsistencies in the SMM itself. The majority of orientation measurements that showed a significant difference (3 of 5) occurred during the same motion type, being fast lateral bending, and 3 of 5 occurred in the same measurement axis, being pitch. Although difficult to definitively conclude, this may allude to measurements taken during lateral bending motions and measurements made in the pitch axis to be less repeatable than other motions and measurement axes.

The average RMSE in the roll, pitch, and yaw axes in this study were found to be 1.98°, 1.78°, and 3.86° respectively and demonstrate the accuracy of the SparkFun Razor IMU, and thus the SMM, in measuring spinal motion in these axes, therefore meeting the aim and hypothesis for this research. The RMSE results are similar to those found for the Dorsa ViMove [49, 209] and lower than 10% ROM, thus showing no clinical difference to the reference measurement system. It should be noted, that the accuracies obtained are for measuring overall spinal posture, as is the intended application of the device, rather than the position of individual vertebrae.

Statistical analysis also showed that 44% (16 of 36) of speed pairs showed a significant difference in RMSEs, thus showing speed to have a greater impact on the repeatability of accuracy than the differences experienced across sessions. This result is consistent with previous outcomes discovered in this research that showed that the measurement of orientations by IMUs and other inertial sensors is affected by speed, in which a higher speed resulted in greater measured ROM when placed on a Katana

robot arm. In this validation study, RMSE increased with speed for the roll and pitch measurement axes, however, for seven of the 12 yaw measurements the RMSE decreased as speed increased thus showing no trend regarding RMSE vs speed for the yaw measurement axis.

When performing statistical analysis on location pairs, 29% (21 of 72) location pairs showed a significant difference in RMSEs. This shows the location of IMU to have a greater impact on RMSEs than the errors induced by collecting data across different sessions, however, the majority of the time it is not a significant issue. The C7 IMU had consistently higher errors in measuring motion than the T12 IMU, which in turn had a consistently higher error than the Sacral IMU. This finding may be due to the C7 IMU undergoing the largest amount of absolute motion, while the T12 experienced the second most motion. However, for the IMU to complete a cycle with greater ROM within the same time, the faster it must travel to complete each cycle. Thus, the speed each IMU experienced was not only adjusted by performing cycles of motions at different rates but by placing them at different spinal levels as well. The IMU placed at C7 travels at a greater speed than the IMUs at T12 and sacrum due to the greater ROM and distance covered in the same amount of time. Although speed is greater at higher spine locations and has already been shown to affect the repeatability of IMU measurements, the greater absolute ROM experienced at the more superior spinal locations may also contribute to the 29% of location pairs that showed a significant difference.

It is demonstrated that there is a greater amount of error associated with yaw measurements compared to roll and pitch (Table 6.1), which has been an issue with IMU based measurements discussed previously in this research and in previous studies [49]. For instance, ViMove has been shown to measure single plane and multiple plane movement with RMSEs of 0.5 – 2.8° and 2.1 – 6.3° respectively, where yaw measurements consistently had higher errors than the other two axes [49]. This increased yaw error is expected, as IMUs cannot use accelerometers to help determine orientation around this axis as they do with the other two axes. This is because the

axis in which yaw occurs aligns with the gravitational axis and thus, when rotation occurs in the yaw axis there is no change in acceleration measured.

Bland-Altman plots (Figure 6.4 and Appendix A) demonstrated a systematic trend in the magnitude of error for the IMUs compared to the VICON increased towards the end range of motion for a number of trial types. This trend is present in fast FE (S and C7), LB (C7), and AR (S and C7), and slow FE (C7), LB (C7), and AR (All locations) simple motions. All other combinations of simple motion and IMU location show no noticeable trend in the extent of error with respect to orientation. Due to these results, the ICC values were calculated using only minima and maxima (i.e. at the end ROM in both directions) values as this is likely to give the lower limit of ICC values as this is where errors are generally the highest.

The ICC values (range 0.775 – 1.00, average 0.956) show excellent agreement between the two measurement systems, and are similar to ICC values obtained by the Spineangel® [54]. As the ICC values represent the lower limit of agreement between the two systems, the reliability of the SMM to measure spinal motion is likely to be greater while measuring motions occurring between two end ROMs. However, the movements in this study can be considered elementary compared to other motion patterns that can be seen in a number of everyday activities, which may see a variation in reliability due to the greater complexity of spinal motion experienced.

The ROM in the primary motion axis for the simple motion was found to be greater than the ROM experienced by the corresponding axis in the coupled motion tasks (Table 6.3). This was expected due to the nature of the experimental tasks, where during single motion tasks the participants were asked to go to full, or close to, ROM whereas they were not in coupled motion. It is for this reason two different thresholds were used for the $ET_{10\%ROM}$ test (Table 6.4). The first threshold was ±10% of the ROM experienced during each specific trial, and the second was ±10% maximum ROM observed for each axis for each participant taken over all trials and both sessions. This is due to the evidence seen in numerous BA plots, in that when ROM increases so does the error thus it is logical to use ±10% of the ROM for each specific trial. However, in some motions such as fast coupled motion, the ROM for some axes, specifically the

pitch axis, was minimal and hence using ±10% of the ROM for this trial would be biased. For instance, the average pitch threshold for the T12 IMU would be 1.90°, being a small threshold to meet, and thus it also valid to use a ±10% maximum ROM observed for each axis of each for each participant tested. Therefore, results were obtained for $ET_{10\%ROM}$ using both threshold conditions.

The percentage of time the error was within ±10% ROM ($ET_{10\%ROM}$) is a new parameter used in this thesis in an attempt to combine accuracy and reliability into a single measure and thus can complement RMSE as a useful output statistic. Often it is desirable for measurement systems to be within this ±10% ROM threshold. When just using RMSE values as commonly reported, it can be misleading as to how often the device is within the ±10% ROM threshold. $ET_{10\%ROM}$ removes any ambiguity from this standard as it reveals what percentage of time the device is within the required threshold. For instance, in this study, it was found the SMM IMUs had average RMSE values of 2.64°, 2.21°, and 4.79° in the FE, LB and AR axes respectively at the C7 vertebrae. When considering the average ROM used by the participants in this study (Table 6.3), C7 can achieve ROM of approximately 100° in flexion-extension and left-right lateral bending, and 150° in left-right axial rotation. Thus, the RMSEs of the IMU are within the required ±10% ROM threshold. However, during various kinematic conditions such as those seen in bending and everyday activities, the accuracy of the device is likely to be inconsistent throughout the movement, thus the importance on conveying the percentage time the device was within the required threshold.

As can be seen from Table 6.4, for threshold 1, the majority of the simple motions have an $ET_{10\%ROM}$ of 100%, but some are as low as 83%. The $ET_{10\%ROM}$ remains high for all axes of motion in the slow coupled motion task, with results generally being above 90%. However, the $ET_{10\%ROM}$ values decrease for the fast-coupled motion. One reason why the values decrease for coupled motion may be due to increased complexity over other motions. However, the largest contributor is likely the lower max ROM experienced for each axis in coupled motion when compared to the simple motions (Table 6.3). Due to the lower ROM, there is also a lower ±10% ROM threshold used for this test. For the roll and yaw axes, this threshold is still larger than the

average RMSEs reported. However, for the pitch axis the threshold approaches, and even goes below, the average RMSE obtained, which would explain the low $ET_{10\%ROM}$ values. When applying the second threshold condition to the coupled motion data, then the $ET_{10\%ROM}$ results become closer to 100% (Table 6.4).

The results obtained from this study show the SMM to be highly accurate and reliable in measuring spinal motion in various axes. In addition, the SMM has been shown to be capable of measuring and outputting orientation-time data, which is a characteristic that many devices discussed in the literature review of this thesis do not have the capability to perform. This proves the usefulness of the SMM compared to similar devices, which along with its low cost, make the SMM an attractive option for inexpensive spinal motion capture.

A limitation of the current study is that although the accuracy of the SMM to measure spine kinematics was determined in a number of spinal motions, it was not tested in normal functional activities such as walking, standing, or sitting for long periods of time. A study to find the accuracy and reliability of the SMM during such activities and others of daily-living would be beneficial to show its effectiveness for use in everyday life and for longer periods of time.

6.5 Summary

In summary, the accuracy and reliability of the spinal kinematic sensors of the SMM (SparkFun Razor IMUs) were found to satisfy the fourth aim of this research. The experimentation accomplished this through numerous tests using a VICON MX Vantage V8 camera system as the gold standard reference measurement. The average RMSE errors were found to be below 2° for the roll and pitch axes, and below 4° for the yaw axis. It was shown through statistical analysis that the major contributor to variations of errors in orientation values experienced by the IMUs was the speed of motion and the location at which the sensors were placed on the spine. Bland-Altmann plots showed the SMM to generally experience the greatest difference in orientation measurement at the end ROM. The SMM results were found to consistently agree with VICON measurements at a high rate, with ICC values for end range of motion values averaging 0.956. The SMM error was found to be within ±10% ROM for the majority of the time, with an average $ET_{10\%ROM}$ value of 92.5% or 98.8%, depending on the threshold condition. The results of this study have shown the SMM, and SparkFun Razor IMU, to be an inexpensive alternative to other motion capture systems for measuring spinal kinematics, especially when unrestricted motion is required.

Chapter 7

Summary and Conclusion

7.1 Thesis Summary

Previous research has shown that back pain is a world leading cause of disability. Back pain is the largest contributor to disability when expressed in years lived with disability (YLD), sixth largest when expressed in terms of disability-adjusted life years (DALYs), and second largest contributor to work leave. Of all major musculoskeletal disorders, only severe rheumatoid arthritis had higher disability weights (DW) than back pain. This shows how much back pain can affect suffering individuals, who often complain of loss of mobility, sleep, and independence.

Back pain has also been found to have a major effect on the economy, with back pain costing approximately AU$9.17 billion in Australia in 2003. In the United States, the cost of back pain is estimated between US$100-200 billion annually. The majority of these costs are due to indirect reasons, such as work days missed, loss of productivity, and training of new staff. This shows that it would be cost effective to use treatment for the prevention of back pain, rather than after the onset of pain.

Back pain has been shown to have numerous risk factors that increase the likelihood of pain occurring, with over 100 risk factors identified. Of these risk factors, however, poor posture, prolonged sedentary behaviour, and high spinal loads are believed to be the most important when designing preventative measures.

Inactivity has been highlighted as a risk factor for numerous non-communicable diseases including coronary heart disease, stroke, type II diabetes, and breast and colon cancer, among others. Inactivity has such a large effect on an individual's health, that in 2010, it was responsible for 5.3 million, or 9% of all, premature deaths globally, the fourth highest contributor. Much research has been performed using longitudinal studies that show the association between a reduced risk of death for many of these non-communicable diseases and adequate amounts of daily exercise. It has also been shown that high enough activity levels can counter-act the negative impact of prolonged sedentary times, such as extended periods of sitting.

Bio-feedback systems, which give a warning (e.g. vibration, alert) to the user when a threshold is reached, have been shown to be effective in training the user to

alter their posture in the long-term. Based on this knowledge and review of previous literature, this research intended to create a new concept device that can track both the user's spinal posture/kinematics and activity by achieving the following aims:

1. Compare a number of commonly used spinal kinematic measurement systems, including a low-cost (<AU$1000) wearable sensor, in their ability to measure motion typically seen in the human spine.

2. Develop an activity classification model capable of predicting everyday activities including standing, sitting, lying, and walking. Extending from this set of activities, it is beneficial to include other commonly used activities of daily living, including jogging, stair ascending and descending, jumping, walking on an incline, and transitions.

3. Create a new, inexpensive (<AU$1000) device with the ability to simultaneously track user spine posture/kinematics and activity. This device should be highly portable, and therefore consist of wearable sensors such that it can be worn during activities of daily living.

4. Validate the device to have accuracy within ±5° for spine kinematics. This accuracy range (±5°) was selected such that it had similar accuracies to previous posture trackers and was within the 10% range of motion threshold used to test clinical significance.

5. Validate the device to have an average positive activity classification rate of 90% or above for standing, sitting, lying, and walking. Extending this aim is to achieve an average classification rate of at least 90% for all activities the created classifier can predict.

These aims we achieved through a number of different studies as discussed in this research. In Chapter 3, a comparison of various measurement systems in their ability

to measure a Katana Robot arm's movement was performed, thus addressing the first aim. From the results, it was discovered that the majority of measurement systems performed better during slower motions and that OptiTrack optical motion capture system performed better than all the inertial sensors. From this analysis, however, it was discovered that the inexpensive SparkFun Razor IMU could measure the ROM at speeds typically seen in the human, to 1.5 times this speed, with accuracies between 0.47° and 4.73° (Table 3.2). During random motion, the errors remained consistent in the axes perpendicular to gravity (X and Y), however, increase to 5.88°- 9.53° in the axes parallel to gravity (Z) (Table 3.3).

Both the second and fifth aim were addressed in Chapter 4. In this study, a new activity classifier using two tri-axial accelerometers was created using machine learning with data from twelve participants. This classifier was trained to predict 13 distinct activities, including standing; sitting; prone, supine, right-side, and left-side lying; walking; jogging; stair ascending and descending; jumping; walking on an incline; and transitions and therefore accomplished the second aim and filled an identified gap in the literature. Upon validation of this model, the average prediction rate was 90.3%, hence slightly above the requirements to satisfy extension to aim five. When considering just standing, sitting, lying, and walking, however, the average prediction rate was 95.6% and therefore this met the conditions of aim five. In this study, it was also found that the experimental protocol can have a significant effect on positive predictive rates. For instance, when validation was performed in protocols without fuzzy border effects due to transitions in activities, the accuracy of the model was much higher than when validation was performed in protocols with transitions. The implications of this for an activity such as walking that had an average positive prediction rate of 87.3%, is that when the walking event persists for an extended period of time (e.g. 30-minute walk for exercise), the accuracy can increase to 99% as shown by the accuracy for walking when on a treadmill.

Both the previous chapters contributed to Chapter 5, which details the design of a new device, the Spinal Motion Measurement device (SMM), which tracks spinal kinematics and activity of the user. The SMM was also designed to be inexpensive and

therefore addressing the third aim of this research and the gap in the literature of there being no inexpensive device currently available to perform this. The SMM consists of three SparkFun Razor IMUs, which were tested for accuracy in Chapter 3, and two ADXL326 tri-axial accelerometers, used to develop for the activity classifier in Chapter 4, were employed into the device. The SMM also consists of an Arduino Mega for collecting and collating sensor data, a Bluetooth module for wireless transmission of data, and a rechargeable lithium-polymer battery for power supply. In total, at the time of development, the SMM had a total build cost of AU$630. The SMM however, was designed to work with any number of inertial sensors between up to a maximum of five (three IMUs and two accelerometers). Therefore, this price can be reduced significantly if fewer sensors are employed, which may be required for widespread use by the general population, along with various other modifications to improve usability.

The final aim to be addressed, aim four, was satisfied with the experimentation discussed in Chapter 6. This chapter shows how the SMM was validated to measure spinal motions to within ±5° at all sensor locations along the spine and all measurement axes. The results obtained in this study, and the study discussed in Chapter 3, show the SMM to have comparable accuracies to similar devices used in other studies [49]. The results found in this research, however, showed that the yaw (angular rotation) axes commonly experienced the highest errors. It was also discovered in this research that the more superiorly placed an IMU is, the higher the measurement error. This conclusion is likely due to the superior locations experiencing higher ROM and angular velocities.

All of the research chapters link together to show that the research performed has developed a new device to simultaneously track two important risk factors for the reduction in occurrence and severity of back pain, as well as other non-communicable disease, to meet the aims of this research. With further development of the SMM to make it more comfortable and easier to use, this device has the potential to help train individuals to use good posture and maintain adequate levels of activity, and hence reduce the risk of back pain occurring through these two risk factors.

7.2 Limitations

There exists a number of limitations with the research performed. In the comparison of sensors on the Katana robot 450, as the testing was performed on a robot arm there were no sources of error commonly present in human kinematic testing. For instance, there was no soft tissue artefact which normally affects the location of the sensor to the underlying bone and therefore diminishing the accuracy of results. Also, the alignment of sensors on the Katana was able to be near-perfect, thus allowing for better inter-session repeatability on the placement of sensors than what would normally occur if human participants were used.

The inability to recreate human motion profiles for all kinematic parameters is another limitation of this study. The Katana motion profile in this study, although matched for the typical ROM and angular velocities of human spine motion, it was harder to match for acceleration. This, therefore, created a sudden, although slight, 'jerk' at the commencement and conclusion of motion, which may negatively affect inertial sensor data and therefore increasing the errors recorded. Although limitations of this study are present, all measurement systems were tested under similar conditions for comparison and therefore these are of no major significance towards the conclusions of this study within the scope of this research.

There are several limitations to the methods used to create the activity classification model developed in this research. Firstly, the number of steps on the staircase used for stair ascending and descending was only four. This, therefore, meant that there is a large proportion of fuzzy border effects when participants transition from one activity to another within both the training data and validation data. So consequently, the model itself may be flawed due to imperfect training data, and the accuracy of the model to predict stair ascending and descending may be lower than expected due to poor validation data. The quality of data and the accuracy of the model may be increased with a greater number of steps within the staircase. A further

limitation on this method is the similarities between turning and both standing and walking. In this research, when a person was turning around on the spot it was always labelled as walking in the training data as participants were moving their feet. However, quite frequently during validation of the model, turns were classified as standing due to participants not moving their feet with as of high intensity as with normal walking. This misclassification, therefore, reduced the accuracy of the model to predict walking, which was found to be 87.3% on average. If a new activity classification was created for turns, instead of labelling turns as walking, then the accuracy of walking would have increased.

The SMM device created in this research also has several limitations. Firstly, is concerned with the ease of use of the SMM. Numerous other devices used to track posture connect to a smartphone application (App), whereas the SMM is required to connect to a computer via Bluetooth and use MATLAB to collect data. This, therefore, shows that at this stage, other devices are simpler and easier to use, and are therefore a more attractive option for the general population. The SMM is also limited to collecting data from the IMUs at 48 Hz, which is significantly lower than other measurement systems used in human kinematics. However, the data logging rate of the SMM is still high enough to track spinal movement [195].

Further limitations on the design of the SMM include the cables that connect the sensors to the rest of the device, comfortability, and the aesthetic appeal. Although to finalise a commercial device is outside the scope of this research, these are three areas, as well as the development of a smartphone App, which need to be addressed before the SMM can be easily used by the general population. Removal of cables allows for a smaller, easier to use device, and ensures no cable interference or entanglement. Currently, the device is connected to users via single-use double-sided tape onto the hard case of the sensors. New cases can be designed to not only to increase the aesthetic appeal but also to incorporate a multiple-use connection system to the human body, as well as a soft interface between the user and sensors to increase the comfort of the device. Sitting on a chair with a back rest may also be uncomfortable

using the SMM. Reducing the size of sensors, and therefore the cases, could would lead to the probable result of a more comfortable device while sitting.

The validation of the device also has a few limitations. The accuracy of the device to classify a number of activities needs to be improved. Of concern, is the device's ability to classify stair descending and walking on a 10% incline as these had accuracies of 61.9% and 80.5% respectively. As discussed previously, however, with improvements in the experimental design for stair descending by including more steps in the staircase, the training and validation data may improve and therefore accuracy also. The results show that when the user is walking on a 10% incline, the model classified this as being either incline walking (80.5%), walking (18.6%), stair ascending (0.8%) and stair descending (0.2%). Therefore, within rounding error, the classifier predicted the user to be performing a walking-like activity 100% of the time. So, although further work is required to increase of the accuracy of the model to predict incline walking at a 10%, the model at least misclassifies this action as activities that are similar to incline walking, rather than ones that are not (e.g. sitting or lying). A limitation on the validation on the accuracy of the SMM to measure spine kinematics was that it was not tested for accuracy during normal functional activities such as walking, standing still, or sitting for long periods of time. A study to find the accuracy and reliability of the SMM during such activities and others of daily-living would be beneficial to show its effectiveness for use in everyday life.

A further limitation on the validation of the SMM is that all testing occurred in a well-controlled laboratory setting and are therefore unlikely to apply to real world scenarios. Firstly, no long-term testing was undertaken for validation of the spinal kinematics measurement aspect of the SMM. Although the testing conducted allowed a comparison between measurement systems in short-term use, it did not permit for an analysis of the effects of drift, which can be a significant issue for gyroscope measurements of orientation. However, these effects may be almost eliminated by drift compensation algorithms within the IMUs, so this is not a major limitation of this research. Secondly, as discussed in Chapter 2, magnetometers are susceptible to errors arising from magnetic interference. Under well-controlled laboratory conditions, as

was the case for this research, these magnetic interferences can be calibrated for. However, this is not the case in the real-world due to numerous changes in the magnetic field caused by a multitude of factors. This limitation should be addressed adequately before the SMM is valid for use in real-world conditions.

7.3 Future Work

Some future work can be conducted to increase the significance of this research. Although out of the scope of this thesis, further work should be performed into making the SMM device more comfortable, cable-free, and easier to use. The benefit of this is not just for commercialisation aspects, but for researchers as well.

As suggested previously, the device could be made more comfortable if the sensors had soft padding on the interface between user and device. To become cable free, each sensor would require a wireless module to transmit data and have its own power supply, similar to how the ViMove (DorsaVi, Melbourne, Australia) operates. This would not only add to the comfort and aesthetic appeal of the device but would eliminate any chance of cables 'tugging' on the sensors. Developing an all-in-one smartphone App, which can track posture and activity simultaneously, as well as log this data for future use, would substantially improve the usability of this device. This is because the data logger (a smartphone) can be easily carried around by the SMM user, and hence puts no restrictions on the movement of the user. This is unlike the current set-up, where the user must remain within 15m of the data logging computer.

Future work should also be completed on the validation of the accuracy in short-term use. In this research, as presented in Chapter 6, marker groups were attached on top of the IMUs of the SMM which was deemed necessary to ensure both measurement systems were measuring the same kinematics. This method however does not necessarily measure the kinematics of the spine due to movement of the IMUs relative to the underlying bone. Therefore, further validation should be performed while also measuring the kinematics of the spine, such as radiography or using validated optical motion capture marker sets. It has been shown in previous studies that high angular velocity of spine motions is another risk factor for back pain [55] and therefore further work should also be performed on validating the gyroscopes within the IMUs.

Although this research has provided a tool to do so, a further study should be performed to validate the device for long-term use, particularly in spinal kinematic

measurements, as well as in the real-world (i.e. outside of a laboratory session). Although unexpected due to the use of drift compensators in IMUs, a study should be performed to measure the accuracy of the device over long periods, as only short-term measurements of approximately 60 seconds have currently been undertaken. Further analysis should also be performed for validating the accuracy of these sensors during activities of daily living. The device has an end goal of tracking posture and activity throughout the user's everyday life to reduce the risk of back pain and other non-communicable diseases. As such, the validation of the device for long-term, real-world use should be performed in the future. This experimentation may be difficult, however, as participants will need to be followed by video cameras (as the reference system) as they perform their daily tasks. This may create issues with line of sight of the camera, equipment power supply, and ethics as interactions with other individuals will cause them to be in the video field of view, and it may be impractical to gain ethics consent from all these people. Nonetheless, a study should be designed to limit the impracticalities of validating the real-world use of the SMM. This could potentially be performed in a work environment in which the individual performs their duties within a certain workspace.

Some further developments can be made to the activity classifier for it to have increased accuracy and improve the SMM. To increase the accuracy of stair descending, increasing the number of steps in the staircase above four will reduce the proportion of fuzzy-border effects and thus increase the quality of both training and validation data. As IMUs are the combination of accelerometers, gyroscopes, and magnetometers, by removing the thoracic spine accelerometer and using one of the IMUs of the SMM instead could have advantages. Firstly, this would reduce the minimum number of sensors required to two. In this case, the thoracic IMU could be used to track spinal kinematics, and both sensors (thoracic IMU and thigh accelerometer) could combine to classify activity. This could therefore significantly reduce the total cost of the device for the general population. The cost could be further decreased if the SparkFun Razor IMU is replaced by its successor, the Razor 9DOF IMU M0, which is 40% less expensive. For the activity classifier of the SMM to

function, it could either use only the accelerometer of the IMU and thus keep the current classifier, or, it could be re-trained to use the gyroscope and magnetometer as well. This could potentially increase the accuracy of the classifier as more data from a variety of sensors is being utilised, thus being the second advantage of replacing the spine accelerometer with one of the IMUs. By using the IMUs gyroscope, turning on the spot may be identified as a separate task. This may be introduced into the activity classifier. Additional future work on the activity classifier would be the inclusion of a tilt angle parameter, calculated using accelerometer measurements in each axis (equation 3.6). The inclusion of this parameter may decrease the confusion between walking and walking on an incline.

7.4 Conclusion

The research performed meets all aims set for the Ph.D. In this research, a comparison of the ability of numerous sensors to measure motion commonly seen in the human spine was performed and from this, it was found that a low-cost IMU (SparkFun Razor) could measure ROM with errors of 0.47° to 4.73°. A new activity classifier was created to predict 13 distinct motions, being standing; sitting; prone, supine, right-side, and left-side lying; walking; jogging; stair ascending and descending; jumping; walking on an incline; and transitions between activities from two tri-axial accelerometers. By combining up to three SparkFun Razor IMUs, two tri-axial accelerometers (ADXL326), an Arduino Mega, Bluetooth module, rechargeable battery, and numerous pieces of software, including the activity classification model, the Spinal Motion Measurement device (SMM) was created. This device has the capabilities to track spinal posture/kinematics, as well as classify the activity of the user. Upon validation of the device for accuracy, it was discovered that it could measure spinal kinematics with an average error of ±5° and could classify standing, sitting, lying, and walking with an average accuracy of 95.6%. When validating for all 13 distinct activities, the average accuracy decreases to 90.3%, narrowly above the aim of 90%.

The developed device has been shown to accurately track spinal posture/kinematics as well as activity. Although limitations exist, they do not reduce the significance of the conclusions derived from this research. For the SMM to overcome these limitations, future work should be performed. This work should include increasing device comfort and usability for the general population. The accuracy of some activities, as well as a decrease in build price, would also be beneficial in future work. While these limitations exist, the SMM developed in this research addresses the limitations of previous devices by being affordable to the general population as well as clinics, and by also giving accurate and complete kinematic data at numerous spinal levels and in activity recognition.

References

1. Dvorák, J., E.G. Vajda, D. Grob, and M. Panjabi, *Normal motion of the lumbar spine as related to age and gender.* Eur Spine J, 1995. **4**(1): p. 18-23.

2. McGregor, A.H., I.D. McCarthy, and S.P. Hughes, *Motion Charachteristics of the Lumbar Spine in the Normal Population.* Spine, 1995. **20**(22): p. 2421-2428.

3. Pearcy, M., I. Portek, and J. Shepherd, *Three-Dimensional X-ray Analysis of Normal Movement in the Lumbar Spine.* Spine, 1984. **9**(3): p. 294-297.

4. Pearcy, M. and S.B. Tibrewal, *Axial Rotation and Lateral Bending in the Normal Lumbar Spine Measured by Three-Dimensional Radiography.* Spine, 1984. **9**(6): p. 582-587.

5. Standring, S., N.R. Borley, P. Collins, A.R. Crossman, M.A. Gatzoulis, J.C. Healy, . . . C.B. Wigley, *The Back*, in *Gray's Anatomy The Anatomical Basis of Clinical Practice*. 2008, Elsevier Health Science UK: London. p. 705-748.

6. Willems, J.M., G. Jull, and J.K.-F. Ng, *An in vivo study of the primary and coupled rotations of the thoracic spine.* Clin Biomech, 1996. **11**(6): p. 311-316.

7. Mitsuhashi, N., K. Fujieda, T. Tamura, S. Kawamoto, T. Takagi, and K. Okubo, *BodyParts3D: 3D structure database for anatomical concepts.* Nucleic acids research, 2008. **37**(suppl_1): p. D782-D785.

8. Robertson, W.S.P. *BodyParts3D in Matlab*. 2018; Available from: https://doi.org/10.5281/zenodo.1490637.

9. Hoy, D., L. March, P. Brooks, F. Blyth, A. Woolf, C. Bain, . . . R. Buchbinder, *The global burden of low back pain: estimates from the Global Burden of Disease 2010 study.* Ann Rheum Dis, 2014. **73**(6): p. 968-974.

10. Cole, M. and P. Grimshaw, *Low back pain and lifting: A review of epidemiology and aetiology.* Work, 2003. **21**(2): p. 173-184.

11. Lahad, A., A.D. Malter, A.O. Berg, and R.A. Deyo, *The Effectiveness of Four Interventions for the Prevention of Low Back Pain.* J Am Med Assoc, 1994. **272**(16): p. 1286-1291.

12. Lidgren, L., *The Bone and Joint Decade 2000 -2010.* Bulletin of the World Health Organization, 2003. **81**: p. 629.

13. Walker, B., R. Muller, and W. Grant, *Low Back Pain in Australian Adults: The Economic Burden.* Asia Pacific Journal of Public Health, 2003. **15**(2): p. 79-87.

14. Duthey, B., *Background Paper 6.24 Low Back Pain. In: Priority Medicines for Europe and the World 2013 Update*, in *Prior Med Eur World*. 2013, WHO Press: Geneva. p. 165-168.

15. Hajihosseinali, M., N. Arjmand, and A. Shirazi-Adl, *Effect of body weight on spinal loads in various activities: A personalized biomechanical modeling approach.* J Biomech, 2015. **48**(2): p. 276-282.

16. Newell, T.M. and S. Kumar, *Comparison of instantaneous and cumulative loads on the low back and neck in orthodontists.* Clin Biomech, 2005. **20**(2): p. 130-137.

17. Norman, R., R. Wells, P. Neumann, J. Frank, H. Shannon, M. Kerr, and O.U.B.P.S.O. Group, *A comparison of peak vs cumulative physical work exposure risk factors for the reporting of low back pain in the automotive industry.* Clin Biomech, 1998. **13**(8): p. 561-573.

18. Sadeghian, F., S. Hosseinzadeh, and R. Aliyari, *Do Psychological Factors Increase the Risk for Low Back Pain Among Nurses? A Comparing According to Cross-sectional and Prospective Analysis.* Safety and Health at Work, 2014. **5**(1): p. 13-16.

19. Linton, S.J., *A review of psychological risk factors in back and neck pain.* Spine, 2000. **25**(9): p. 1148-1156.

20. Waters, T.R. and V. Putz-Anderson, *Manual materials handling.* Occupational Safety and Health -New York-, 1996. **27**: p. 329-350.

21. Sato, K., S. Kikuchi, and T. Yonezawa, *In Vivo Intradiscal Pressure Measurement in Healthy Individuals and in Patients With Ongoing Back Problems.* Spine, 1999. **24**(23): p. 2468-2474.

22. Wilke, H.-J., P. Neef, M. Caimi, T. Hoogland, and L.E. Claes, *New In Vivo Measurements of Pressures in the Intervertebral Disc in Daily Life.* Spine, 1999. **24**(8): p. 755-762.

23. Arjmand, N., A. Plamondon, A. Shirazi-Adl, C. Larivière, and M. Parnianpour, *Predictive equations for lumbar spine loads in symmetric lifting tasks.* J Biomech, 2011. **44**(1): p. 84-91.

24. Dreischarf, M., A. Shirazi-Adl, N. Arjmand, A. Rohlmann, and H. Schmidt, *Estimation of loads on human lumbar spine: A review of in vivo and computational model studies.* Journal of Biomechanics, 2016. **49**(6): p. 833-845.

25. Hajihosseinali, M., N. Arjmand, A. Shirazi-Adl, F. Farahmand, and M.S. Ghiasi, *A novel stability and kinematics-driven trunk biomechanical model to estimate muscle and spinal forces.* Med Eng Phys, 2014. **36**(10): p. 1296-1304.

26. Nachemson, A., *The effect of forward leaning on lumbar intradiscal pressure.* Acta Orthopaedica Scandinavica, 1965. **35**(1-4): p. 314-328.

27. Nachemson, A. and J.M. Morris, *In Vivo Measurements of Intradiscal Pressure: Discometry, A Method For The Determination Of Pressure In The Lower Lumbar Discs.* JBJS, 1964. **46**(5): p. 1077-1092.

28. Nachemson, A.L., *Disc pressure measurements.* Spine, 1981. **6**(1): p. 93-97.

29. Lee, I.M., E.J. Shiroma, F. Lobelo, P. Puska, S.N. Blair, and P.T. Katzmarzyk, *Effect of physical inactivity on major non-communicable diseases worldwide: an analysis of burden of disease and life expectancy.* The Lancet, 2012. **380**(9838): p. 219-229.

30. Kohl, H.W., C.L. Craig, E.V. Lambert, S. Inoue, J.R. Alkandari, G. Leetongin, and S. Kahlmeier, *The pandemic of physical inactivity: global action for public health.* The Lancet, 2012. **380**(9838): p. 294-305.

31. Australian Government Department for Health. *Sedentary Behaviour*. 2019 [cited 2019 30th of June]; Available from: https://www.health.gov.au/internet/main/publishing.nsf/Content/sbehaviour.

32. Pate, R.R., J.R. O'neill, and F. Lobelo, *The evolving definition of" sedentary"*. Exercise and sport sciences reviews, 2008. **36**(4): p. 173-178.

33. Kent, P., R. Laird, and T. Haines, *The effect of changing movement and posture using motion-sensor biofeedback, versus guidelines-based care, on the clinical outcomes of people with sub-acute or chronic low back pain-a multicentre, cluster-randomised, placebo-controlled, pilot trial.* BMC Musculoskelet Dis, 2015. **16:131**: p. 1-19.

34. Aminian, K., P. Robert, E.E. Buchser, B. Rutschmann, D. Hayoz, and M. Depairon, *Physical activity monitoring based on accelerometry: validation and comparison with video observation.* Medical & Biological Engineering & Computing, 1999. **37**(3): p. 304-308.

35. Lee, S.H., H.D. Park, S.Y. Hong, K.J. Lee, and Y.H. Kim. *A study on the activity classification using a triaxial accelerometer*. in *Proceedings of the 25th Annual International Conference of the IEEE Engineering in Medicine and Biology Society (IEEE Cat. No.03CH37439)*. 2003.

36. Lugade, V., E. Fortune, M. Morrow, and K. Kaufmann, *Validity of using tri-axial accelerometers to measure human movement - Part I: Posture and movement detection.* Med Eng Phys, 2014. **36**(2): p. 169-176.

37. Casale, P., O. Pujol, and P. Radeva. *Human Activity Recognition from Accelerometer Data Using a Wearable Device*. in *Pattern Recognition and Image Analysis*. 2011. Berlin, Heidelberg: Springer Berlin Heidelberg.

38. Godfrey, A., A.K. Bourke, G.M. Ólaighin, P. van de Ven, and J. Nelson, *Activity classification using a single chest mounted tri-axial accelerometer.* Medical Engineering and Physics, 2011. **33**(9): p. 1127-1135.

39. Karantonis, D.M., M.R. Narayanan, M. Mathie, N.H. Lovell, and B.G. Celler, *Implementation of a real-time human movement classifier using a triaxial accelerometer for ambulatory monitoring.* IEEE Transactions on Information Technology in Biomedicine, 2006. **10**(1): p. 156-167.

40. Khan, A.M., M. Lawo, and P. Homer. *Wearable Recognition System for Physical Activities*. in *2013 9th International Conference on Intelligent Environments*. 2013.

41. Kwapisz, J.R., G.M. Weiss, and S.A. Moore, *Activity recognition using cell phone accelerometers.* SIGKDD Explor. Newsl., 2011. **12**(2): p. 74-82.

42. Mannini, A. and A.M. Sabatini, *Machine Learning Methods for Classifying Human Physical Activity from On-Body Accelerometers.* Sensors, 2010. **10**(2): p. 1154-1175.

43. Mathie, M.J., B.G. Celler, N.H. Lovell, and A.C.F. Coster, *Classification of basic daily movements using a triaxial accelerometer.* Med Biol Eng Comput, 2004. **42**(5): p. 679-687.

44. Mathie, M.J., N.H. Lovell, A.C.F. Coster, and B.G. Celler. *Determining activity using a triaxial accelerometer*. in *Proceedings of the Second Joint 24th Annual Conference and the Annual Fall Meeting of the Biomedical Engineering Society] [Engineering in Medicine and Biology*. 2002.

45. Mathie, M.J., B.G. Celler, N.H. Lovell, and A.C.F. Coster, *Classification of basic daily movements using a triaxial accelerometer.* Medical and Biological Engineering and Computing, 2004. **42**(5): p. 679-687.

46. Jetté, M., K. Sidney, and G. Blümchen, *Metabolic equivalents (METS) in exercise testing, exercise prescription, and evaluation of functional capacity.* Clinical Cardiology, 1990. **13**(8): p. 555-565.

47. Mansoubi, M., N. Pearson, S.A. Clemes, S.J. Biddle, D.H. Bodicoat, K. Tolfrey, . . . T. Yates, *Energy expenditure during common sitting and standing tasks: examining the 1.5 MET definition of sedentary behaviour.* BMC Public Health, 2015. **15**(1): p. 516-523.

48. *2011 Compendium of Physical Activities.*

49. Charry, E., M. Umer, and S. Taylor, *Design and validation of an ambulatory inertial system for 3-D measurements of low back movements*, in *Intelligent Sensors, Sensor Networks and Information Processing (ISSNIP), 2011 Seventh International Conference on*. 2011, IEEE: Adelaide. p. 58-63.

50. Page, P., *Beyond statistical significance: clinical interpretation of rehabilitation research literature.* International journal of sports physical therapy, 2014. **9**(5): p. 726.

51. Intolo, P., A.B. Carman, S. Milosavljevic, J.H. Abbott, and G.D. Baxter, *The Spineangel®: Examining the validity and reliability of a novel clinical device for monitoring trunk motion.* Manual Therapy, 2010. **15**(2): p. 160-166.

52. Lumo Bodytech Inc. *Lumo Lift Posture Coach*. 2016 [cited 2016 31st October]; Available from: https://www.lumobodytech.com/.

53. Ribeiro, D.C., S. Milosavljevic, and J.H. Abbott, *Effectiveness of a lumbopelvic monitor and feedback device to change postural behaviour: a protocol for the ELF cluster randomised controlled trial.* BMJ Open, 2017. **7**(1): p. e015568.

54. Ribeiro, D.C., G. Sole, J.H. Abbott, and S. Milosavljevic, *Validity and reliability of the Spineangel® lumbo-pelvic postural monitor.* Ergonomics, 2013. **56**(6): p. 977-991.

55. Marras, W.S., S.A. Lavender, S.A. Ferguson, R.E. Splittstoesser, and G. Yang, *Quantitative dynamic measures of physical exposure predict low back functional impairment.* Spine, 2010. **35**(8): p. 914-923.

56. Yezak, M. *Thoracic Spine Anatomy and Upper Back Pain*. 2011 [cited 2015 21st May]; Available from: http://www.spine-health.com/conditions/spine-anatomy/thoracic-spine-anatomy-and-upper-back-pain.

57. Davis, E. *Lumbar Spine Anatomy and Pain*. 2011 [cited 2015 21st May]; Available from: http://www.spine-health.com/conditions/spine-anatomy/lumbar-spine-anatomy-and-pain.

58. Ullrich, P.F.J. *Cervical Spine Anatomy and Neck Pain*. 2009 [cited 2015 21st May]; Available from: http://www.spine-health.com/conditions/spine-anatomy/cervical-spine-anatomy-and-neck-pain.

59. Murray, C.J.L., T. Vos, R. Lozano, M. Naghavi, A.D. Flaxman, C. Michaud, . . . A.D. Lopez, *Disability-adjusted life years (DALYs) for 291 diseases and injuries in 21 regions, 1990–2010: a systematic analysis for the Global Burden of Disease Study 2010.* Lancet, 2012. **380**(9859): p. 2197-2223.

60. Institute for Health Metrics and Evaluation, *The Global Burden of Disease: Generating Evidence, Guiding Policy*. 2013, Seattle, WA: IHME.

61. Hoy, D.G., E. Smith, M. Cross, L. Sanchez-Riera, R. Buchbinder, F.M. Blyth, . . . L.M. March, *The global burden of musculoskeletal conditions for 2010: an overview of methods.* Ann Rheum Dis, 2014. **73**(6): p. 982-989.

62. Qaseem, A., T.J. Wilt, R.M. McLean, M.A. Forciea, and f.t.C.G.C.o.t.A.C.o. Physicians, *Noninvasive Treatments for Acute, Subacute, and Chronic Low Back Pain: A Clinical Practice Guideline From the American College of PhysiciansNoninvasive Treatments for Acute, Subacute, and Chronic Low Back Pain.* Annals of Internal Medicine, 2017. **166**(7): p. 514-530.

63. Balagué, F., A.F. Mannion, F. Pellisé, and C. Cedraschi, *Non-specific low back pain.* The Lancet, 2012. **379**(9814): p. 482-491.

64. Souza, L.D. and A. Frank, *Experiences of living with chronic back pain: The physical disabilities.* Disabil Rehabil, 2007. **29**(7): p. 587-596.

65. Daffner, S.D., A.S. Hilibrand, B.S. Hanscom, B.T. Brislin, A.R. Vaccaro, and T.J. Albert, *Impact of Neck and Arm Pain on Overall Health Status.* Spine, 2003. **28**(17): p. 2030-2035.

66. Viikari-Juntura, E., E.-P. Takala, H. Riihimäki, R. Martikainen, and P. Jäppinen, *Predictive validity of symptoms and signs in the neck and shoulders.* J Clin Epidemiol, 2000. **53**(8): p. 800-808.

67. Steiner, C., *Man vs. machine.* Forbes, 2007. **180**: p. 104-109.

68. Hartvigsen, J., C. Leboeuf-Yde, S. Lings, and E.H. Corder, *Is sitting-while-at-work associated with low back pain? A systematic, critical literature review.* Scandinavian journal of public health, 2000. **28**(3): p. 230-239.

69. Arjmand, N., O. Ekrami, A. Shirazi-Adl, A. Plamondon, and M. Parnianpour, *Relative performances of artificial neural network and regression mapping tools in evaluation of spinal loads and muscle forces during static lifting.* J Biomech, 2013. **46**(8): p. 1454-1462.

70. Arjmand, N., A. Plamondon, A. Shirazi-Adl, M. Parnianpour, and C. Larivière, *Predictive equations for lumbar spine loads in load-dependent asymmetric one- and two-handed lifting activities.* Clin Biomech, 2012. **27**(6): p. 537-544.

71. Forde, K.A., W.J. Albert, M.F. Harrison, J.P. Neary, J. Croll, and J.P. Callaghan, *Neck loads and posture exposure of helicopter pilots during simulated day and night flights.* Int J Ind Ergon, 2011. **41**(2): p. 128-135.

72. McGill, S.M. and R.W. Norman, *Dynamically and Statically Determined Low Back Moments During Lifting.* J Biomech, 1985. **18**(12): p. 877-885.

73. McGill, S.M., R.W. Norman, and J. Cholewicki, *A simple polynomial that predicts low-back compression during complex 3-D tasks.* Ergonomics, 1996. **39**(9): p. 1107-1118.

74. Merryweather, A.S., M.C. Loertscher, and D.S. Bloswick, *A revised back compressive force estimation model for ergonomic evaluation of lifting tasks.* Work, 2009. **34**(3): p. 263-272.

75. Potvin, J.R., *Use of NIOSH equation inputs to calculate lumbosacral compression forces.* Ergonomics, 1997. **40**(7): p. 691-707.

76. Vette, A.H., T. Yoshida, T.A. Thrasher, K. Masani, and M.R. Popovic, *A comprehensive three-dimensional dynamic model of the human head and trunk for estimating lumbar and cervical joint torques and forces from the upper body kinematics.* Med Eng Phys, 2012. **34**(5): p. 640-649.

77. Rajaee, M.A., N. Arjmand, A. Shirazi-Adl, A. Plamondon, and H. Schmidt, *Comparative evaluation of six quantitative lifting tools to estimate spine loads during static activities.* Appl Ergon, 2015. **48**: p. 22-32.

78. Arjmand, N., D. Gagnon, A. Plamondon, A. Shirazi-Adl, and C. Larivière, *A comparative study of two trunk biomechanical models under symmetric and asymmetric loadings.* J Biomech, 2010. **43**(3): p. 485-491.

79. Damsgaard, M., J. Rasmussen, S.T. Christensen, E. Surma, and M. de Zee, *Analysis of musculoskeletal systems in the AnyBody Modelling System.* Simul Model Pract and Theory, 2006. **14**(8): p. 1100-1111.

80. Stenlund, T.C., F. Öhberg, R. Lundström, O. Lindroos, C. Häger, and B. Rehn, *Inter- and intra-tester reliability when measuring seated spinal postures with inertial sensors.* Int J Ind Ergon, 2014. **44**(5): p. 732-738.

81. Chiu, T., W. Ku, M. Lee, W. Sum, M. Wan, C. Wong, and C. Yuen, *A Study on the Prevalence of and Risk Factors for Neck Pain Among University Academic Staff in Hong Kong*. J Occup Rehabil, 2002. **12**(2): p. 77-91.

82. Chiu, T., K. Lau, C. Ho, M. Ma, T. Yeung, and P. Cheung, *A study on the prevalence of and risk factors for neck pain in secondary school teachers.* Public Health, 2006. **120**(6): p. 563-565.

83. Veritashealth. *Spine Anatomy Interactive Video*. copyright 1999-2018 [cited 2018 May 2nd].

84. Schulze, M., F. Trautwein, T. Vordemvenne, M. Raschke, and F. Heuer, *A method to perform spinal motion analysis from functional X-ray images.* J Biomech, 2011. **44**(9): p. 1740-1746.

85. Frobin, W., P. Brinckmann, G. Leivseth, M. Biggermann, and O. Reikeras, *Precision measurement of segmental motion from flexion-extension radiographs of the lumbar spine.* Clin Biomech, 1996. **11**(8): p. 457-465.

86. Dvorák, J., M. Panjabi, D. Grob, J. Novotny, and J. Antinnes, *Clinical Validation of Functional Flexion/Extension Radiographs of the Cervical Spine*. Spine, 1993. **18**(1): p. 120-127.

87. Tousignant, M., L.d. Bellefeuille, S. O'Donoughues, and S. Grahovac, *Criterion validity of the cervical range of motion (CROM) goniometer for cervical flexion and extension.* Spine, 2000. **25**(3): p. 324-330.

88. Marin, F., N. Hoang, P. Aufaure, and M. Ho Ba Tho, *In vivo intersegmental motion of the cervical spine using an inverse kinematics procedure.* Clin Biomech, 2010. **25**(5): p. 389-396.

89. Wong, W.Y. and M.S. Wong, *Detecting spinal posture change in sitting positions with tri-axial accelerometers.* Gait Posture, 2008. **27**(1): p. 168-171.

90. Campbell-Kyureghyan, N., M. Jorgensen, D. Burr, and W. Marras, *The prediction of lumbar spine geometry: method development and validation.* Clin Biomech, 2005. **20**(5): p. 455-464.

91. Ehara, Y., H. Fujimoto, S. Miyazaki, M. Mochimaru, S. Tanaka, and S. Yamamoto, *Comparison of the performance of 3D camera systems II.* Gait Posture, 1997. **5**(3): p. 251-255.

92. Papić, V., V. Zanchi, and M. Cecić, *Motion analysis system for identification of 3D human locomotion kinematics data and accuracy testing.* Simul Model Pract and Theory, 2004. **12**(2): p. 159-170.

93. Quesada, P.M. and G.S. Rash, *Measurement of Human Movement*, in *International Encyclopedia of Ergonomics and Human Factors*, W. Karwowski, Editor. 2006, CRC Press: Boca Raton, Florida, USA,. p. 3238-3242.

94. Ehara, Y., H. Fujimoto, S. Miyazaki, S. Tanaka, and S. Yamamoto, *Comparison of the performance of 3D camera systems.* Gait Posture, 1994. **3**(3): p. 166-169.

95. Richards, J., *The measurement of human motion: A comparison of commercially available systems.* Hum Mov Sci, 1999. **18**(5): p. 589-602.

96. Carse, B., B. Meadows, R. Bowers, and P. Rowe, *Affordable clinical gait analysis: An assessment of the marker tracking accuracy of a new low-cost optical 3D motion analysis system.* Physiother, 2013. **99**(4): p. 347-351.

97. Fuller, J., L. Liu, M. Murphy, and R. Mann, *A comparison of lower-extremity skeletal kinematics measured using skin- and pin-mounted markers.* Hum Mov Sci, 1997. **16**(2): p. 219-242.

98. Benoit, D., D. Ramsey, M. Lamontagne, L. Xu, P. Wretenberg, and P. Renström, *Effect of skin movement artifact on knee kinematics during gait and cutting motions measured in vivo.* Gait Posture, 2006. **24**(2): p. 152-164.

99. Lu, T.W. and J.J. O'Connor, *Bone position estimation from skin marker co-ordinates using global optimisation with joint constraints.* J Biomech, 1999. **32**(2): p. 129-134.

100. Reinschmidt, C., A. van den Bogert, B. Nigg, A. Lundberg, and N. Murphy, *Effect of skin movement on the analysis of skeletal knee joint motion during running.* J Biomech, 1997. **30**(7): p. 729-733.

101. Mayagoitia, R.E., A.V. Nene, and P.H. Veltink, *Accelerometer and rate gyroscope measurement of kinematics: an inexpensive alternative to optical motion analysis systems.* J Biomech, 2002. **35**(4): p. 537-542.

102. Alqhtani, R.S., M.D. Jones, P.S. Theobald, and J.M. Williams, *Reliability of an Accelerometer-Based System for Quantifying Multiregional Spinal Range of Motion.* J Manip Physiol Ther, 2015. **38**(4): p. 275-281.

103. Morrison, M.M., *Inertial measurement unit*, G. Patents, Editor. 1987: United States of America.

104. Goodvin, C., E. Park, K. Huang, and K. Sakaki, *Development of a real-time three-dimensional spinal motion measurement system for clinical practice.* Med Biol Eng Comput, 2006. **44**(12): p. 1061-1075.

105. Brodie, M.A., A. Walmsley, and W. Page, *The static accuracy and calibration of inertial measurement units for 3D orientation.* Computer Methods in Biomechanics and Biomedical Engineering, 2008. **11**(6): p. 641-648.

106. Schall, M.C.J., N.B. Fethke, H. Chen, and F. Gerr, *A comparison of instrumentation methods to estimate thoracolumbar motion in field-based occupational studies.* Appl Ergon, 2015. **48**: p. 224-231.

107. Han, S. and J. Wang, *A Novel Method to Integrate IMU and Magnetometers in Attitude and Heading Reference Systems.* J Navigation, 2011. **64**(4): p. 727-738.

108. LORD Corporation MicroStrain Sensing Systems, *3DM-GX3 -25 Miniature Attitude Heading Reference System*, in *LORD Product Datasheet*, L. Corporation, Editor. 2014: Williston, VT, USA.

109. Xsens Technologies B.V., *Motion Tracker Technical Documentation MT9-B and MT6-B* Xsens Technologies B.V., Editor. 2005: Netherlands.

110. Xsens Technologies B.V., *MTi and MTx User Manual and Technical Documentation*, Xsens Technologies B.V., Editor. 2006: Netherlands.

111. Xsens Technologies. *MTi-G-700-GPSINS-6A5G4-DK*. Xsens Online Shop 2015 [cited 2015 15th April]; Available from: http://shop.xsens.com/shop/mti-g-100-series/mti-g-700-gps-ins/mti-g-700-gpsins-6a5g4-dk.

112. Ronchi, A., *A Reliability Study of a New Back Strain Monitor Based on Clinical Trials*, in *School of Electrical and Computer Engineering*. 2008, Royal Melbourne Institute of Technology.

113. SparkFun. *9 Degrees of Freedom - Razor IMU SEN-10736 ROHS*. [cited 2015 16th June]; Available from: https://www.sparkfun.com/products/10736.

114. Marras, W.S., F.A. Fathallah, R.J. Miller, S.W. Davis, and G.A. Mirka, *Accuracy of a three-dimensional lumbar motion monitor for recording dynamic trunk motion characteristics.* Int J Ind Ergon, 1992. **9**(1): p. 75-87.

115. Petersen, C.M., R.D. Johnson, and D. Schuit, *Reliability of cervical range of motion using the OSI CA 6000 Spine Motion Analyser on asymptomatic and symptomatic subjects.* Man Ther, 2000. **5**(2): p. 82-88.

116. Petersen, C.M., D. Schuit, R.D. Johnson, H. Knecht, and P. Levine, *Agreement of measures obtained radiographically and by the OSI CA-6000 Spine Motion Analyzer for cervical spinal motion.* Man Ther, 2008. **13**(3): p. 200-205.

117. Wang, P.T., C.E. King, A.H. Do, and Z. Nenadic, *A durable, low-cost electrogoniometer for dynamic measurement of joint trajectories.* Med Eng Phys, 2011. **33**(5): p. 546-552.

118. Tesio, L., M. Monzani, R. Gatti, and F. Franchignoni, *Flexible electrogoniometers: kinesiological advantages with respect to potentiometric goniometers.* Clin Biomech, 1995. **10**(5): p. 275-277.

119. Shiratsu, A. and H.J.C.G. Coury, *Reliability and accuracy of different sensors of a flexible electrogoniometer.* Clin Biomech, 2003. **18**(7): p. 682-684.

120. Biometrics Ltd., *GBP Price List - Sreptember 2014*, in *Biometrics Ltd Pounds Sterling Price List*. 2014. p. 3.

121. Mills, P.M., S. Morrison, D.G. Lloyd, and R.S. Barret, *Repeatability of 3D gait kinematics obtained from an electromagnetic tracking system during treadmill locomotion.* J Biomech, 2007. **40**(7): p. 1504-1511.

122. Amiri, M., G. Jull, and J. Bullock-Saxton, *Measuring range of active cervical rotation in a position of full head flexion using the 3D FASTRAK measurement system: an intra-tester reliability study.* Man Ther, 2003. **8**(3): p. 176-179.

123. Jordan, K., K. Dziedzic, P.W. Jones, B.N. Ong, and P.T. Dawes, *The reliability of the three-dimensional FASTRAK measurement system in measuring cervical spine and shoulder range of motion in healthy subjects.* J Rheumatol, 2000. **39**(4): p. 382-388.

124. Jordan, K., K.L. Haywood, K. Dziedzic, A.M. Garratt, P.W. Jones, B.N. Ong, and P.T. Dawes, *Assessment of the 3-dimensional FASTRAK measurement system in measuring range of motion in ankylosing spondylitis.* J Rheumatol, 2004. **31**(11): p. 2207-2215.

125. Sterling, M., G. Jull, Y. Carlsson, and L. Crommert, *Are cervical physical outcome measures influenced by the presence of symptomatology.* Physiother Research Int, 2002. **7**(3): p. 113-121.

126. Koerhuis, C.L., J.C. Winters, F.C.T. van der Helm, and A.L. Hof, *Neck mobility measurement by means of the 'Flock of Birds' electromagnetic tracking system.* Clin Biomech, 2003. **18**(1): p. 14-18.

127. Assink, N., G.J.D. Bergman, B. Knoester, J.C. Winters, P.U. Dijkstra, and K. Postema, *Interobserver reliability of neck-mobility measurement by means of the Flock-Of-Birds electromagnetic tracking system.* J Manip Physiol Ther, 2005. **28**(6): p. 408-413.

128. Bull, A.M. and A.H. McGregor, *Measuring spinal motion in rowers: the use of an electromagnetic device.* Clin Biomech, 2000. **15**(10): p. 772-776.

129. Morphett, A.L., C.M. Crawford, and D. Lee, *The use of electromagnetic tracking technology for measurement of passive cervical range of motion: A Pilot Study.* J Manip Physiol Ther, 2003. **26**(3): p. 152-159.

130. Polhemus, *FASTRAK Brochure*. 2008.

131. Polhemus, *LIBERTY Brochure*. 2008.

132. Ascension Technology Corporation, *Flock Of Birds Brochure*. 2000.

133. Schuler, N.B., M.J. Bey, J.T. Shearn, and D.L. Butler, *Evaluation of an electromagnetic position tracking device for measuring in vivo, dynamic joint kinematics.* J Biomech, 2005. **38**(10): p. 2113-2117.

134. Banaee, H., M.U. Ahmed, and A. Loutfi, *Data Mining for Wearable Sensors in Health Monitoring Systems: A Review of Recent Trends and Challenges.* Sensors, 2013. **13**: p. 17472-17500.

135. Bonato, P., *Wearable Sensors/Systems and Their Impact on Biomedical Engineering*, in *IEEE Engineering in Medicine and Biology Magazine*. 2003. p. 18-20.

136. Patel, S., H. Park, P. Bonato, L. Chan, and M. Rodgers, *A review of wearable sensors and systems with application in rehabilitation.* J NeuroEng Rehabil, 2012. **9**(1): p. 21.

137. Statista. *Facts and statistics on Wearable Technology*. [cited 2016 17th Novemeber]; Available from: https://www.statista.com/topics/1556/wearable-technology/.

138. Atallah, L., B. Lo, and G.Z. Yang, *Can Pervasive Sensing Address Current Challenges in Global Healthcare?* J Epidemiol Global Health, 2012. **2**(1): p. 1-13.

139. Avci, A., S. Bosch, M. Marin-Perianu, R. Marin-Perianu, and P. Havinga. *Activity Recognition Using Inertial Sensing for Healthcare, Wellbeing and Sports Applications: A Survey*. in *Architecture of Computing Systems (ARCS), 2010 23rd International Conference on*. 2010.

140. Nangalia, V., D.R. Prytherch, and G.B. Smith, *Health technology assessment review: Remote monitoring of vital signs - current status and future challenges.* Crit Care, 2010. **14**(5): p. 233.

141. Ding, D., K.D. Lawson, T.L. Kolbe-Alexander, E.A. Finkelstein, P.T. Katzmarzyk, W. van Mechelen, and M. Pratt, *The economic burden of physical inactivity: a global analysis of major non-communicable diseases.* The Lancet, 2016. **388**(10051): p. 1311-1324.

142. Andersen, L.B., J. Mota, and L. Di Pietro, *Update on the global pandemic of physical inactivity.* The Lancet, 2016. **388**(10051): p. 1255-1256.

143. Bames, J., T.K. Behrens, M.E. Benden, S. Biddle, D. Bond, P. Brassard, . . . J. Chaput, *Letter to the Editor: Standardized use of the terms "sedentary" and "sedentary behaviours".* Applied Physiology, Nutrition, and Metabolism, 2012. **37**(3): p. 540-542.

144. Ekelund, U., J. Steene-Johannessen, W.J. Brown, M.W. Fagerland, N. Owen, K.E. Powell, . . . I.M. Lee, *Does physical activity attenuate, or even eliminate, the detrimental association of sitting time with mortality? A harmonised meta-analysis of data from more than 1 million men and women.* The Lancet, 2016. **388**(10051): p. 1302-1310.

145. Kyu, H.H., V.F. Bachman, L.T. Alexander, J.E. Mumford, A. Afshin, K. Estep, . . . M.H. Forouzanfar, *Physical activity and risk of breast cancer, colon cancer, diabetes, ischemic heart disease, and ischemic stroke events: systematic review and dose-response meta-analysis for the Global Burden of Disease Study 2013.* BMJ, 2016. **354**.

146. Lozano, R., M. Naghavi, K. Foreman, S. Lim, K. Shibuya, V. Aboyans, . . . C.J.L. Murray, *Global and regional mortality from 235 causes of death for 20 age groups in 1990 and 2010: a systematic analysis for the Global Burden of Disease Study 2010.* The Lancet, 2012. **380**(9859): p. 2095-2128.

147. Morris, J.N., J.A. Heady, P.A.B. Raffle, C.G. Roberts, and J.W. Parks, *Coronary Heart-Disease and Physical Activity of Work.* The Lancet, 1953. **262**(6795): p. 1053-1056.

148. Morris, J.N., J.A. Heady, P.A.B. Raffle, C.G. Roberts, and J.W. Parks, *Coronary Heart-Disease and Physical Activity of Work.* The Lancet, 1953. **262**(6796): p. 1111-1120.

149. Morris, J.N. and M.D. Crawford, *Coronary Heart Disease and Physical Activity of Work.* British Medical Journal, 1958. **2**(5111): p. 1485-1496.

150. Heady, J.A., J.N. Morris, A. Kagan, and P.A.B. Raffle, *Coronary Heart Disease in London Busmen: A Progress Report with Particular Reference to Physique.* British Journal of Preventive & Social Medicine, 1961. **15**(4): p. 143-153.

151. Paffenbarger, J.R.S., A.L. Wing, and R.T. Hyde, *Physical Activity as an Index of Heart Attack Risk in College Alumni.* American Journal of Epidemiology, 1978. **108**(3): p. 161-175.

152. Paffenbarger , R.S.J., R. Hyde , A.L. Wing , and C.-c. Hsieh *Physical Activity, All-Cause Mortality, and Longevity of College Alumni.* New England Journal of Medicine, 1986. **314**(10): p. 605-613.

153. Paffenbarger , R.S.J., M.E. Laughlin , A.S. Gima , and R.A. Black *Work Activity of Longshoremen as Related to Death from Coronary Heart Disease and Stroke.* New England Journal of Medicine, 1970. **282**(20): p. 1109-1114.

154. Benjamin, E.J., S.S. Virani, C.W. Callaway, A.M. Chamberlain, A.R. Chang, S. Cheng, . . . P. Muntner, *Heart Disease and Stroke Statistics – 2018 Update: A Report From the American Heart Association.* Circulation, 2018. **137**(12): p. e67.

155. Feigin, V.L., M.H. Forouzanfar, R. Krishnamurthi, G.A. Mensah, M. Connor, D.A. Bennett, . . . C. Murray, *Global and regional burden of stroke during 1990–2010: findings from the Global Burden of Disease Study 2010.* The Lancet, 2014. **383**(9913): p. 245-255.

156. Soares-Miranda, L., D.S. Siscovick, B.M. Psaty, W.T. Longstreth, and D. Mozaffarian, *Physical Activity and Risk of Coronary Heart Disease and Stroke in Older Adults: The Cardiovascular Health Study.* Circulation, 2015.

157. McDonnell, M.N., S.L. Hillier, S.E. Judd, Y. Yuan, S.P. Hooker, and V.J. Howard, *Association between television viewing time and risk of incident stroke in a general population: Results from the REGARDS study.* Preventive Medicine, 2016. **87**: p. 1-5.

158. Pandey, A., U. Salahuddin, S. Garg, and et al., *Continuous dose-response association between sedentary time and risk for cardiovascular disease: A meta-analysis.* JAMA Cardiology, 2016. **1**(5): p. 575-583.

159. Chomistek, A.K., J.E. Manson, M.L. Stefanick, B. Lu, M. Sands-Lincoln, S.B. Going, . . . C.B. Eaton, *Relationship of Sedentary Behavior and Physical Activity to Incident Cardiovascular Disease: Results From the Women's Health Initiative.* Journal of the American College of Cardiology, 2013. **61**(23): p. 2346-2354.

160. Jefferis, B.J., P.H. Whincup, O. Papacosta, and S.G. Wannamethee, *Protective Effect of Time Spent Walking on Risk of Stroke in Older Men.* Stroke, 2014. **45**(1): p. 194.

161. Tikk, K., D. Sookthai, S. Monni, M.-L. Gross, C. Lichy, M. Kloss, and R. Kaaks, *Primary Preventive Potential for Stroke by Avoidance of Major Lifestyle Risk Factors.* Stroke, 2014.

162. Blomstrand, A., C. Blomstrand, N. Ariai, C. Bengtsson, and C. Björkelund, *Stroke incidence and association with risk factors in women: a 32-year follow-up of the Prospective Population Study of Women in Gothenburg.* BMJ Open, 2014. **4**(10).

163. Armstrong, M.E.G., J. Green, G.K. Reeves, V. Beral, and B.J. Cairns, *Frequent Physical Activity May not Reduce Vascular Disease Risk as Much as Moderate Activity: Large Prospective Study of UK Women.* Circulation, 2015.

164. Åberg, N.D., H.G. Kuhn, J. Nyberg, M. Waern, P. Friberg, J. Svensson, . . . M. Nilsson, *Influence of Cardiovascular Fitness and Muscle Strength in Early Adulthood on Long-Term Risk of Stroke in Swedish Men.* Stroke, 2015.

165. Joshua, Z.W., P.M. Yeseon, L.S. Ralph, G. Heather, M.D. Keith, B.W. Clinton, . . . K.C. Yuen, *Physical inactivity is a strong risk factor for stroke in the oldest old: Findings from a multi-ethnic population (the Northern Manhattan Study).* International Journal of Stroke, 2016. **12**(2): p. 197-200.

166. Bell, E.J., P.L. Lutsey, B.G. Windham, and A.R. Folsom, *Physical Activity and Cardiovascular Disease in African Americans in ARIC.* Medicine and science in sports and exercise, 2013. **45**(5): p. 901-907.

167. Biswas, A., P.I. Oh, G.E. Faulkner, and et al., *Sedentary time and its association with risk for disease incidence, mortality, and hospitalization in adults: A systematic review and meta-analysis.* Annals of Internal Medicine, 2015. **162**(2): p. 123-132.

168. Sallis, J.F., F. Bull, R. Guthold, G.W. Heath, S. Inoue, P. Kelly, . . . P.C. Hallal, *Progress in physical activity over the Olympic quadrennium.* The Lancet, 2016. **388**(10051): p. 1325-1336.

169. Warburton, D.E.R., C.W. Nicol, and S.S.D. Bredin, *Health benefits of physical activity: the evidence.* Canadian Medical Association Journal, 2006. **174**(6): p. 801.

170. King, A.C., C.B. Taylor, W.L. Haskell, and R.F. DeBusk, *Influence of regular aerobic exercise on psychological health: a randomized, controlled trial of healthy middle-aged adults.* Health Psychology, 1989. **8**(3): p. 305.

171. Taylor, C.B., J.F. Sallis, and R. Needle, *The relation of physical activity and exercise to mental health.* Public Health Reports, 1985. **100**(2): p. 195-202.

172. Bouten, C.V.C., K.T.M. Koekkoek, M. Verduin, R. Kodde, and J.D. Janssen, *A triaxial accelerometer and portable data processing unit for the assessment of daily physical activity.* IEEE Transactions on Biomedical Engineering, 1997. **44**(3): p. 136-147.

173. The Mathworks Inc., *Applying Supervised Learning*, in *Machine Learning with MATLAB*. 2016.

174. Hussain, R.G., M.A. Ghazanfar, M.A. Azam, U. Naeem, and S. Ur Rehman, *A performance comparison of machine learning classification approaches for robust activity of daily living recognition.* Artificial Intelligence Review, 2018.

175. Liaw, A. and M. Wiener, *Classification and regression by randomForest.* R news, 2002. **2**(3): p. 18-22.

176. Breiman, L., *Random Forests.* Machine Learning, 2001. **45**(1): p. 5-32.

177. Cunningham, P. and S.J. Delany, *k-Nearest neighbour classifiers.* Multiple Classifier Systems, 2007. **34**(8): p. 1-17.

178. Hechenbichler, K. and K. Schliep, *Weighted k-nearest-neighbor techniques and ordinal classification.* 2004.

179. Begg, R. and J. Kamruzzaman, *A machine learning approach for automated recognition of movement patterns using basic, kinetic and kinematic gait data.* Journal of Biomechanics, 2005. **38**(3): p. 401-408.

180. Bourke, A.K., J.V. O'Brien, and G.M. Lyons, *Evaluation of a threshold-based tri-axial accelerometer fall detection algorithm.* Gait & Posture, 2007. **26**(2): p. 194-199.

181. Bourke, A.K., K.J. O'Donovan, and G. ÓLaighin, *The identification of vertical velocity profiles using an inertial sensor to investigate pre-impact detection of falls.* Medical Engineering & Physics, 2008. **30**(7): p. 937-946.

182. Doughty, K., R. Lewis, and A. McIntosh, *The design of a practical and reliable fall detector for community and institutional telecare.* Journal of Telemedicine and Telecare, 2000. **6**(1_suppl): p. 150-154.

183. Diaz, A., M. Prado, L. Roa, J. Reina-Tosina, and G. Sanchez. *Preliminary evaluation of a full-time falling monitor for the elderly*. in *Engineering in Medicine and Biology Society, 2004. IEMBS'04. 26th Annual International Conference of the IEEE*. 2004. IEEE.

184. Hwang, J.-Y., J. Kang, Y.W. Jang, and H.-C. Kim. *Development of novel algorithm and real-time monitoring ambulatory system using Bluetooth module for fall detection in the elderly*. in *Engineering in Medicine and Biology Society, 2004. IEMBS'04. 26th Annual International Conference of the IEEE*. 2004. IEEE.

185. Noury, N., P. Barralon, G. Virone, P. Boissy, M. Hamel, and P. Rumeau. *A smart sensor based on rules and its evaluation in daily routines*. in *Engineering in medicine and biology society, 2003. Proceedings of the 25th annual international conference of the IEEE*. 2003. IEEE.

186. Baker, S.P. and A.H. Harvey, *Fall injuries in the elderly.* Clinics in geriatric medicine, 1985. **1**(3): p. 501-512.

187. Hoyert, D.L., K.D. Kochanek, and S.L. Murphy, *Deaths: final data for 1997.* Natl Vital Stat Rep, 1999. **47**(19): p. 1-104.

188. Lord, S.R., J.A. Ward, P. Williams, and K.J. Anstey, *An epidemiological study of falls in older community-dwelling women: the Randwick falls and fractures study.* Australian Journal of Public Health, 1993. **17**(3): p. 240-245.

189. Tinetti, M.E., M. Speechley, and S.F. Ginter, *Risk Factors for Falls among Elderly Persons Living in the Community.* New England Journal of Medicine, 1988. **319**(26): p. 1701-1707.

190. Project, T.G.C., *The Rotation Problem*. 2009; Available From: https//vimeo.com/2649637

191. Consmüller, T., A. Rohlmann, D. Weinland, C. Druschel, G.N. Duda, and W.R. Taylor, *Velocity of Lordosis Angle during Spinal Flexion and Extension.* PLoS ONE, 2012. **7**(11): p. e50135.

192. STMicroelectronics, *Tilt measurement using a low-g 3-axis accelerometer*, in *AN 3182 Application Note*. 2010.

193. Landers, R., *Computing Intraclass Correlations (ICC) as Estimates of Interrater Reliability in SPSS.* The Winnower, 2015. **2**.

194. Mayo Clinic. *Bedsores (pressure ulcers)*. 2018 30th August 2018]; Available from: https://www.mayoclinic.org/diseases-conditions/bed-sores/symptoms-causes/syc-20355893.

195. Mathie, M.J., A.C.F. Coster, N.H. Lovell, and B.G. Celler, *Accelerometry: providing an integrated, practical method for long-term, ambulatory monitoring of human movement.* Physiol Meas, 2004. **25**(2): p. R1.

196. Mannini, A. and A.M. Sabatini, *Machine Learning Methods for Classifying Human Physical Activity from On-Body Accelerometers.* Sensors, 2010. **10**(2).

197. Fan, L., Z. Wang, and H. Wang. *Human Activity Recognition Model Based on Decision Tree*. in *2013 International Conference on Advanced Cloud and Big Data*. 2013.

198. Shoaib, M., H. Scholten, and P.J.M. Havinga. *Towards Physical Activity Recognition Using Smartphone Sensors*. in *2013 IEEE 10th International Conference on Ubiquitous Intelligence and Computing and 2013 IEEE 10th International Conference on Autonomic and Trusted Computing*. 2013.

199. Ravi, N., N. Dandekar, P. Mysore, and M.L. Littman. *Activity recognition from accelerometer data*. in *Aaai*. 2005.

200. Himann, J.E., D.A. Cunningham, P.A. Rechnitzer, and D.H. Paterson, *Age-related changes in speed of walking.* Medicine and science in sports and exercise, 1988. **20**(2): p. 161-166.

201. Marras, W.S. and P.E. Wongsam, *Flexibility and velocity of Normal and Impaired Lumbar Spine.* Arch Phys Med Rehab, 1986. **67**: p. 213-217.

202. Faber, G.S., I. Kingma, S.M. Bruijn, and J.H.v. Dieën, *Optimal inertial sensor location for ambulatory measurement of trunk inclination.* J Biomech, 2009. **42**(14): p. 2406-2409.

203. Bergamini, E., P. Guillon, V. Camomilla, H. Pillet, W. Skalli, and A. Cappozzo, *Trunk Inclination Estimation During the Sprint Start Using an Inertial Measurement Unit: A Validation Study.* J Appl Biomech, 2013. **29**(5): p. 622-627.

204. Lee, J.K., G.T. Desmoulin, A.H. Khan, and E.J. Park, *Comparison of 3D spinal motions during stair-climbing between individuals with and without low back pain.* Gait Posture, 2011. **34**(2): p. 222-226.

205. Ashouri, S., M. Abedi, M. Abdollahi, F. Dehghan Manshadi, M. Parnianpour, and K. Khalaf, *A novel approach to spinal 3-D kinematic assessment using inertial sensors: Towards effective quantitative evaluation of low back pain in clinical settings.* Comput Biol Med, 2017. **89**(Supplement C): p. 144-149.

206. Faber, G.S., C.C. Chang, I. Kingma, J.T. Dennerlein, and J.H. van Dieën, *Estimating 3D L5/S1 moments and ground reaction forces during trunk bending using a full-body ambulatory inertial motion capture system.* J Biomech, 2016. **49**(6): p. 904-912.

207. Trott, P.H., M.J. Pearcy, S.A. Ruston, I. Fulton, and C. Brien, *Three-dimensional analysis of active cervical motion: the effect of age and gender.* Clin Biomech, 1996. **11**(4): p. 201-206.

208. Ordway, N.R., R. Seymour, R.G. Donelson, L. Hojnowski, E. Lee, and W.T. Edwards, *Cervical Sagittal Range-of-Motion Analysis Using Three Methods.* Spine, 1997. **22**(5): p. 501-508.

209. Mjøsund, H.L., E. Boyle, P. Kjaer, R.M. Mieritz, T. Skallgård, and P. Kent, *Clinically acceptable agreement between the ViMove wireless motion sensor system and the Vicon motion capture system when measuring lumbar region inclination motion in the sagittal and coronal planes.* BMC Musculoskelet Dis, 2017. **18**(1): p. 124.

Appendix A:

Accelerometer Frequency Domain Plots

In this section is an example of data collected from all three axes of both accelerometers for each of the activities of the activity classifier, presented in the frequency domain. The majority of the signal for static activities occurs at 0 Hz, with various axes being the dominant axis depending on the orientation of the accelerometer in three-dimensional space. For dynamic activities, there is an increased response from accelerometers at numerous frequencies with the amplitude of these depending on the type and intensity of activity performed.

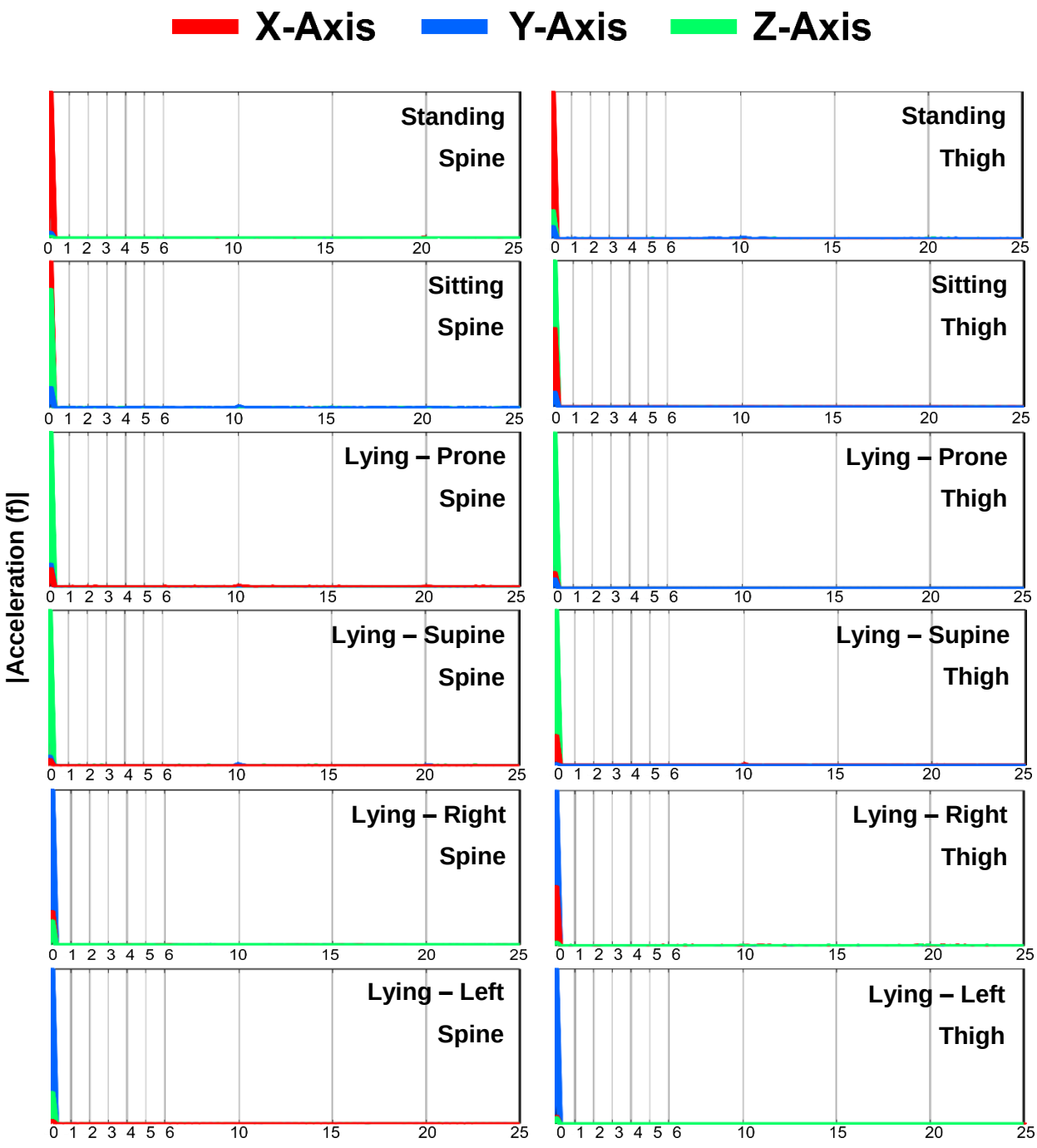

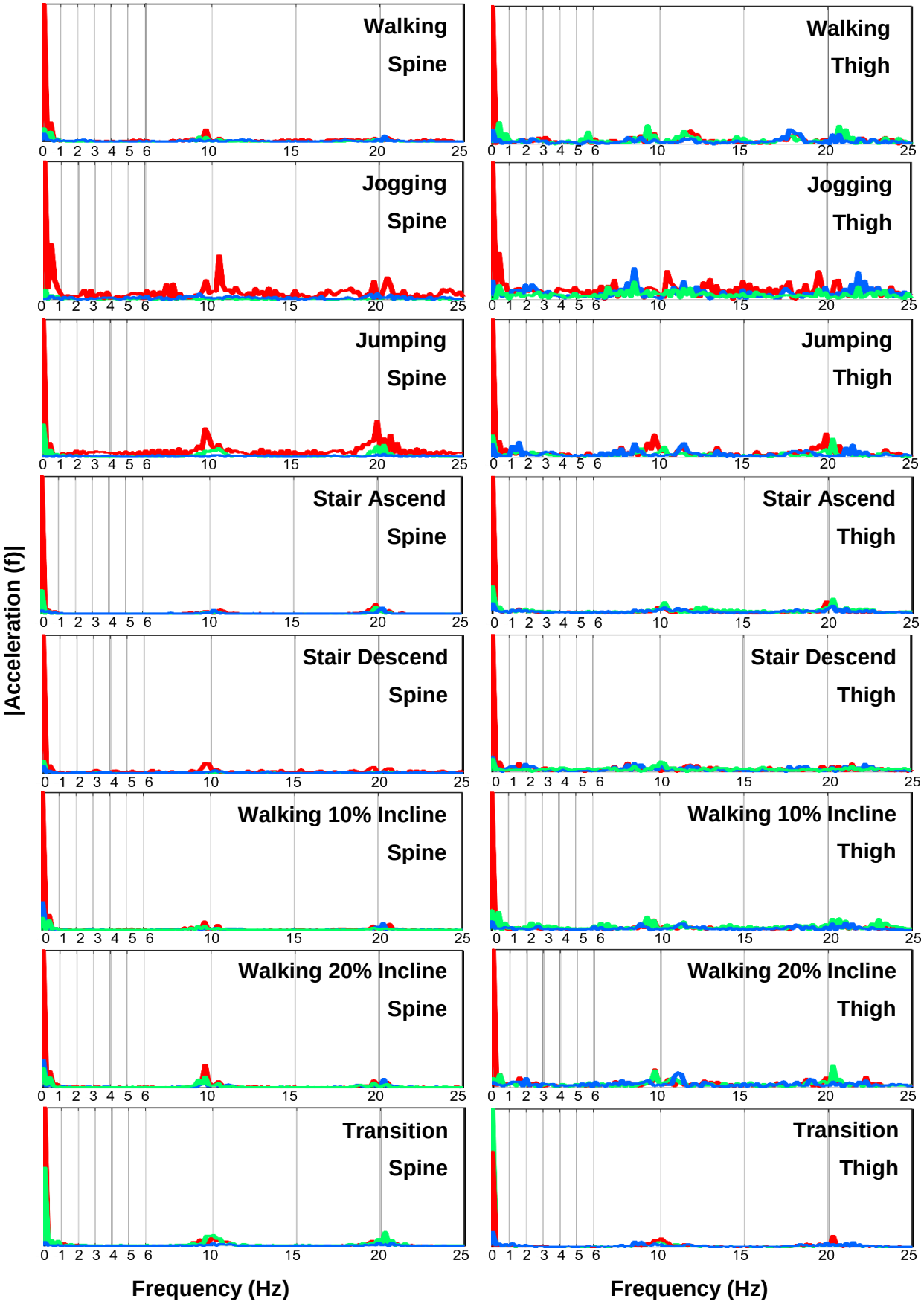
Walking
Spine
Walking
Thigh
Jogging
Spine
Jogging
Thigh
Jumping
Spine
Jumping
Thigh
Stair Ascend
Spine
Stair Ascend
Thigh
Stair Descend
Spine
Stair Descend
Thigh
Walking 10% Incline
Spine
Walking 10% Incline
Thigh
Walking 20% Incline
Spine
Walking 20% Incline
Thigh
Transition
Spine
Transition
Thigh
0 1 2 3 4 5 6 10 15 20 25
|Acceleration (f)|
Frequency (Hz)
Frequency (Hz)

Appendix B:

Spine Orientation Bland-Altman Plots

Participant # 1 2 3 4 5 6

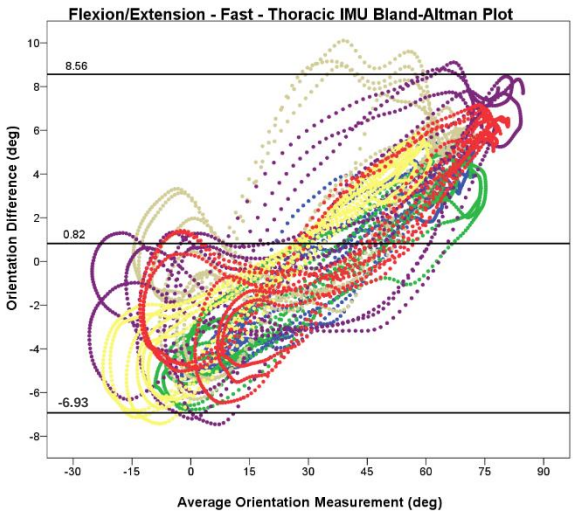

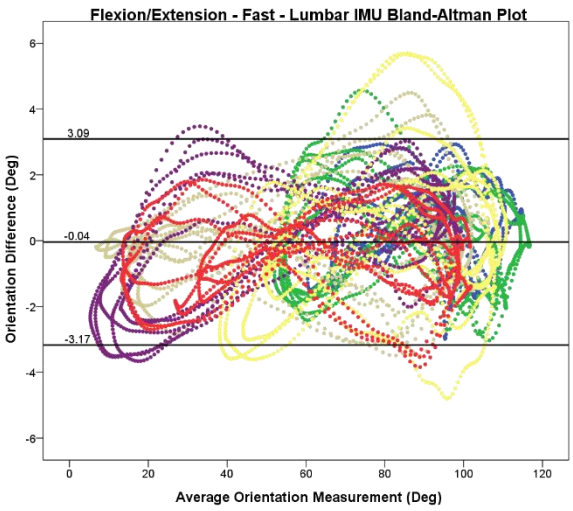

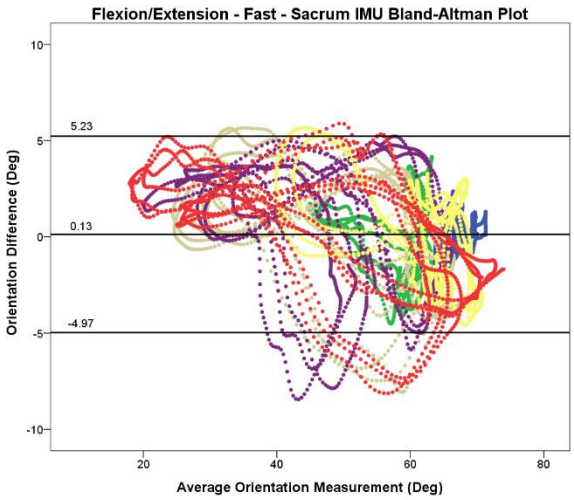

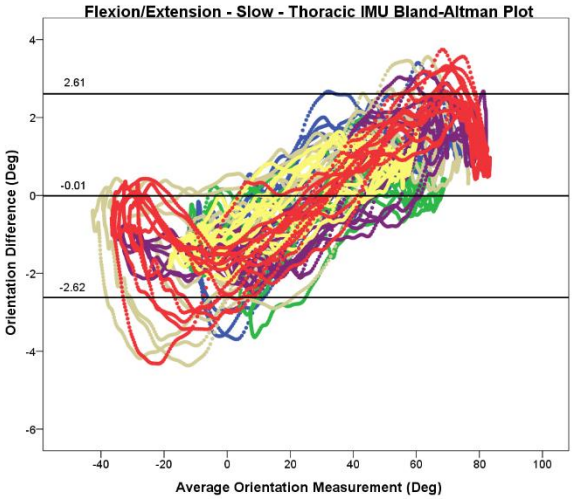

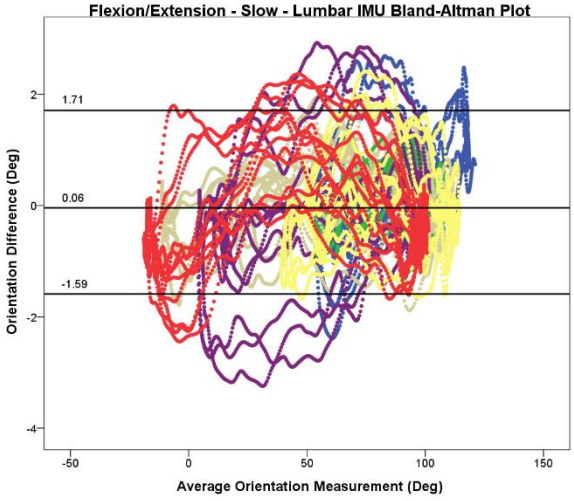

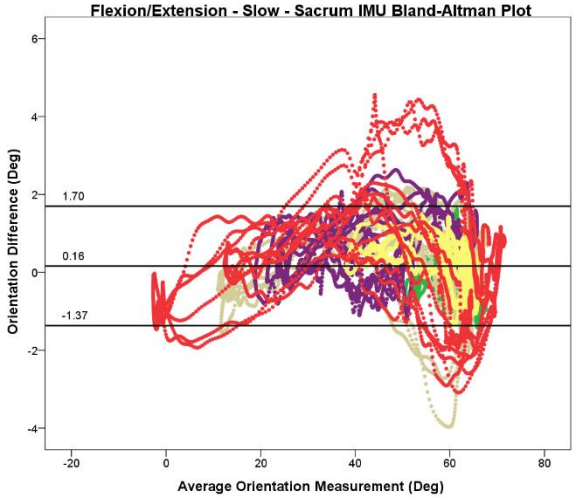

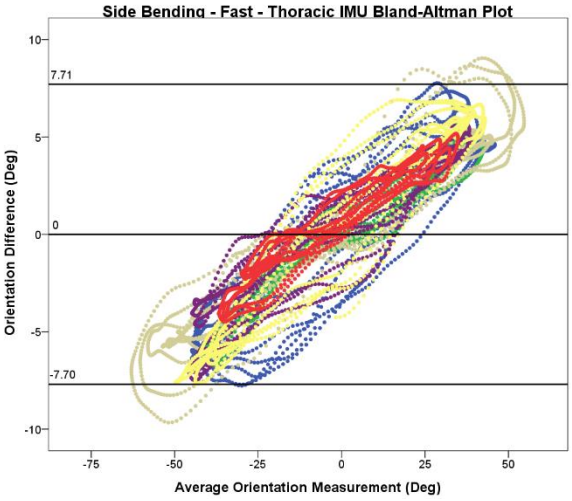
Side Bending - Fast - Thoracic IMU Bland-Altman Plot
Orientation Difference (Deg)
Average Orientation Measurement (Deg)
7.71
0
-7.70

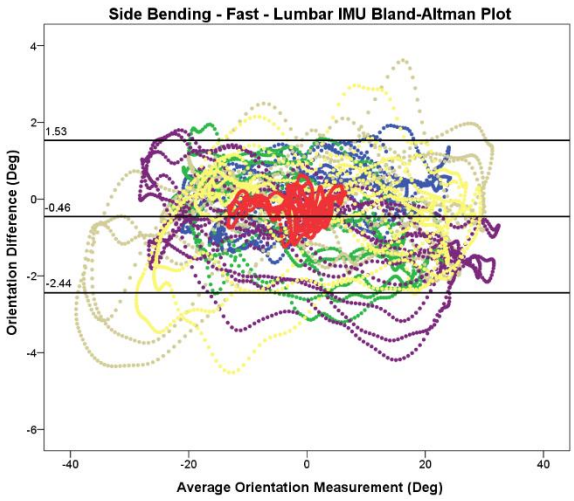
Side Bending - Fast - Lumbar IMU Bland-Altman Plot
Orientation Difference (Deg)
Average Orientation Measurement (Deg)
1.53
-0.46
-2.44

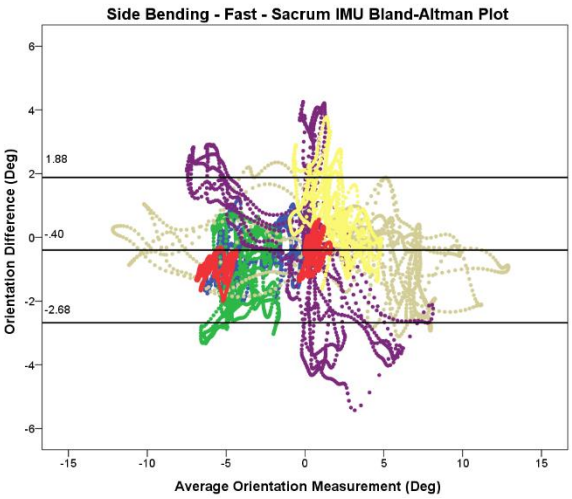
Side Bending - Fast - Sacrum IMU Bland-Altman Plot
Orientation Difference (Deg)
Average Orientation Measurement (Deg)
1.88
-.40
-2.68

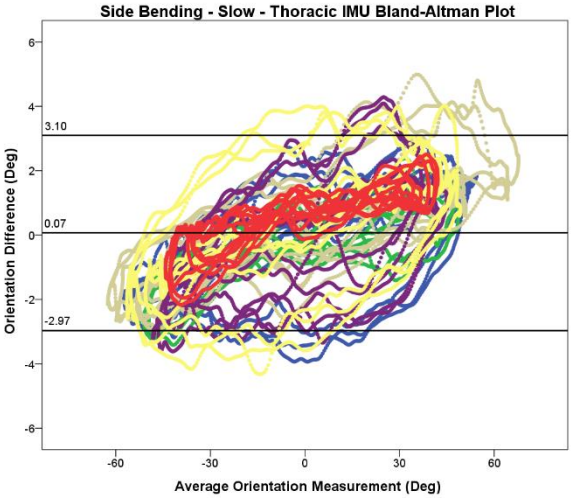
Side Bending - Slow - Thoracic IMU Bland-Altman Plot
Orientation Difference (Deg)
Average Orientation Measurement (Deg)
3.10
0.07
-2.97

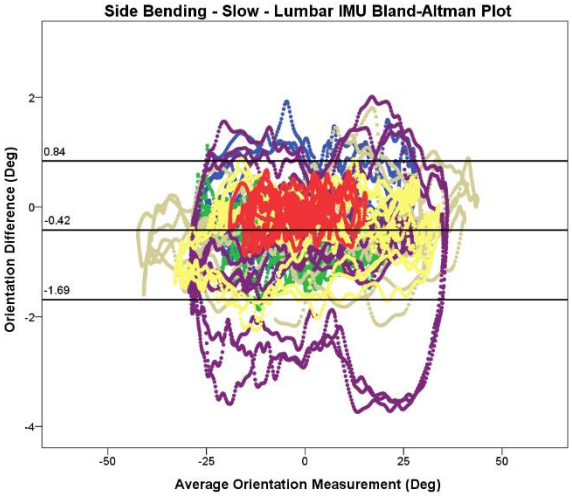
Side Bending - Slow - Lumbar IMU Bland-Altman Plot
Orientation Difference (Deg)
Average Orientation Measurement (Deg)
0.84
-0.42
-1.69

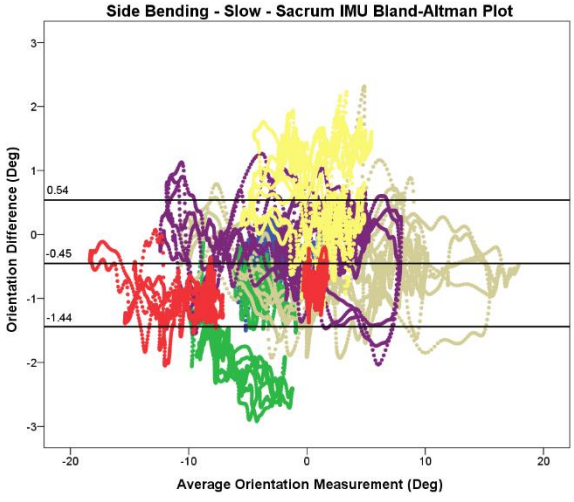
Side Bending - Slow - Sacrum IMU Bland-Altman Plot
Orientation Difference (Deg)
Average Orientation Measurement (Deg)
0.54
-0.45
-1.44

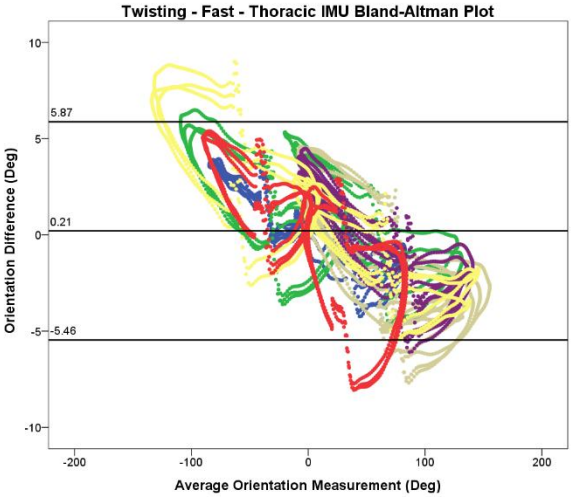
Twisting - Fast - Thoracic IMU Bland-Altman Plot
Orientation Difference (Deg)
Average Orientation Measurement (Deg)
5.87
0.21
-5.46

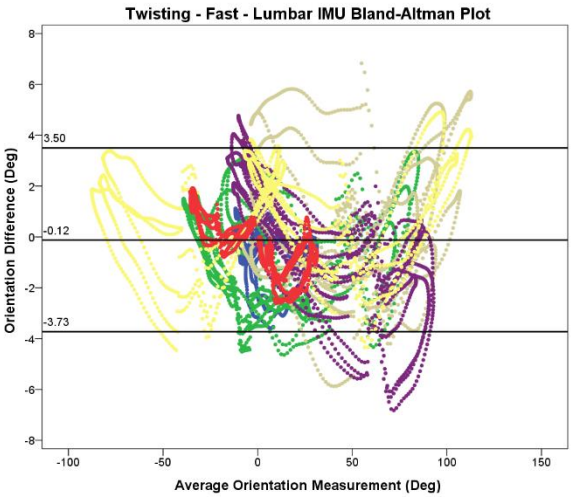
Twisting - Fast - Lumbar IMU Bland-Altman Plot
Orientation Difference (Deg)
Average Orientation Measurement (Deg)
3.50
-0.12
-3.73

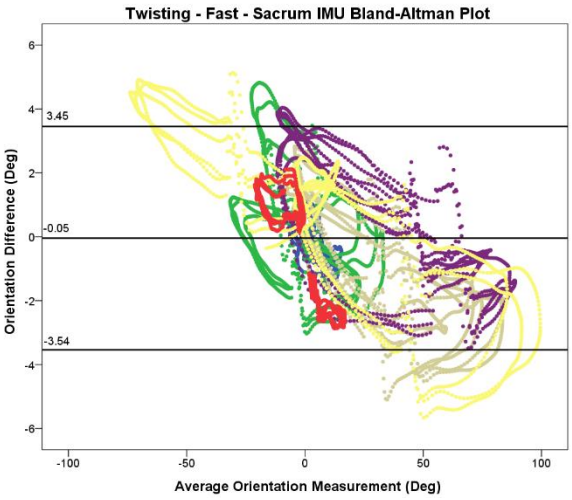
Twisting - Fast - Sacrum IMU Bland-Altman Plot
Orientation Difference (Deg)
Average Orientation Measurement (Deg)
3.45
-0.05
-3.54

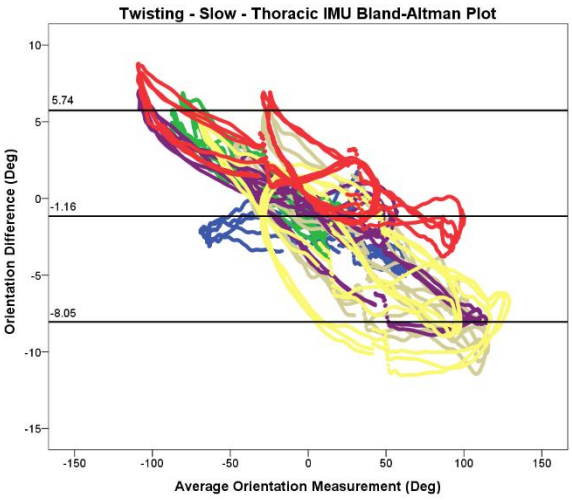
Twisting - Slow - Thoracic IMU Bland-Altman Plot
Orientation Difference (Deg)
Average Orientation Measurement (Deg)
5.74
-1.16
-8.05

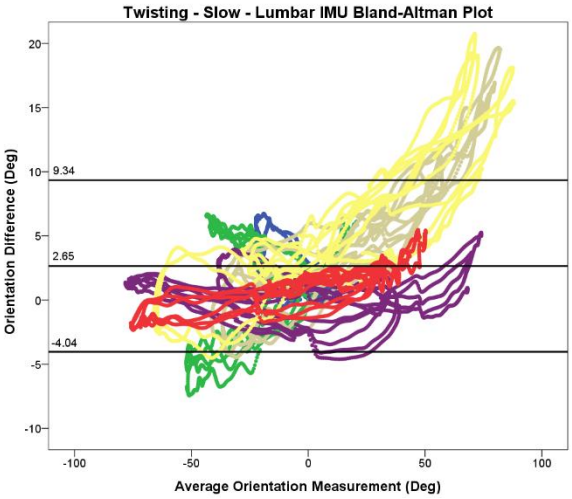
Twisting - Slow - Lumbar IMU Bland-Altman Plot
Orientation Difference (Deg)
Average Orientation Measurement (Deg)
9.34
2.65
-4.04

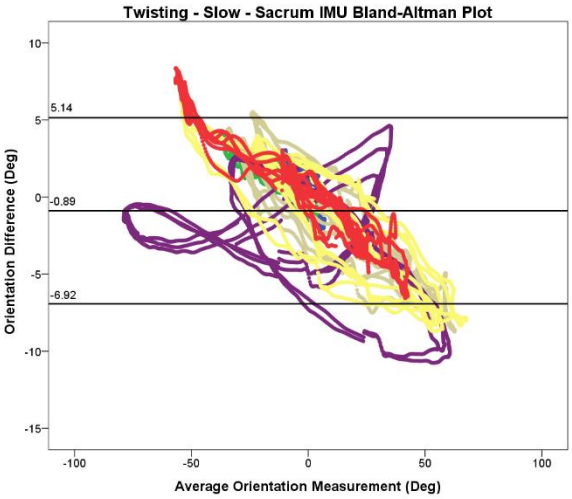
Twisting - Slow - Sacrum IMU Bland-Altman Plot
Orientation Difference (Deg)
Average Orientation Measurement (Deg)
5.14
-0.89
-6.92